# Modelling of the deaerator system in Flownex


**Prepared by:**

Richard Bobby Banda

BNDRIC005

Department of Mechanical Engineering

University of Cape Town

**Supervisor:**

Dr Wim Fuls

**December 2015**



Submitted to the Department of Mechanical Engineering at the University of Cape Town in partial fulfilment of the academic requirements for a Master's of Science degree in Mechanical Engineering

**Key Words:** Deaerator, Spray-type, Tray-type, Mass Transfer Coefficients, Modelling, Flownex

# *Abstract*

The study of the steady-state and dynamic behaviour of thermal power plants is of interest and significant benefit in different engineering fields ranging from research and design, to the assistance of operator training, plant optimization, fault finding and failure analysis. In light of the these benefits, and the increasing electrical energy demand in South Africa, the Eskom Power Plant Engineering Institute Centre for Energy Efficiency intends to build a transient simulation model of a coal fired power plant. The software identified for this task is Flownex SE. Flownex is a one-dimensional thermal-hydraulic solver that solves user defined networks by obtaining a numerical solution of the governing equations of fluid dynamics and heat transfer. The software contains a vast library of low level standard industrial components such as valves and pipes that can be linked together to form networks. Due to the overall size and complexity of the intended plant model, it was suggested that individual plant components be modelled separately and then integrated together to form the complete model. The primary objective of this study was to develop one such model, of a deaerator, in Flownex. In addition to being a building block for the complete plant model, the deaerator model will also be used as a standalone model to predict the steady state, transient and non-condensable gas extraction characteristics of the equipment.

The first activity performed was to establish the types and operating principles of the deaerators used in industry, particularly in Eskom power stations. This was achieved through a literature survey complemented by six power station visits and a review of some assets owned by Eskom. It was established that the tray and spray type deaerators were the most commonly used deaerator types, and that their operating principle was based on the temperature-solubility relationship of gases in water and Henry's Law. Based on this knowledge, an analytical model of a deaerator was developed. The purpose of this analytical model was to serve as a verification tool for the final Flownex Model. The analytical model was developed by writing a Mathcad algorithm that solved the steady state one-dimensional mass and energy conservation equations around the deaerator boundary together with the oxygen component continuity equation. The model was successfully validated by comparing its predictions to acceptance tests data from an Eskom's Plant 1 power station. The final step was the development, verification and validation of the Flownex model. The Flownex model was developed and successfully verified by comparing its predictions to that of the analytical model. Three case studies were then performed as a validation exercise in order to demonstrate the integrity of the model in simulating both steady state and transient scenarios. In all three studies the model predicted the unknown values satisfactorily and within acceptable error margins. It was therefore concluded that the primary objective of the study had been met.

# *Declaration*

I, Richard Bobby Banda hereby declare the work contained in this dissertation to be my own. All information which has been gained from various journal articles, text books or other sources has been referenced accordingly. I have not allowed, and will not allow, anyone to copy my work with the intention of passing it off as their own work or part thereof.

Signed by candidate

Richard Bobby Banda

# *Acknowledgements*

The author wishes to express his deepest gratitude to his supervisor, Dr Wim Fuls, for his unparalleled commitment in providing academic support throughout the course of this study. His input has not only assisted in completing this work, but has also contributed significantly into building a competent and confident mechanical engineer.

Many thanks go to the author's colleagues at the Eskom Power Plant Engineering Institute Centre for Energy Efficiency. Their assistance and companionship is greatly appreciated and forever treasured.

The author thanks the academic staff at the University of Cape Town and industrial experts for their guidance and advice throughout the course of this project. Special mention goes to Professor Louis Jestin, Professor Pieter Rousseau, Dr Francois du Preez and Jack Pratt.

The author would like to thank the Eskom Power Plant Engineering Institute for funding this project. Their provisions made this study and the accompanying qualification possible.

The financial assistance of the National Research Foundation (NRF) towards this research is hereby acknowledged. Opinions expressed and conclusions arrived at, are those of the author and are not necessarily to be attributed to the NRF.

Many thanks go to Eskom staff members for their input and for providing verification and validation data. Special mention goes to Mr Rahendra Neerputh and Mr Abel Rudman.

The author's sincere gratitude goes to his parents Gift and Jesca for their encouragement, prayers and supplementary financial provisions throughout the course of this project. The author also thanks his siblings Rocky, Ruth and Rachel for motivation and prayers throughout the project.

The author's deepest gratitude and indebtedness go to Ruvimbo Hapanyengwi, to whom this project is dedicated. Her constant support, encouragement and prayers are forever cherished.

Finally the author would like to thank the Lord for seeing this project to a successful completion.

# *Table of Contents*

# List of Figures

# List of Tables

# List of Nomenclature

## General symbols

| | |
|---|---|
| $A$ | Area [$m^2$] |
| $A_0$ | Nozzle discharge area [$m^2$] |
| $c$ | Molar concentration [$mol/m^3$] |
| $C_k$ | Pressure loss coefficient [$1/m^4$] |
| $c_p$ | Isobaric specific heat capacity [J/kg K] |
| $d_0$ | Nozzle discharge diameter [m] |
| $D$ | Diameter [m] |
| $D_{32}$ | Sauter Mean Diameter [m] |
| $D_{AB}$ | Mass diffusivity of A in B [$m^2/s$] |
| $h$ | Specific heat [kJ/kg] |
| $h_c$ | Convective mass transfer coefficient [$W/m^2 ˚C$], [$W/m^2$ K] |
| $J$ | Molecular flux in terms of coordinates moving at the molar average velocity [$mol/m^2$ s] |
| $k$ | Thermal conductivity [$W/m ˚C$], [W/m K] |
| $k_c$ | Convective mass transfer coefficient [m/s], [mol/s $m^2$ Pa] |
| $K$ | Overall mass transfer coefficient [m/s], [mol/s $m^2$ Pa] |
| $K_H$ | Henry's Law constant [Pa $m^3$/mol] |
| $K_{H\theta}$ | Henry's Law constant at ambient conditions [1.3 x $10^{-3}$ kmol/$m^3$ atm] |
| $L$ | Length [m] |
| $m$ | Mass flow rate [kg/s] |
| $M$ | Molecular weight [g/mol] |
| $N$ | Molecular flux relative to mass average velocity [$mol/m^2$ s] |
| $N_{noz}$ | Number of nozzles [-] |
| $n$ | Number of elements [-] |
| $p$ | Partial pressure [Pa], [bar] |
| $P$ | Total pressure [Pa], [bar] |
| $\Delta P$ | Pressure drop [Pa], [bar] |
| $q$ | Heat transfer rate [W] |
| $\dot{q}$ | Energy generated per unit volume [$W/m^3$] |
| $r$ | Radius [m] |
| $R_{ideal}$ | Ideal gas constant [8.314 J/K mol] |
| $t$ | Time [s] |
| $T$ | Temperature [˚C], [K] |

| | |
|---|---|
| $T_0$ | Ambient temperature [˚C], [K] |
| v | Velocity [m/s] |
| $V_m$ | Molal volume [$cm^3$/mol] |
| x | Mole fraction (liquid and solid) [-] |
| X | Nozzle “X” factor [-] |
| y | Mole fraction (gas) [-] |

## Greek symbols and subscripts

| | |
|---|---|
| $\alpha$ | Thermal diffusivity [$m^2/s$] |
| $\kappa$ | Boltzmann constant [$1.38064852 \times 10^{-23} m^2\ kg/s^2\ K$] |
| $\mu$ | Dynamic viscosity [Pa s] |
| $\rho$ | Mass concentration or density [$kg/m^3$] |
| $\sigma$ | Surface tension [N/m] |
| $\omega$ | Mass fraction [ppb] |
| $\Phi$ | Solvent association parameter [-] |

## Subscripts

| | |
|---|---|
| avg | Average |
| bs | Bled steam |
| dea | Deaerator |
| dw | Deaerated water |
| G | Gas phase |
| ht | Heat transfer |
| L | Liquid phase |
| mc | Main condensate |
| mt | Mass transfer |
| Noz | Nozzle |
| rc | Return condensate |
| s | Saturated liquid |
| vs | Vent steam |

## Acronyms and Abbreviations

| | |
|---|---|
| DALC | Deaerator Level Control |
| FW | Feedwater |

| | |
|---|---|
| FWH | Feedwater heater |
| FR | Flow resistance |
| GE | General Empirical |
| HTC | Heat transfer coefficient |
| MTC | Mass transfer coefficient |
| NCG | Non-condensable gas |
| NPSH | Net Positive Suction Head |
| ppm | Parts per million |
| ppb | Parts per billion |
| SMD | Sauter mean diameter |

# Glossary

**Mass fraction** Mass of component A per unit mass of the mixture given by;

$$\omega_A = \frac{\rho_A}{\rho}$$

**Molal volume** The volume occupied by one mole of a gas, liquid or solid. Also called the molar volume.

**Molar concentration** A measure of the concentration of a solute in a solution, or of any molecular species in a given volume. The molar concentration is given by;

$$c = \frac{\rho}{M} \text{ for liquids and solids}$$

$$c = \frac{P}{R_{ideal} T} \text{ for gases}$$

**Mole fraction** Concentration of any molecular species as a fraction of the total molar concentration given by;

$$x_A = \frac{c_A}{c} \text{ for liquids}$$

$$y_A = \frac{c_A}{c} \text{ or } y_A = \frac{p_A}{P} \text{ for gases}$$

**Nusselt number**

$$Nu = \frac{h_c L}{k}$$

**Peclet number**

$$Pe = \frac{h_c L}{k}$$

**Reynolds number**

$$. \mathrm{Re} = \frac{\rho v d}{\mu} .$$

**Schmidt number** $$Sc = \frac{\mu}{\rho D_{AB}}$$

**Sherwood number** $$Sh = \frac{K_L d_{32}}{D_{AB}}$$

**Stanton number** $$St = \frac{h_c}{\rho v c_p}$$

# 1. Introduction

## 1.1 Background to study

The study of the steady-state and dynamic behaviour of thermal power plants is of interest and significant benefit in different engineering fields ranging from research and design, to the assistance of operator training, plant optimization, fault finding and failure analysis [1]. Several dynamic power plant models have been developed and used successfully for some of these activities. An example of such a model is reported in [2], where it was used to understand the effects of adding new components to a power plant in an effort to reduce the risk of failure and increase plant safety. In some cases, the plant models consist of several component models integrated together in order to simulate the behaviour of an entire system. Depending on the level of detail included in these component models, they too can be used as standalone models to further understand the behaviour of a component or group of components independently. Examples of such models and their applications are reported in [1], [3] and [4].

In light of the aforementioned benefits associated with using thermal-hydraulic models, and the increasing electrical energy demand in South Africa, the Eskom Power Plant Engineering Institute (EPPEI) Centre for Energy Efficiency at the University of Cape Town intends to build a transient simulation model of a coal fired power plant. The software identified for this task is Flownex SE, hereafter referred to as Flownex. Flownex is a one-dimensional thermal-hydraulic solver that solves user defined networks by obtaining a numerical solution of the governing equations of fluid dynamics and heat transfer. The software contains a vast library of low level standard industrial components such as valves and pipes that can be linked together to form networks. Due to the overall size and complexity of the intended plant model, it was suggested that individual plant components be modelled separately and then integrated together to form the complete plant model.

## 1.2 Objectives of the study

### 1.2.1 Primary objective

The primary objective of this study is to develop a thermal-hydraulic model of a deaerator in Flownex. The model shall be used to predict the steady state, transient and non-condensable gas (NCG) extraction behaviour of a typical deaerator system. In addition to being a building block for the full plant model, the deaerator model will also serve as a standalone model that can be used to simulate and understand the behaviour of typical deaerator systems independently.

### 1.2.2 Secondary objectives

In order to meet the primary objective of this study, the following secondary objectives were laid down;

1. Establishment of the types and operating principles of the deaerators used in industry, particularly in Eskom power stations.
2. Development and validation of an analytical model of a deaerator in Mathcad.
3. Development, verification and validation of the Flownex model using the analytical model as a reference.

## 1.3 Methodology

The methodology followed in this study can be grouped into three main activities, each aimed at satisfying the secondary objectives listed in section 1.2.2. The first activity was to perform a literature survey mainly aimed at establishing the types and operating principles of the deaerators used in industry, particularly in Eskom power stations. The survey also included six power station visits, studies on previous deaerator models that were developed by other researchers, and studies performed on the transport processes and properties that govern deaeration.

Using the knowledge gained in the first activity, the following activity was to develop a validated analytical model of a deaerator. The purpose of this model was to serve as a reference model for the Flownex model. The analytical model was developed by writing a Mathcad algorithm that solved the steady state one-dimensional mass and energy conservation equations around the deaerator boundary, together with the oxygen component continuity equation. The model was validated by comparing its predictions to plant acceptance data from Plant 1 power station.

Using the validated analytical model as reference, the Flownex model was then developed. The model was verified through comparing its predictions to the analytical model and validated through three case studies, two of which were steady state studies and one transient study.

## 1.4 Scope and limitations of the study

Most deaerator manufacturers do not readily disclose information relating to the detailed design of their products because of competition between manufacturers, and also to protect their intellectual property. This in turn means that modelling of deaerators using exact design dimensions becomes difficult as a large number of assumptions will be necessitated. Such assumptions may significantly compromise the accuracy of the model. Another approach is therefore required and was used in this study. This is to use information from the deaerator

performance data to predict or determine key characteristics and inputs that can then be used to build a suitable model.

The model developed in this study therefore focuses on defining the systems level characteristics of the deaerator. This means that the model uses average fluid and material properties and aims to define the properties of the deaerator that will affect surrounding components. The model will therefore not be able to predict some local effects. This might affect the accuracy of the model especially in conditions that extend beyond the typical operating range of the equipment.

The model will be developed with control capabilities but without actual control elements or loops. Such additions require a detailed knowledge of other plant components and are therefore deemed to be out of the scope of this work. A fully detailed control system will be added to the full plant model once all components are completed and integrated. The absence of a control system for this model makes it difficult to validate its transient characteristics since those are significantly dependant on the level and conditions inside the deaerator feed tank.

The model developed shall be applicable to the two main types of deaerators available in industry as it is based on the following two assumptions;

- The deaerating dome and feedwater tank are considered as one vessel as postulated by [5].
- The heating and deaeration processes are completed in the preheater stage of the deaerating dome (which is common to both deaerator types) [6].

## 1.5 Report Outline

The next chapter of this report focuses on the theoretical concepts that were considered in the development of the model. These concepts set a foundation for the literature used to formulate the modelling approach that was finally adopted. The chapter starts off by discussing the Rankine cycle and the role of feedwater heaters (FWH). It then narrows down to deaerators and discusses the different deaerator types and their working principles. This is followed by fundamental considerations of the processes of heat and mass transfer, which play pivotal roles in the deaeration process. The chapter is concluded with a discussion of liquid atomization and spray nozzles; this information is used in the model to provide necessary parameters required to solve the heat and mass transfer relations that characterize deaeration.

Chapter 3 presents the literature used to formulate the modelling methodology followed. The chapter describes two mathematical deaerator models and reviews the methodologies employed in their development. Following this, the processes of heat and mass transfer in deaerators are

looked at in detail; this is achieved through presenting previous works that were carried out by other researchers on the subjects.

Chapters 4 and 5 present the development, verification and validation exercises performed on the analytical and Flownex models respectively. In general, the chapters start off by describing the constituent relations or components that make up the models. This is followed by a description of the calibration exercises required before the models can be used. Following this, the models are then run and the results are compared to actual plant data and discussed.

The last chapter contains the conclusion to the study, limitations of the models and some recommendations on possible further studies.

# 2. Theoretical Background

The purpose of this chapter is to present the theoretical foundation of the material discussed and used in the following chapters. The chapter starts off by describing the regenerative Rankine cycle and the role played by FWH and deaerators. This is followed by a description of the operating principles and functionality of deaerators, and a survey of the deaerators used in industry and in Eskom power stations. The following sections then narrow down to the fundamental concepts of heat and mass transfer which are followed by an overview of liquid atomization and spray nozzles. After this, the key aspects of the chapter are then summarised in the closing remarks.

## 2.1 The regenerative Rankine cycle

Most fossil, nuclear and solar power stations in the world are based on the Rankine cycle (Figure 1). The cycle can be carried out in four pieces of equipment which are appropriately joined by pipes for conveying the working medium from one component to the next [7]. In its simplest form the ideal cycle consists of the following four stages [8];

- Isentropic compression in a pump
- Constant pressure heat addition in a boiler
- Isentropic expansion in a turbine
- Constant pressure heat rejection in a condenser

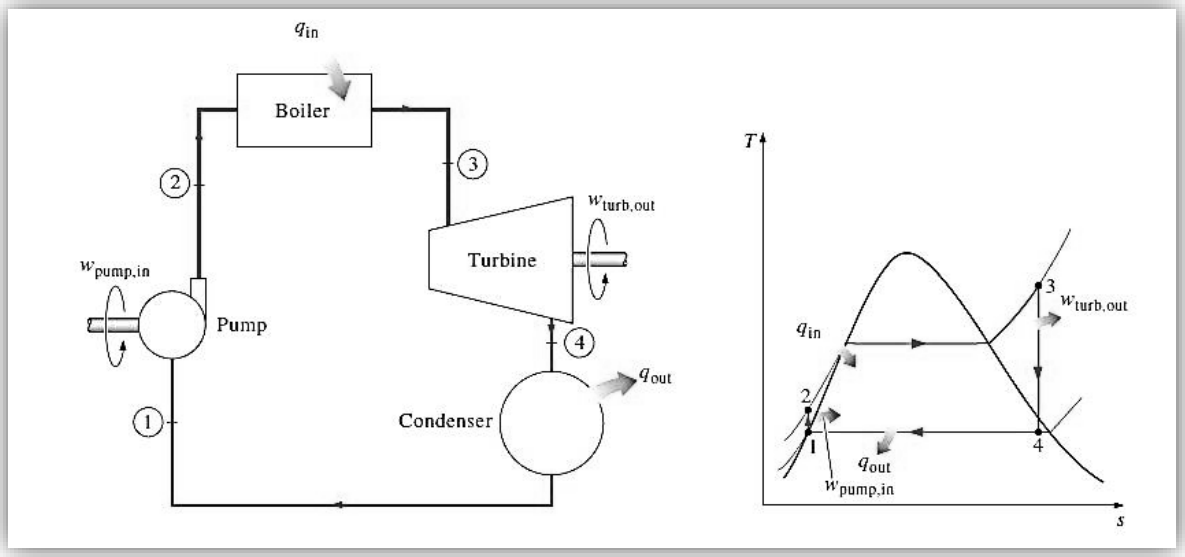


*Figure 1: Simple Ideal Rankine cycle schematic and the corresponding T-s diagram [8]*

Studies on the Rankine cycle have shown that efficiency improvements require either an increase of the thermal state of the high pressure steam, or a decrease in that of the exhaust steam, or both. These changes require an increased boiler pressure, higher initial superheat and lower condenser pressures. However, the operational and material limits of these conditions have long been reached and as such, cycle modifications were investigated with the hope of increasing the thermal efficiency of the cycle. One such modification, which made significant progress in increasing the efficiency of the cycle resulted in the Regenerative cycle first proposed by Ferranti in 1905 [5]. The principle feature of this cycle is the thermal regeneration of condensate into high temperature feedwater (FW) by the use of steam extracted from the turbine. A high level schematic of the cycle and the associated T-s diagram are shown below;

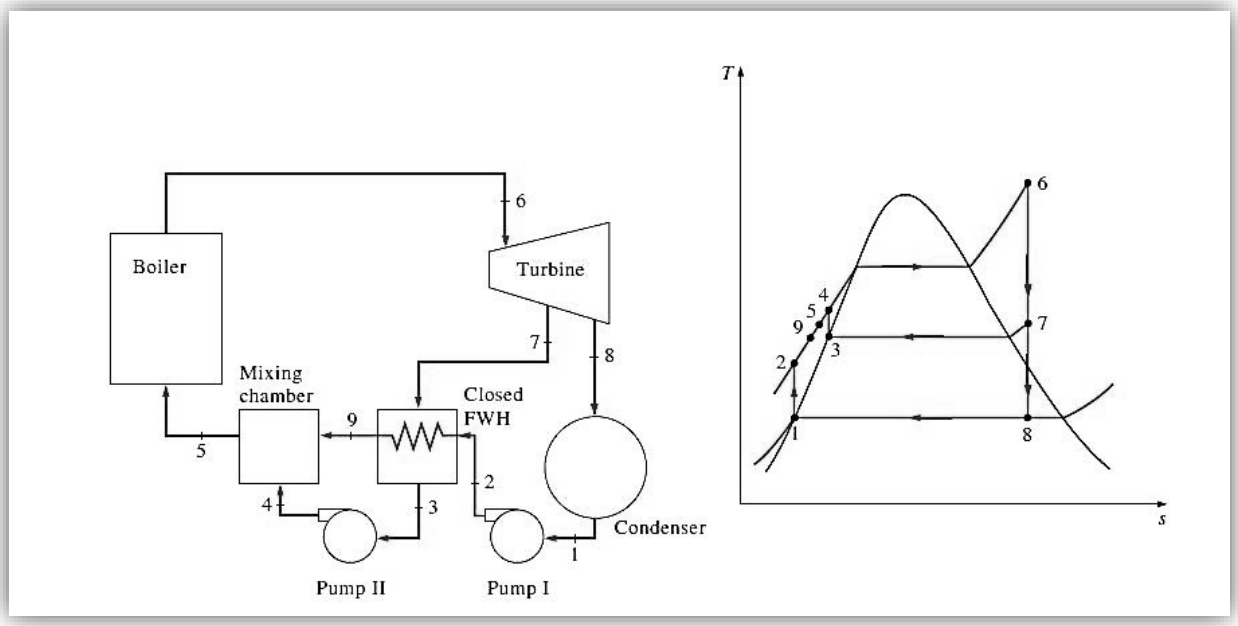


*Figure 2: Regenerative Rankine cycle schematic and T-s diagram [8]*

The main advantage of this cycle over the simple Rankine cycle is that the heating steam as extracted from the turbine, has released considerably most of the mechanical work represented in its available energy, whilst retaining most of its heating capacity which would have otherwise been rejected in the condenser. Using this steam, the FW is progressively heated using feedwater heaters (FWHs), nearly to the boiler saturation temperature – thereby reducing the necessary heat input to the cycle. This decrease in the heat input and the accompanying reduction in the amount of heat rejected in the condenser increase the overall efficiency of the cycle. The gain in efficiency becomes higher as the boiler pressure is increased due to the fact that the heat of the liquid will then form a larger part of the total fluid enthalpy [7].

Although the Regenerative cycle presents many other advantages over the simple Rankine cycle, it does however, require more auxiliary equipment in the form of heaters, pumps, traps and piping. These components make up what is called the Feedwater loop.

### 2.1.1 The Feedwater loop

*"The purpose of the FW loop can be said to be that of converting the cycle condensate into high temperature boiler feed, at a pressure sufficiently above that of the boiler to cause the correct flow into the boiler under variable loads"* [7]. The loop is located between the condenser outlet and the boiler inlet and its constituent components are shown below;

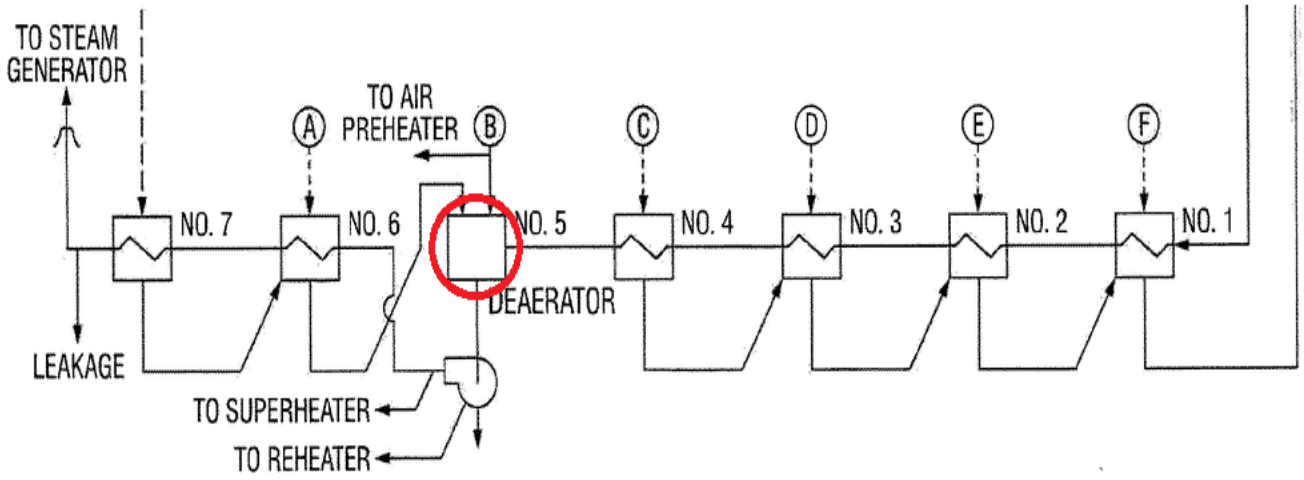


*Figure 3: Typical components of the FW loop (Feedwater heaters numbered 1 to 7).*

The configurations of the components in the FW loop are innumerable and no comprehensive description can thus be given. The key elements of the loop are the heating components. These components may comprise of FWHs and low and high heat saving equipment. Although the economiser and part of the boiler also constitute actual water heating surfaces, it is customary to label as "FWHs" those elements in which the FW is heated by obtaining heat from steam [7]. A comprehensive analysis of all heating components of the loop is out of the scope of this work, however, attention shall be given to FWHs, particularly of the open or contact type.

## 2.2 Feedwater heaters

A Feedwater Heater is a heat exchanger in which FW is heated via a heat transfer operation, with heat being transferred from steam extracted from the turbine [8]. The heat is transferred from the steam to the FW by either mixing the two streams in open or contact FWHs, or without mixing the streams in closed or surface FWHs. The two types of heaters will be briefly discussed below.

### 2.2.1 Closed FWHs

Heaters that are used to heat pressurised FW without any contact between the FW and heating steam are known as closed or surface FWHs [7]. In these heaters, one medium flows in a tube bundle and the other in a shell surrounding the bundle. Heat is transferred through the tube walls from the hot to the cold medium. Ideally the FW is heated to the saturation temperature corresponding to its pressure, but to enable effective heat transfer, there is a temperature difference of a few degrees Celsius between the outlet FW temperature, and the saturation temperature at the heater pressure. From a design standpoint, surface FWHs can be classified into steam tube and water tube heaters. Steam tube heaters are more commonly used in evaporators [7] whereas water tube heaters are most commonly used as extraction heaters. These heaters can also be classified according to the geometry of the tubes, into straight tube and bent tube (U tube and steam coils), and into single or multi-pass heaters. From a process standpoint, closed FWHs are classified into high pressure and low pressure FWHs. This designation emanates from the pressure of the FW flowing inside that heater, which is in turn driven by which side of the boiler feed pump the heater lies.

*Figure 4: Typical surface heater construction [9]*

The ordinary surface heater (Figure 4) is housed in a very well insulated cylindrical shell of steel. The tubes are normally made of steel or copper alloy and may be floating to allow for expansion

due to heat fluctuations [7]. FWHs of the surface type are considerably more expensive and complex than their open type counterparts, but offer the advantage of not needing a pump after each heater as the heat transferring streams can be at different pressures [8].

### 2.2.2 Open FWHs

FWHs that function by mixing of the steam and FW are known as open FWHs. This name is a holdover from the days when FW was heated to between 98.9°C - 100°C in heaters that were open to the atmosphere to maintain their pressure at approximately 1.013 bar [5]. A preferred and more common name for these heaters is direct contact heaters. In this type of heater, the FW is heated via direct contact conduction from steam to water, and the water can be heated to the temperature of the saturated steam if no foreign gas phases are present [7]. Although there are numerous internal designs of this equipment, all of them include some mechanism of increasing the surface area of the FW to allow rapid and efficient heat transfer from the heating steam. In addition to its heating function, the ordinary open heater also performs the following functions [7];

- Acts as a storage reservoir for heated FW.
- Provides a convenient receiver for condensation from various sources.
- Liberates non condensable gases (NCGs) to a greater or lesser degree depending on the design [5].

A contact heater especially designed for the removal of NCGs is known as a deaerating heater, or more commonly, a deaerator. Some scholars consider this a misnomer due to the fact that the equipment is not necessarily designed to remove air from the FW and steam, but rather a few unwanted gases, some of which are found in air. This type of heater forms the crux of this work and the following section is devoted to discussing the heater, and most of its process linked characteristics.

## 2.3 Deaerators

NCGs are gases that do not easily condense when cooling [10] and require temperatures in the cryogenic range to start condensing [11]. Examples of NCGs that are commonly found in boiler FW streams are Oxygen, Carbon Dioxide, Nitrogen and Ammonia Dioxide. These gasses usually enter the FW stream via the following channels [5];

- Leaks, especially in those areas of the plant that operate below atmospheric pressure e.g. the low pressure turbine exhaust and condenser.
- By chemical reactions due to water treatment.

- By dissociation of the water and steam in the cycle due to prevailing high temperature conditions.

The effects of NCGs on normal boiler operation are numerous, and include blanketing of heat transfer surfaces, and increasing the average operating pressure of various plant components. The most prominent and most catastrophic effect however, is the corrosion they cause as a result of their chemical properties. The mechanisms of corrosion are a highly complex matter and a subject of much debate and work [12]. These mechanisms will not be covered in this study but it is sufficient to state that it is desirable to reduce the oxygen concentration in boiler FW to zero, or practically so [7]. In practice, international standards have stipulated that the oxygen concentrations in the boiler feedwater be less than 7ppb, and consequently most deaerators are designed to achieve this goal [13]. The remaining oxygen is normally further reduced by the use of chemicals called oxygen scavengers [14] [15]. These react with the oxygen in the water and form relatively harmless compounds that can be safely carried along through the remaining parts of the cycle.

### 2.3.1 Operating principle

Before describing the operating principle behind deaeration, it is necessary to briefly look at the physics governing the dissolution of gases in water. When non-polar molecules, like oxygen, are brought in close proximity with polar molecules such as water, the negative charge on the water molecule repels the oxygen electrons and pushes them farther away from the water. This results in a temporary uneven distribution of electrons in the oxygen molecule, known as an induced dipole [16]. During this period, the oxygen molecule behaves in a polar fashion and is attracted to water molecules via electrical forces called induced dipole-dipole forces. The same situation may arise due to the random motion of electrons within non-polar molecules, making the molecules temporarily polar. When a dipole-dipole bond is formed, the normally non-polar molecule is said to be dissolved in the dipole fluid. Regardless of how the dipole is induced, induced dipole-dipole forces are relatively weak and therefore non-polar molecules have low solubility in water.

Thermal deaeration is based on two physical principles, both aimed at disrupting the weak induced dipole-dipole forces holding NCG and water molecules together. These are [17];

1. The temperature-solubility relationship of gases in water and,
2. Henry's law.

The first principle says that as the temperature of water is increased, the solubility of gases in it decreases [18]. This is a result of the decrease in the time available to form induced dipoles as the

molecules move around faster with a higher kinetic energy. This principle is exploited in thermal deaeration by heating the FW using steam, and so reducing the solubility of NCGs in it [19].

The second principle can be represented by equation(1), and is a statement that relates the concentration of a gas dissolved in water, to the partial pressure of that gas in contact with the free surface of the water.

$$p_A = K_H c_A \tag{1}$$

Where;

- $p_A$ is the partial pressure of gas A in contact with the free surface of the water.
- $K_H$ is Henry's Law constant.
- $c_A$ is the concentration of the gas dissolved in the water.

This principle is exploited in deaeration by introducing another gas (steam) and heating the FW to its boiling point at the deaerator pressure. By so doing, the partial pressures of all other gases in contact with the water are reduced to zero, meaning that by equation(1), no other gas can be absorbed by the water. The two principles work simultaneously during thermal deaeration as the same heating medium is responsible for the reduction in NCG partial pressures.

Simply rendering the gases insoluble by heating the water to its boiling point does not itself eliminate the molecules of gas dissolved in the water. On a molecular level, heating the water to boiling only means that the NCG molecules are no longer bound to the water molecules by the weak induced dipole-dipole forces, but they are still physically intermixed between the water molecules. In this state, the NCG molecules exist as small bubbles inside the water body [18]. If they are not separated, they will be reabsorbed by the water once the temperature is reduced, or their partial pressure is increased. In order to escape from the mass of water, the gas molecules must diffuse through the surface film surrounding the water particle [7]. The rate of this diffusion is function of the concentration difference of the gas between the water particle and the surrounding steam, and the total surface area available for diffusion. It is necessary to agitate the water in order to reduce the surface tension and increase the surface area available for diffusion. Deaerators are therefore designed to repeatedly agitate and break down the water particles to enable the gaseous molecules to reach the water surface rapidly, and eliminate the need for movement from the interior of the water particle to the surface purely by diffusion [7]. How the water is agitated depends on the temperature difference of the incoming and outgoing water streams, and in turn, to the particular deaerator design. As such, there exists a number of deaerator types, some of which are discussed in the next section.

## 2.3.2 Deaerator Types

The principles mentioned in the preceding section can be carried out in deaerators of varying designs, some of which are not direct contact heaters [20]. This work will be focused on deaerating heaters as these are the ones used in thermal power generation utilities, including Eskom power stations. Some of the other types will be mentioned and discussed very briefly at the end of this section for sake of completeness. Deaerating heaters are usually designed to perform the following three functions [18];

1. Remove NCGs from boiler FW.
2. Heat the FW.
3. Store FW (In this case the deaerator is usually located on top of a horizontal storage tank).

In addition to the points listed, deaerators are usually placed at a high elevation in order to provide a Net Positive Suction Head (NPSH) for the boiler feed pump [1].

Deaerating heaters are classified into two types, the spray-tray and spray-scrubber or atomizer types [13]. Both types have sprays in them, hence the prefix “spray” in their names. The preferred industrial names for these deaerators, which will be used from here onwards, are tray and spray type deaerators respectively.

**Tray Type Deaerator**

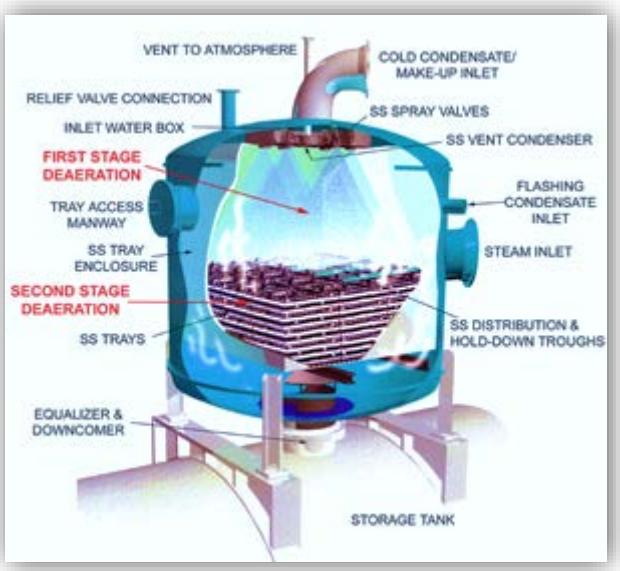


*Figure 5: Tray type deaerator (showing the deaerating section only) [21]*

Figure 5 shows a schematic of a tray type deaerator. The deaerator consists of two sections, called the first and second deaerating stages, or more commonly, the preheater and tray sections respectively.

The incoming feedwater is first introduced into the preheater via a system of atomizers or nozzles, the purpose of which is to break down the water and increase the surface area available for heat and mass transfer. Once inside the preheater, the feedwater is mixed with steam, which is introduced through the side, top or bottom of the deaerator, depending on the particular design. The steam heats the feedwater to a few degrees within saturation, and deaerates it according the principles discussed in section 2.3.1. More than 90% of the heating and deaeration are achieved in this stage [22] [13] [6]. The NCGs are liberated into the steam, where they rise to the upper part of the deaerator because of their relatively low densities. The gases are then vented out of the deaerator, along with a small amount of steam, through a vent pipe. The vent pipe may discard the steam-NCG mixture into the atmosphere or into a lower pressure vessel like the condenser. The heating steam loses energy and condenses around the feedwater droplets. Together, the mixture flows by gravity to the second deaerating stage.

The final deaeration to prescribed industrial limits is achieved in the tray section, sometimes called the polishing zone [22]. Here the FW drips down layers of slightly tilted perforated trays, emerging as hundreds or even thousands of little waterfalls [5]. This is done in order to further increase the surface areas for heat and mass transfer, and also to increase the residence time of the FW inside the vessel. As the FW falls from tray to tray, it is mixed with the fresh steam rising from the bottom. The violent mixing of the water and steam under these conditions allows the remaining NCGs to be removed from the FW and into the steam, where they are carried to the preheater section. The trays are made of cast iron or stainless steel, the latter being preferred due to its light weight and corrosion resistance characteristics [5].

The FW leaving the tray section passes through a down comer pipe into the storage section. For power utility deaerators, this is usually a horizontal tank upon which the vertical deaerator is mounted. The storage tank usually contains a sparge line through which heating steam is admitted at low flow rates. This is primarily done to keep the FW heated and to provide a steam blanket over the free surface of the water in order to avoid recontamination. This tank may also serve as a convenient drains receiver, allowing drains from high pressure FW heaters to be collected and reintroduced into the FW loop. The operation described above and suggested by Figure 5 shows one of three steam flow arrangements [20], in which the FW and steam are flowing in opposite directions (counter-flow). The steam and the FW may flow in the same direction, in an arrangement known as a co-counter or parallel flow arrangement [22]. In this arrangement the steam is introduced through the top of the deaerator and flows in the same direction as the FW.

The steam flow may also be orthogonal to the water flow in an arrangement known as cross-current flow [20].

As an additional accessory, some deaerating heaters are fitted with a vent condenser [5]. This may be an external U-tube surface FW heater mounted on top of the deaerator before the spray nozzle(s) [5], or simply a length of piping inside the deaerator on top of the spray nozzle(s) [18] [13]. The purpose of the vent condenser is to recover the steam from vapour gas mixture vented out of the deaerator. It has the advantage of also heating the FW before it passes through the nozzle.

**Spray type deaerator**

The general anatomy and operating principle of this deaerator type is very similar to that of the tray type deaerator (Figure 6). Some spray type deaerators are also mounted on horizontal tanks and therefore have an external appearance similar to that of the tray type deaerator discussed in the preceding section. Both deaerators consist of two deaerating stages with an identical preheater section and venting mechanism. This section will therefore not be re-described here. The fundamental difference is in the second deaeration stage.

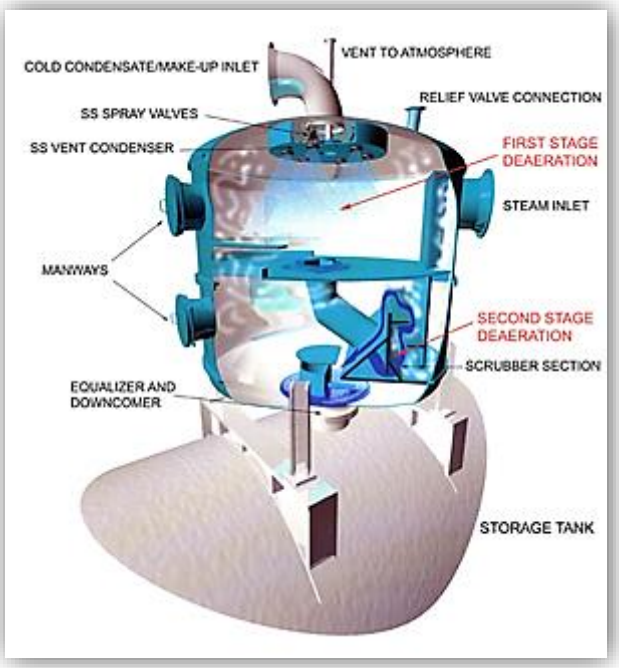


*Figure 6: Spray type deaerator (showing the deaerating section only) [21]*

For the spray type deaerator, the FW is collected in a space below the preheater section, called the scrubber section [21]. A high velocity steam jet is then bubbled into the water through a steam orifice. The purpose of this action is to violently mix the water and perform a scrubbing action. The kinetic energy of the steam is imparted to the water causing it to break down into fine droplets,

thereby increasing the surface area for heat and mass transfer. The NCGs pass almost instantaneously into the surrounding steam, little of which would have been condensed during the atomizing process. The NCG-steam mixture then flows upwards to meet the incoming water in the preheater section. The steam orifice may be of the fixed or variable type, the latter being preferred because of its adaptation and suitability to changing operating conditions [22].

Spray type deaerators are usually preferred for maritime practice because deaeration will be adversely affected in the tray type deaerator by rolling and pitching of the vessel (the motion affects the thickness of the water film spilling over the edge of the trays) [22], and because they are generally lighter in weight. Although spray type deaerators have been used in stationary plants (utilities), two disadvantages have prevented their general acceptance viz. the terminal difference and the inability to efficiently remove NCGs in the event of a pressure loss in the deaerating section [5].

**The Stork Spray Deaerator**

The stork spray type deaerator has been mentioned separately because of its unique geometry and slightly different operating principle to the conventional spray type deaerator. The uniqueness of this deaerator is responsible for the common perception that the Stork spray type deaerator is a different deaerator type altogether. The deaerator combines the deaeration and storage functions into one vessel (Figure 7) and is used widely in power utilities including some owned by Eskom.

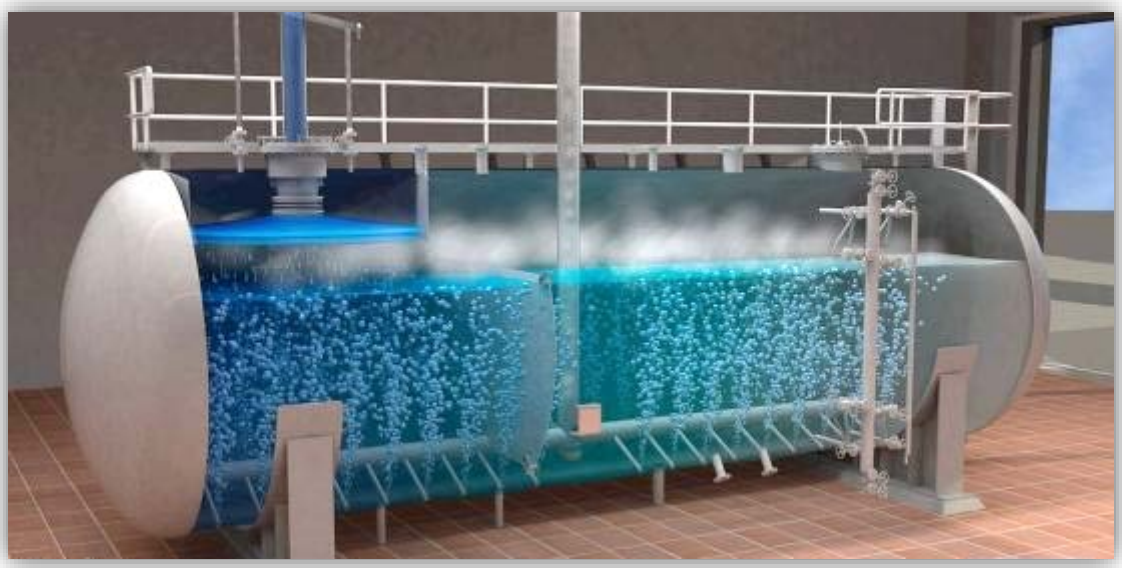

*Figure 7: Stork type deaerator [23]*

In principle, the stork type deaerator is a spray-scrubber type deaerator. The preheating section of this deaerator is the space below the nozzle ring (also known as the “stork disc sprayer”) [23]. In this section, the water is heated close to saturation and most of the NCGs are liberated into the

steam atmosphere. The steam condenses around the water droplets, leaving the low density gases to rise to the space above the spray, and to be finally vented into the atmosphere in a fashion similar to that of the tray and spray type deaerators previously discussed. The water from the preheating section then flows into the second deaerating section directly below the nozzle ring. In this section, steam is sparged via stork sprays at the bottom of the vessel. This steam serves to agitate the water therefore increasing the surface area for heat and mass transfer. The remaining NCGs are liberated into the sparging steam which rises to the preheater section. The deaerated water then flows over the baffle into the storage tank where it continues to be heated by the same sparging action to avoid recontamination.

**Other deaerator types**

Henry's Law has been exploited in other deaerator designs, different from the ones mentioned so far. This section will briefly describe two of these deaerators. The first one is called a vacuum deaerator, and works on the principle of creating a vacuum inside a packing-filled tower in order to bring the FW to saturation at lower temperatures [18]. This eliminates the need for heating the water and is useful in situations where heating the water may be costly or impractical. The packing used is normally small pieces of ceramic or plastics stacked randomly inside a vertical tower. The packing acts as splash blocks so a lot of surface area is exposed as the water tumbles down from the top to the bottom. As long as the FW is warmer than the saturation temperature at the vacuum drawn, it will be boiling and a little is actually vaporized. Under these conditions the water cannot hold any gases. NCGs are then liberated and drawn out of the deaerator using steam ejectors or vacuum pumps. This deaerator type is not used in power generation set ups because the water is heated anyway.

The second deaerator type worth mentioning is the flash type deaerator. In this deaerator the pressure inside the deaerating vessel is maintained at a value slightly above atmospheric. The water to be deaerated is heated using an external source to a temperature slightly above that corresponding to the pressure inside the deaerator, and then introduced into the vessel via a spray nozzle. Due to the fact that the water is slightly warmer than saturation conditions inside the deaerator, some of it will flash into steam and the rest will be at boiling point and therefore cannot hold any gases [18]. The gases then pass out into the "flash" steam and are pushed out into the atmosphere using a vent mechanism similar to that described for the tray and spray type deaerators.

### 2.3.3 Deaerator location and level control

It was mentioned in section 2.3.2 that deaerators play the role of providing a NPSH for the boiler feed pump. This is achieved by locating the deaerating unit at the highest possible part of the plant, typically at 18.3m for combined cycle plants and at 36.6m for conventional fuel plants [24] [1]. The unit is usually located directly above the boiler feed pump and after the last low pressure feedwater heater. In addition to providing a NPSH for the boiler feed pump, this may be driven by cost considerations and an effort to appropriately distribute workloads on the condensate extraction and boiler feed pumps. The operating temperature of thermal deaerators is normally above 107 °C as this is the minimum temperature at which Carbon dioxide can be removed from the feedwater [25]. The removal of carbon dioxide is regarded as an important factor in controlling the conductivity of the water.

As the deaerator storage tank is responsible for keeping a steady supply of condensate to the boiler feed pump in the case of a loss of supply form the condenser feed, the level of FW in the tank is monitored and controlled [6]. The actual control system varies per plant and is determined by the philosophy employed during the design of the plant. In general, the level control is effected by the Deaerator Level Control Valve (DALC valve) which is located somewhere in the lower levels of the plant depending on the specific design [24]. Essentially the system consists of a sensor which measures the water level in the tank and triggers the DALC valve to act in one of two ways. In the case of a decrease in the level, the DALC valve will introduce make up water, typically from the demineralised tank, into the deaerator condensate feed. This will steadily increase the level in the deaerator as there is a net inflow of water. In the case of an increase in the deaerator level, the DALC valve will dump a fraction of the condensate feed into a hotwell or other storage device and decrease the flow of condensate to the deaerator. This will decrease the level in the deaerator as the water entering the deaerator will be less than that exiting the unit [6].

### 2.3.4 Deaerators used in Eskom

Eskom currently has thirteen coal fired power stations all fitted with deaerator units. Due to financial, time and logistical constraints, only six of these stations were visited during the course of this study. The stations visited and the types of deaerators available at each station are listed in the following table.

From Table 1 it is clear that Eskom predominantly uses tray type deaerators. This is quite expected considering that spray type deaerators are predominantly used in the maritime industry and have not been widely adopted in stationary plants [5].

*Table 1: Eskom power stations visited and the respective deaerator types installed*

| ***Power Station*** | ***Deaerator type*** |
|---|---|
| | |
| *Arnot* | *Tray type* |
| *Duvha* | *Tray type* |
| *Hendrina* | *Tray type* |
| *Plant 2* | *Stork type* |
| *Plant 1* | *Tray type* |
| *Tutuka* | *Tray type* |

The deaerators available in Eskom power stations are of differing designs and are made by different manufacturers. As a result, some important differences exist in the manner in which they operate. The main differences noted are those concerning the spray devices used in the first deaerating stage. More light shall be shed on this matter in section 2.6 where liquid atomization and spray nozzles are discussed.

### 2.3.5 Mass and energy balance calculations for deaerators

The mass and energy balance calculations for deaerators are similar to those for direct contact FWHs. The following assumptions are usually made when carrying out the balances [5];

- The heater is perfectly insulated.
- The enthalpy of the vent steam is that of saturated steam at the deaerator pressure.
- The water exiting the vessel is fully saturated, i.e. extraction is below the fill level, and the hydraulic pressure increase is insignificant.
- The process is one of steady flow.
- The kinetic energies of the flows are insignificant, thus static and total pressure is assumed equal.
- The energy extracted contribution of the NCGs is negligible.
- The deaerator and storage tank can be treated as one vessel.

In the case where a vent condenser is fitted to the equipment, it is often dealt with as being part of the heater itself so no separate heat balance is required. The balance itself is carried out by conserving incoming and outgoing energy and mass of the deaerator. Shown below are typical heat balance equations for a simplified deaerator (Figure 8). More often than not, the inlet steam mass flow rate and inlet water enthalpy are the unknown quantities. The naming convention suggested in Figure 8 should be carefully noted as it is used extensively in Chapters 4 and 5. It is presented and explained below for clarity.

- Main condensate (*mc*) refers to the incoming feedwater from the low pressure feedwater heaters.
- Return condensate (*rc*) refers to the drains coming from the high pressure feedwater heaters and being collected in the deaerator.
- Bled steam (*bs*) refers to the heating steam that is extracted or bled from the turbine.
- Vent steam (*vs*) refers to the NCG-steam mixture vented out of the deaerator through the vent pie.
- Deaerated water (*dw*) refers to the deaerated water leaving the deaerator.

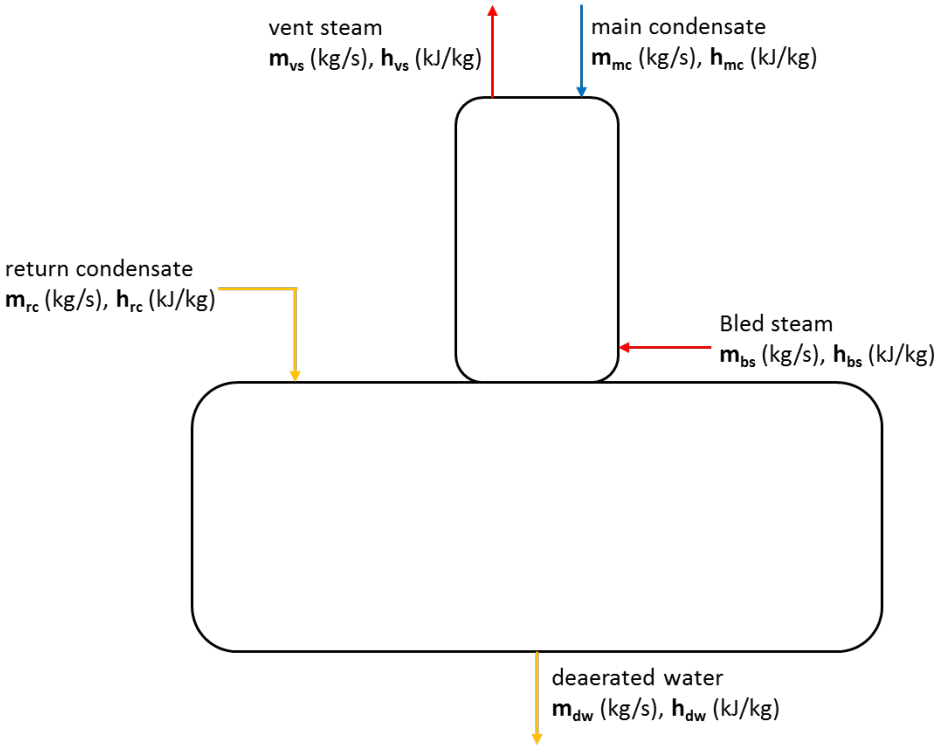


*Figure 8: Simple deaerator schematic*

- Mass balance;

$$m_{mc} + m_{rc} + m_{bs} = m_{vs} + m_{dw} \tag{2}$$

- Energy balance;

$$m_{mc}h_{mc} + m_{rc}h_{rc} + m_{bs}h_{bs} = m_{vs}h_{vs} + m_{dw}h_{dw} \tag{3}$$

Where *m* represents the mass flow rates and *h* represents the specific enthalpies. These two equations can be rearranged to solve for any two unknowns.

## 2.4 Heat transfer overview

The descriptions of the deaeration process presented in the preceding sections have made it apparent that deaeration is essentially a process of simultaneous heat and mass transfer. As such, it is necessary to present the fundamental basis of the two transport processes before considering their application in the analysis of deaeration. This section is devoted to presenting some heat transfer principles that will be elaborated on in the following chapters.

The principles presented here will not be too detailed as it is generally assumed that the water will be heated to its saturation temperature during deaeration. The main aim of this section is to give an overall description of the heat transfer basics from which mass transfer analogies will be drawn.

### 2.4.1 Heat transfer by conduction

It has been shown that when a temperature gradient exists within a body, energy will flow from the high temperature region to the low temperature region in order to even out the temperature distribution. This flow of energy is termed conductive heat transfer and is described by Fourier's law of heat conduction as:

$$q = -kA\frac{\partial T}{\partial x} \tag{4}$$

Where

- $q$ represents the heat transfer rate.
- $k$ is the thermal conductivity of the material.
- $A$ represents the area normal to the temperature gradient.
- $\frac{\partial T}{\partial x}$ is the temperature gradient in the x-direction in °C/m.

Equation (4) is written in terms of the x-direction and Cartesian coordinates but can be extended and applied to any direction and coordinate system of choice. The negative sign in the equation shows that the energy will flow in the direction of a negative temperature gradient in accordance with the second law of thermodynamics [26].The equation can be used in the derivation of the heat conduction equation by applying it in the energy balance of an elemental three-dimensional volume. The derivation is of no significant assistance in understanding the material presented in this report, and will not be shown here. However, it is necessary to present the equation as it plays a part in the analysis to follow.

$$\frac{\partial^2 T}{\partial x^2}+\frac{\partial^2 T}{\partial y^2}+\frac{\partial^2 T}{\partial z^2}+\frac{\dot{q}}{k}=\frac{1}{\alpha}\frac{\partial T}{\partial t} \tag{5}$$

Where $\dot{q}$ and $\alpha$ are the energy generated per unit volume and the thermal diffusivity of the material in question respectively. By solving equation(5) for suitable boundary and initial conditions, it is possible to fully describe a heat-conduction scenario in terms of the temperature distribution in the time domain.

### 2.4.2 Heat transfer by convection

When heat is transferred between a surface and a moving fluid, or between two moving fluids, the transfer process is termed convective heat transfer. The rate of energy transferred in this way can be computed using Newton's law of cooling;

$$q = h_c A(T_1 - T_2) \tag{6}$$

Where $(T_1 - T_2)$ represent the temperature difference between the two streams or the stream and the body, and $h_c$ the convective heat transfer coefficient (HTC). The HTC is essentially a function of the flow and thermal properties of the fluids between which the heat is being transferred. Although it can be computed analytically via a boundary layer analysis, in most cases this is far too difficult or even impossible to achieve and so empirical and semi-empirical methods are used to compute its value. The empirical methods often result in correlations expressed in various dimensionless numbers and fluid properties.

## 2.5 Mass transfer overview

When a system contains two or more fluids whose concentrations vary from point to point there is a natural tendency for mass to be transferred in order to minimise the concentration difference. This movement of mass is called mass transfer and can be defined as the movement of one component from a region of higher concentration to that of a lower concentration. The transportation phenomena of mass is very similar to that of heat and therefore many of the concepts and underlying principles are the same.

Mass can be transferred in two distinct modes, namely, molecular diffusion and convective mass transfer. These two modes are analogous to conduction and convective heat transfer respectively.

### 2.5.1 Molecular diffusion

Molecular diffusion is the transfer of mass due to random molecular movements within a system [27]. Mass transfer laws have shown that the flux of the diffusing substance is related to the

concentration gradient of that species, and that the mass will always move in the direction of a negative concentration gradient. Before presenting the relations used to evaluate this flux, it is necessary to briefly discuss the use of average velocities commonly used to describe the phenomena.

In a multi component system the species usually move at different velocities. Therefore if one wishes to evaluate the velocity of the mixture, some averaging technique is required. In this light, two average velocities are defined in mass transfer operations, namely, the mass-average velocity and the molar-average velocity. These can be evaluated using the equations shown below;

*Mass-average velocity*

$$v_{mass} = \frac{\sum_{i=1}^{n} \rho_i v_i}{\rho} \tag{7}$$

*Molar-average velocity*

$$v_{molar} = \frac{\sum_{i=1}^{n} c_i v_i}{c} \tag{8}$$

Where

- $v_i$ represents the absolute velocity of species *i* in m/s.
- $\rho_i$ represents the mass concentration or density of species *i* in kg/m$^3$.
- $c_i$ represents the molecular concentration of species *i* in mol/m$^3$.
- $\rho$ represents the mass concentration or density of the mixture in kg/m$^3$.
- $c$ represents the total molar concentration of the mixture in mol/m$^3$.

The velocity of a species relative to the mass or molar-average velocity is known as the diffusion velocity. Two diffusion velocities can therefore be defined, one relative to each average velocity.

The mass or molar flux of a given species is a vector representing the amount of that species, in either mass or molar units, passing through a unit area normal to that vector in a given time interval. The flux can be defined relative to stationary or moving coordinates. In the latter case, the coordinates may be moving with either the mass-average velocity or molar-average velocity of the mixture. In its most basic form, the flux of a species due to molecular diffusion $J_{A,}$ is defined in terms of coordinates moving at the molar average velocity. An empirical definition for this flux defined for isothermal, isobaric conditions is;

$$J_{A,z} = -D_{AB} \frac{dc_A}{dz} \tag{9}$$

Where

- $D_{AB}$ is the mass diffusivity of component *A* in component *B*.
- $\frac{dc_A}{dz}$ is the concentration gradient in the z-direction in mol/m$^4$.

The above relation is known as Fick's Rate equation, commonly called Fick's Law defined in the z-direction. This is the mass transfer equivalent to Fourier's law of heat conduction and can also be extended to other directions other than the z-direction. A more general relation not restricted to isothermal, isobaric systems was proposed by Groot [27] and can be shown as;

$$J_{A,z} = -cD_{AB}\frac{dy_A}{dz} \tag{10}$$

Where $y_A$ is the mole fraction of species *A*, written here for gases.

Since the total concentration does not change in isothermal and isobaric systems, it can be seen from the above equation that Fick's Law is merely a special case of Groot's expression for the case where *c* is constant. Flux can also be represented with respect to the mass average velocities in relationships that are considered equivalent to the expressions shown above. One such relation is shown below;

$$j_{A,z} = -\rho D_{AB}\frac{d\omega_A}{dz} \tag{11}$$

Where $\omega_A$ is the mass fraction of component A. When density is constant this becomes;

$$j_{A,z} = -D_{AB}\frac{d\rho_A}{dz} \tag{12}$$

**The diffusion coefficient**

The diffusion coefficient is analogous to the thermal diffusivity α, of a medium [27]. For binary mixtures, it is sometimes referred to as the mass diffusivity of component *A* in component *B*. The diffusion coefficient is dependent on the temperature, pressure and composition of a system, and its values have mostly been obtained experimentally. Due to the different molecular mobilities in the three states of matter, diffusion coefficients are generally higher for gases than they are for liquids, which are higher than those for solids. In the absence of experimental data, semi-theoretical expressions have been developed which give approximations for the diffusion coefficient, sometimes as good as the experimental data.

*Liquid-Mass Diffusivity*

The matter of theoretically determining the diffusion coefficient for components in liquids has been complicated by the inadequacies of the theories describing the structure and transportation

properties of liquids. Moreover, there has been much debate on the subject of defining diffusion coefficients for electrolyte solutions and what this would physically mean [27]. For non-electrolyte solutions, two theories have been postulated as possible explanations for diffusion in low concentration solutions; the Erying "hole" theory and the hydrodynamic theory. The two theories have been combined to come up with an accepted general form to describe the diffusion coefficient of components in low concentration solutions. The general form is sown below;

$$\frac{D_{AB}\mu_B}{\kappa T} = f(V) \tag{13}$$

where *f(V)* is a function of the molecule volume of the diffusing solute, $\mu_B$ is the solvent viscosity, $\kappa$ is the Boltzmann constant and $T$ is the absolute temperature. Researchers have developed empirical relations using this general form with the aim to predict the liquid diffusion coefficient in terms of the solute and solvent properties. To this effect, Wilke and Chang [27] [28] have proposed a widely accepted correlation for non-electrolytes in an indefinitely dilute solution;

$$\frac{D_{AB}\mu_B}{T} = \frac{117.3x10^{-18}(\Phi_B \cdot M_B)^{1/2}}{Vm_A^{0.6}} \tag{14}$$

Where

- $\Phi_B$ is the solvent association parameter for solvent *B.*
- $M_B$ is the molecular weight of solvent *B* in g/mol.
- $Vm_A$ is the molal volume of solute *A* at the normal boiling temperature in $cm^3/mol$.
- $\mu_B$ is the viscosity of solvent *B* in centipoises.
- $T$ is the temperature of the mixture in K.

## 2.5.2 Convective mass transfer

Convective mass transfer is the exchange of mass between a boundary surface and a moving fluid, or between two immiscible moving fluids separated by a mobile interface. In the former case the transfer is essentially within a single phase and the flux is related to an individual convective mass transfer coefficient (MTC). Many mass transfer operations however, including deaeration, include the transfer of mass between two contacting phases. In this case the flux is related to an overall convective MTC. Convective mass transfer is dependent on both the transport properties and the dynamic characteristics of the flow, and can be further classified into two forms depending on the force behind the fluid flow. When the fluid flow is caused by an external pump or similar device, the process is called forced convection, if the flow is due to density differences, the process is called natural or free convection. The rate equation for convective mass transfer is shown below.

$$N_A = k_c \Delta c_A \tag{15}$$

Where

- $N_A$ is the flux of species *A* diffusing from the stationary boundary into the fluid stream. Note the use of *N* instead of *J* to represent the flux. This is to show that the flux is measured relative to a stationary coordinate system.
- $\Delta c_A$ is the concentration difference of species A between the surface boundary and the bulk of the fluid.
- $k_c$ is the convective MTC.

Equation (15) is also the defining equation for the MTC and is analogous to Newton's Law of cooling. As with molecular diffusion, convective mass transfer occurs in the direction of decreasing concentration.

**The mass transfer coefficient**

In general, the convective MTC is a function of the system geometry, the fluids in question, the fluid flow properties and the concentration differences. The reciprocal of the convective MTC, $1/k_c$, represents the resistance to mass transfer and shall be used extensively in the following sections. The convective MTC is analogous to the convective HTC in Newton's law of cooling and the techniques used to evaluate the two are very similar. For convective mass transfer between a stationary boundary and moving fluid, four methods of evaluating the MTC have been used, these are [27];

- Dimensional analysis coupled with experiment;
- Exact laminar boundary-layer analysis
- Approximate boundary layer analysis
- Analogy between momentum, energy and mass transfer

No further discussion of convective mass transfer operations between stationary boundaries and moving fluids shall be presented in this work as it offers no direct insight into the task at hand. The remaining sections on convective mass transfer shall focus solely on the transfer of mass between two phases.

**Equilibrium and equilibrium relations**

The transport of mass within a single phase has been shown to be directly dependent upon the component concentration gradient. Such a departure from equilibrium conditions is also required for mass to be transferred between two phases. If the average or bulk concentrations of the phases are different, mass will be transferred between the two until an equilibrium is attained. This however, does not mean that the concentrations of the component in the two phases need to

be equal. For multi-phase problems, a dynamic equilibrium can be achieved between phases with unequal concentrations, and laws have been established to describe the conditions under which this occurs. For problems involving liquids and gases, many equations on this matter have been developed and reported. The choice of equations to use is generally dependent on the conditions of the system and the chemistry of the interacting fluids.

For cases involving gas and liquid phases, some fairly simple yet useful relationships are documented. A few of them will be discussed here as they are relevant to this work. When the liquid phase is ideal, equilibrium conditions can be described by Raoult's Law which relates the equilibrium partial pressure of the component *A* in the vapour phase above the liquid, $p_A$, to the molar fraction of the component in the liquid $x_A$, and the vapour pressure of the pure *A* at the equilibrium pressure $P_A$.

$$p_A = x_A P_A \tag{16}$$

When the gas phase is ideal the equilibrium condition can be described by Dalton's law which relates the equilibrium partial pressure of component *A,* the mole fraction of the component *A* in the gas phase $y_A$, and the total pressure of the system *P*.

$$p_A = y_A P \tag{17}$$

In cases where both the liquid and gaseous phases are ideal, Raoult's and Dalton's laws can be combined into the Raoult-Dalton equilibrium law which stipulates;

$$y_A P = x_A P_A \tag{18}$$

When dilute solutions are involved, Henry's Law can be used to describe the equilibrium conditions. This law relates the concentration of a gas dissolved in liquid $c_A$, to the partial pressure of that gas in contact with the free surface of the liquid $p_A$. The constant of proportionality $K_H$, is called Henry's Law constant.

$$p_A = K_H c_A \tag{19}$$

A detailed discussion of equilibrium relations is beyond the scope of this study. However, it is necessary to highlight the following basic concepts involving the distribution of a component between two phases in an interphase mass transfer operation [27];

- At any fixed set of conditions such as temperature and pressure, it can be shown via Gibbs's phase rule that a set of equilibrium relations exist.
- There is no net exchange of mass in a system that is at equilibrium.

- If and when a system is out of equilibrium, mass will be exchanged in such a manner to cause the composition to shift towards an equilibrium point. If enough time is permitted, the system will eventually reach equilibrium.

**Whitman's two film theory**

Interphase mass transfer between liquids and gases consists of three steps (Figure 9), (1) the transfer of mass from the bulk conditions of one phase to the interfacial surface between the two phases, (2) the transfer of mass across the interface into the second phase and (3) the transfer of the mass into the bulk conditions of the second phase.

A two resistance theory proposed by Whitman and Lewis is usually used to describe this process [27]. The theory assumes that a thin film exists on either side of the phase interface and has two principle assumptions;

1. The rate of mass transfer between the two phases is controlled by the rates of diffusion through thin stagnant films on either side of the interface.
2. There is no resistance to mass transfer across the interface.

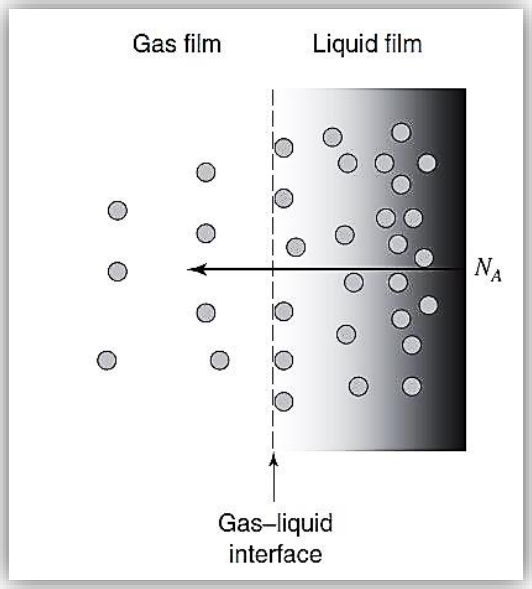


*Figure 9: Pictorial representation of the Two Film Theory [27]*

The theory can be used to explain the transfer of mass from the liquid to the gaseous phase and vice versa. The following discussion assumes that mass is transferred from the liquid to the gaseous phase in steady state (Figure 9). The driving force required to transfer mass from the bulk liquid phase to the liquid-gas interface is provided by the difference in the liquid phase bulk concentration $c_{AL}$ and the liquid phase interfacial concentration $c_{Ai}$ (Figure 10). Likewise, the driving force required to transfer mass from the liquid-gas interface to the bulk gas phase is

provided by the difference between the gas phase interfacial concentration (expressed in partial pressure form) $p_{Ai}$, and the gas phase bulk concentration $p_{AG}$. Since the theory assumes that there is no resistance to mass transfer across the interface, it follows that the liquid phase interfacial concentration and the gaseous phase interfacial partial pressure are in a thermodynamic equilibrium state that may be described by one of the laws previously presented.

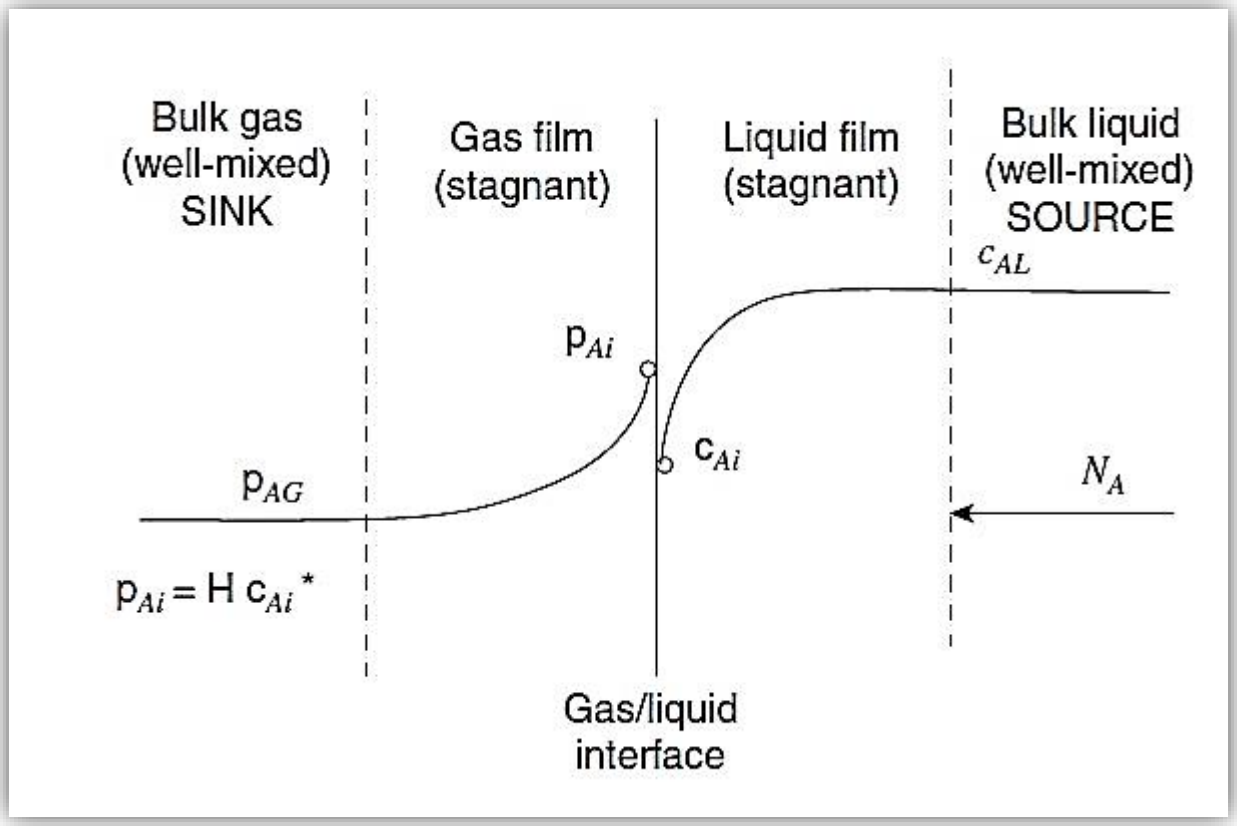


*Figure 10: Graphical view of the Two Film Theory [27]*

The mass flux transferred during the process can be defined on both sides of the liquid-gas interface. For the liquid side this is given as;

$$N_A = k_L(c_{AL} - c_{Ai}) \tag{20}$$

Where $k_L$ is the convective MTC in the liquid phase (m/s) and the quantity in brackets is the concentration difference driving the transport (mol/m$^3$). Likewise the flux on the gas side of the interface can be described as;

$$N_A = k_G(p_{Ai} - p_{AG}) \tag{21}$$

Where $k_G$ is the convective MTC in the gas phase (mol/s m$^2$ Pa) and the term in brackets is the concentration difference expressed in partial pressures (Pa). During steady-state convective mass

transfer, the fluxes on either side of the interface should be equal. By mathematically equating equations (20) and (21) one can come up with a ratio for the two convective MTCs expressed as;

$$-\frac{k_L}{k_G}=\frac{p_{AG}-p_{Ai}}{c_{AG}-c_{Ai}} \tag{22}$$

This ratio can be used in a graphical method to evaluate the interfacial compositions for a specific set of bulk conditions. This method is commonly used to evaluate the equilibrium conditions at an arbitrary plane in gas-liquid contactors including gas strippers and absorbers.

It is significantly difficult however, to obtain this ratio because of the difficulties associated with physically measuring the interfacial concentrations and partial pressures. It is desirable therefore, to somehow express the mass flux of the diffusing species in terms of the bulk properties of the contacting phases which are relatively easier to establish. This notion is similar to that used to motivate the need to define an overall heat transfer coefficient, *U*, in heat transfer applications. The challenge with this approach however, is that the overall driving force cannot simply be expressed as the difference between $c_{AL}$ and $p_{AG}$, $(c_{AL}-p_{AG})$, because the quantities have different units. This hurdle can be overcome by considering the equilibrium relations discussed previously. It can be shown that the partial pressure of the component in the bulk gas phase $p_{AG}$, is in thermodynamic equilibrium with some arbitrary concentration $c_A^*$, at any system pressure and temperature. By employing one of the equilibrium relations previously described, the equilibrium concentration $c_A^*$ can be evaluated and substituted for $p_{AG}$ in the expression for the overall driving force and the flux can then be written as;

$$N_A=K_L(c_{AL}-c_A^{\,*}) \tag{23}$$

Where $K_L$ is the overall convective MTC based on a liquid driving force (note the use of a capital *K* to denote the overall MTC). The same procedure can be followed for the gas phase and similarly an overall convective MTC based on a gas driving force can be defined. For low concentrations, as in power plant deaeration cases, Henry's law can be used to relate the equilibrium concentration $c_A^*$ and the bulk partial pressure on the gaseous side $p_{AG}$. The relationship is given by;

$$p_{AG}=K_H c_A^{\,*} \tag{24}$$

$$p_{Ai}=K_H c_{Ai} \tag{25}$$

The same relation exists between the interfacial properties and they can be expressed in a similar manner as shown in equation(25) by combining these two equations and the definitions of the flux on either side of the liquid-gas interface, the overall MTC based on either the liquid or gas driving force can be expressed as a function of the individual phase MTCs and Henry's law constant as;

$$\frac{1}{K_L} = \frac{1}{K_H k_G} + \frac{1}{k_L} \tag{26}$$

$$\frac{1}{K_G} = \frac{1}{k_G} + \frac{K_H}{k_L} \tag{27}$$

Equations (26) and (27) show that the relative contributions of the individual phase resistances to the overall resistance depend on the solubility of the gas, as indicated by the magnitude of the proportionality constant, Henry's Law constant $K_H$. For a system involving a soluble gas such as ammonia in water, $K_H$ is very low and the overall MTC is essentially equal to the gas phase MTC. In such a situation the mass transfer is said to be gas phase controlled. If the gas in question is a low solubility gas such as carbon dioxide in water, the overall MTC is essentially equal to the liquid phase MTC and the system is said to be liquid phase controlled. It should be stated however that many systems encountered in mass transfer operations are controlled by both phases and therefore both transfer coefficients need to be evaluated. Although the individual MTCs $k_L$ and $k_G$ may be independent of the concentration, the overall MTCs $K_L$ and $K_G$ may vary with concentrations unless the equilibrium relation is linear as is Henry's Law. If this is not the case the evaluated coefficients should only be used in the concentration ranges used when they were originally evaluated.

The two film theory is one of many theories put forward in an attempt to explain interphase mass transfer. Other theories of notable recognition are the Film and Penetration theories [27] [29]. Most industrial data have however been interpreted in terms of the two film theory.

**Convective mass transfer correlations**

Some convective mass transfer applications have been dealt with analytically and by using analogies to momentum and heat transfer as mentioned in 2.5.1. It is often desired to validate the analytical solutions experimentally and in so doing, dimensionless correlations are usually developed [27]. Dimensionless correlations have also been developed for instances that have not been successfully dealt with analytically. This section presents correlations pertaining to one such instance, the mass transfer between spheres and moving fluids.

Before these correlations are presented it is necessary to discuss the relevance of the associated dimensionless numbers. The form of these numbers is presented in the nomenclature and the main ones are presented below;

- The Reynolds number *(Re)* relates the inertial forces of the fluid to the forces due to the viscosity of the fluid.
- The Schmidt number *(Sc)* is a ratio of the momentum diffusivity to the mass diffusivity (analogous to the Prandtl *(Pr)* number in heat transfer). [29]

- The Sherwood number ( $Sh = \frac{k_L D}{D_{AB}}$ ) is a ratio of the transfer of mass due to convection to the transport of mass through molecular diffusion (analogous to the Nusselt *(Nu)* number in heat transfer) [29]

In addition, the Stanton *(St)* number involves the convection MTC, the Reynold *(Re)*, Peclet *(Pe)* and Grasshof *(Gr)* numbers are used to describe fluid flow.

Mass transfer correlations for single spheres consider the sum of the molecular diffusion and forced convection contributions [27]. The general form of the correlations is;

$$Sh = Sh_0 + C\,\mathrm{Re}^m\, Sc^{1/3} \tag{28}$$

Where *C* and *m* are correlating constants dependant on the application in question. For mass transfer into gas streams where the effects of free or natural convection are negligible, the Froessling equation is applicable for Reynolds numbers ranging from 2 to 800 and Schmidt numbers ranging from 0.6 to 2.7 [27];

$$Sh = 2 + 0.552\,\mathrm{Re}^{1/2}\, Sc^{1/3} \tag{29}$$

The effects of free or natural convection can be considered to be negligible if;

$$\mathrm{Re} \geq 0.4 Gr^{1/2} Sc^{-1/6} \tag{30}$$

When the effects of free or natural convection are significant, Steinberger and Treybal equation is recommended for transport of mass from spheres into moving gases.

$$Sh = Sh_0 + 0.347(\mathrm{ReSc}^{1/2})^{0.62} \tag{31}$$

Where $Sh_0$ is dependent on *GrSc*

$$Sh_0 = 2 + 0.569(GrSc)^{0.25}, GrSc \leq 10^8 \tag{32}$$

$$Sh_0 = 2 + 0.0254(GrSc)^{0.25}\,\mathrm{Sc}^{0.244}, GrSc \geq 10^8 \tag{33}$$

It is possible to rearrange the correlations presented into forms convenient for the evaluation of the MTC if all other parameters in the chosen correlation can be found.

## 2.5.3 Modelling of mass transfer processes

There are two model types commonly used to analyse two-phase (liquid-gas) mass transfer equipment, the ideal stage model and the mass transfer rate based model [30]. The following sections will briefly describe the two model types.

**The Ideal Stage Model**

The present discussion of this model type shall be of a very general nature. For a detailed treatment of the matter, the reader is referred to mass exchanger design dedicated literature [31] [30]. The ideal stage model has been used to design mass transfer equipment for over a century and is based on the assumption of thermodynamic equilibrium being attained at each stage or theoretical stage in a mass exchanger. This modelling approach entails simultaneously solving the component material balance equations, thermodynamic equilibrium relations and the enthalpy data of a system bearing in mind that the summation of mole fractions in each phase should equal to one. Collectively, these equations and relations are referred to as (**M**ass, **E**quilibrium, **S**ummation and **H**eat), MESH equations. The key assumptions of this approach are [30];

- Thermodynamic equilibrium is obtained on each stage
- The vapour and liquid phase are so perfectly mixed so that the vapour and liquid leaving a stage are at the same composition as the material in the stage.
- The vapour and liquid phase are at the same temperature.

Graphical techniques are often employed to solve the material and energy balances assuming thermodynamic equilibrium exists. Common examples of these are the Ponchon-Savarit diagram and McCabe-Thiele graphical methods which are applicable in different system types [32]. As some of the assumptions listed above are not achievable in most industrial-type applications, several types of efficiencies can be used either for a single stage or theoretical stage, [31] or for the overall mass exchanger [30] to "calibrate" the calculations and make them applicable to real-life scenarios.

The ideal-stage model is relatively easy to use as a full detailed equipment design is not required and also because it requires a minimum amount of input data – only equilibrium relationships and enthalpy data for the heat balance.

**The Mass transfer Rate-Based Model**

The theoretical foundation for mass transfer rate-based or non-equilibrium stage models was presented in section 2.5.2. This modelling approach forgoes the use of stage efficiencies and attempts to model mass-exchange equipment using the actual geometry of construction e.g. number of trays, packing height etc. This is achieved by computing the actual rates of interphase mass transfer in the equipment using relations presented in section 2.5.2 [30]. The mass transfer rates are solved simultaneously with energy and mass relations written in forms specific to the particular mass transfer application. If fully implemented, the modelling approach also includes the pressure drops across the mass exchanger so that a hydraulic balance is also performed. The

combination of these equations is occasionally referred to as the (**M**ass, **E**nergy, **R**ate, **S**ummation, **H**ydraulic, energy **= Q**) MERSHQ equations. The principle assumptions of this approach are;

- Thermodynamic equilibrium is achieved at the vapour-liquid interface.
- The temperatures of the two bulk phases need not be equal.
- Summation of the vapour and liquid mole fraction at the interface needs to be one.

**Mass transfer vs. Ideal Stage modelling**

The choice of modelling technique to use is dependent on the equipment being modelled, inputs available and the level of detail required as both are suitable for significantly detailed studies [30]. The ideal stage model is relatively simple to use, requires less data and computational time. However the empiricism of scaling up from ideal to real stages when assigning efficiencies can be a disadvantage when accurate overall efficiencies are not available. The mass transfer rate-based model offers detailed composition and temperature profiles and is generally more predictive in nature, but not necessarily more accurate, as it also depends on the assumption of equilibrium relations at the vapour-liquid interface. Although computationally intensive and requiring more detailed inputs, *"the mass transfer model does not use artificial parameters such as residence time per artificial stage"* [33] and does not rely on engineering-supplied estimates any more than heat-transfer calculations do. As this is the case, some researchers [33] have felt that it is necessary to eliminate the need to assume efficiencies and reliance on past experience and instead use the mass transfer rate based modelling approach to model mass transfer equipment. Also, advocates for the ideal-stage model [30] have conceded that in the absence of well-established overall efficiencies, using the mass transfer rate-based model becomes the only option.

## 2.6 Liquid atomization

It has been mentioned that the first deaeration stage consists of a spray device or devices which break down the water into small droplets in order to increase its surface area. This stage is responsible for more than 90% of the heating and deaeration [6] [13] [22] and this portion of the chapter is devoted to describing the principles that characterise this stage.

### 2.6.1 Atomizers

The transformation or breakdown of a bulk water body into a spray or dispersion consisting of smaller droplets is termed atomization [34] [35]. This breakdown of the bulk water body is carried out using spray devices known as atomizers, or more commonly nozzles. The process of atomization is one in which a liquid jet or sheet is disintegrated by the kinetic energy of the liquid itself, or by exposure to a high velocity gas or air, or as a result of mechanical energy applied

externally through a rotating or vibrating device [34]. This work focuses on atomization due to the kinetic energy of the liquid as the others to do not pertain to the deaerators modelled in this work.

The atomization process in which liquid disintegration is brought on by the kinetic energy of the liquid itself is carried out using nozzle types known collectively as pressure atomizers [35]. This name stems from the fact the pressure drop across this nozzle is the source of the liquid kinetic energy which in is responsible for the breaking up of the water body. Pressure atomizers are the most economical of all atomizer types where power demand is considered and they can be classified into three types.

- Jet atomizers
- Swirl atomizers
- Jet-swirl atomizers

The three nozzle types are described below.

**Jet Atomizers**

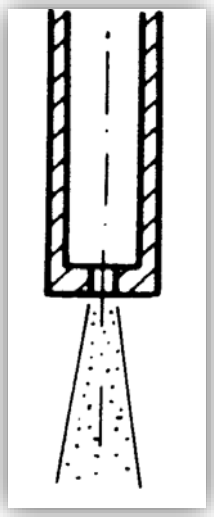

*Figure 11: Schematic of a jet atomizer [35]*

Jet atomizers function by forcing the liquid body through a small circular hole. The liquid emerges from the atomizer as a continuous body of cylindrical form. On the surface of this cylindrical body, a competition exists between cohesive and disruptive forces which results in oscillations and perturbations. If the liquid pressure exceeds the ambient pressure by about 150kPa [34], the oscillations are amplified and the liquid body disintegrates into drops, in a process known as primary atomization. If the droplets formed in the primary atomization stage exceed a certain critical diameter, they will further disintegrate into even smaller droplets in a process then known as secondary atomization. The process of this disintegration and the final result are a function of

the liquid type, discharge orifice diameter, discharge velocity and ambient conditions. For a given jet atomizer it can be said that the disintegration of the jet can be accelerated by increasing the discharge velocity which in turn means increasing the pressure drop across the atomizer. Jet atomizers are considered the simplest of all atomizers due to their relatively simple construction and principle of operation.

**Swirl atomizers**

Swirl atomizers operate in a manner similar to jet atomizers. The principle difference between the two atomizer types is the fact that the liquid body enters into a swirl chamber before it is discharged through the circular orifice. Various designs and types of swirl atomizers are used in industry. The following section applies to swirl atomizers of the simplex type as these are the most commonly encountered ones.

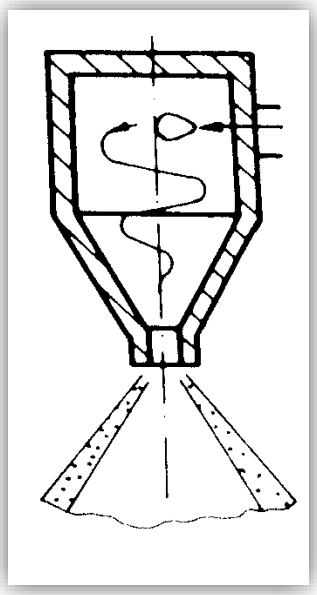

*Figure 12: Schematic of a pressure swirl atomizer [35]*

The swirling motion of the liquid inside the swirl chamber creates a core of air or gas that extends from the discharge orifice to the rear of the swirl chamber. This core is accordingly termed the air core. The liquid then emerges through the discharge orifice as an annular sheet which spreads outwards to form a hollow cone spray with a cone angle ranging from 15 to 90 degrees depending on the application [34]. The subsequent development of the emerging cone is heavily influenced by the initial velocity and the physical properties of the liquid and the ambient gas. In order to expand the sheet against the contracting surface tension forces, a minimum sheet velocity is required, which is provided by the pressure drop across the nozzle.

If the initial velocity is increased, the sheet is expanded and elongated until a leading edge is formed where an equilibrium exists between the surface tension and inertial forces. At this point the sheet disintegrates into ligaments and finally into droplets in a manner that depends on the velocity of the sheet. Three modes of sheet disintegration are known to exist, these are 1. Rim disintegration 2. Wave disintegration and 3. Perforated sheet disintegration. The three may occur simultaneously or only two at a time. The relative contributions of the different modes will significantly influence both the mean droplet size and droplet size distributions. The details of the modes of sheet disintegration will not be described further as they offer no immediate insight to task at hand.

For now it is suffice to state that swirl atomizers function best at high velocities and wide cone angels [34]. They generally ensure satisfactory disintegration for moderate and even small pressure drops and for this reason, and their relatively simple design, they are the most widely used of all types of atomizers [35].

**Jet-Swirl Atomizers**

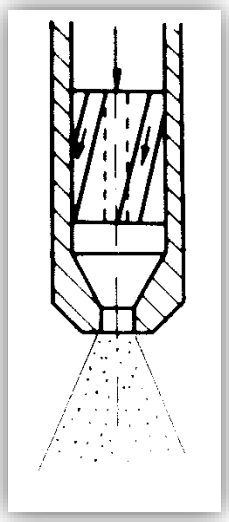

*Figure 13: Schematic of a jet swirl atomizer [35]*

For applications in which a “solid” cone is desired, jet-swirl atomizers are employed. As the name suggests, this atomizer type is essentially a combination of the jet and swirl atomizers. The principle feature of this atomizer is the use of an axial jet or some other device to inject droplets into the centre of the hollow conical spray pattern produced by the swirl chamber [34]. The resulting spray is one in which the jet density in the section perpendicular to the jet axis can be can be arbitrarily adjusted according to one’s need [35]. This may result in a uniform distribution; an advantage for most heat and mass transfer applications.

## 2.6.2 External characteristics of liquid sprays

The rest of the discussion on atomizers and atomizer performance shall be restricted to pressure swirl simplex atomizers. The theory on jet and jet-swirl atomizers was only introduced to allow for extensions to this work to be performed. These atomizer types shall not be discussed any further.

When one encounters a problem involving the atomization of a liquid in engineering applications, there are a few parameters of interest that may be required to perform calculations involving the performance of the atomizer, or the bigger system being analysed. Listed below are some of these parameters that are relevant to this work.

- Droplet size distribution in the spray
- Mean droplet diameter
- Spray sheet thickness
- Cone angle

The parameters listed above shall be discussed below in turn.

**Droplet size distribution**

The droplet size in a spray is determined by both controllable factors (e.g. nozzle geometry, type of liquid) and uncontrollable factors (e.g. liquid turbulence, vibrations). As a result, droplets with varying sizes are generated giving rise to a non-uniform (polydisperse) system. The process of droplet generation is therefore statistical in character and a theoretical prediction of the droplet number and sizes based on the disintegration mechanism itself is not feasible [35]. Although some scholars have attempted to deal with the problem theoretically, their success has been limited to certain atomizer types [34].

Statistical models have however been developed to represent the droplet size distribution and can been used to establish the mean droplet diameter. Of note are the Rosin-Rammler equation [36], the Nukiyama-Tanasawa equation [37], and the log normal distribution function [34].

**Mean droplet diameter**

A mean droplet diameter is a conventional quantity that characterises a set of droplets substituted for the real set. It can be used to determine characteristics such as the number, diameter, surface and volume of droplets depending on how it is calculated. Although a mean diameter will not provide any information about the droplet set itself, it is the most informative quantity for atomization quality assessment and can be used satisfactorily for engineering calculations [35].

There are different mean diameters that are in use and the choice of which one to use is based on the application in question. All mean diameters however are derived from the following equation;

$$D_{pq} = \sqrt[p-q]{\frac{\sum_{i=1}^{m} D_i^p \Delta n_i}{\sum_{i=1}^{m} D_i^q \Delta n_i}} \tag{34}$$

Where *p* and *q* are used simultaneously for the determination of a particular diameter. In order to gain a better understanding of the mean diameter concept, consider Figure 14 shown below to define the arithmetic mean diameter $D_{10}$ *(p=1, q=0)*. $D_{10}$ is the diameter of an equivalent droplet set (b) with the same number of droplets and sum of diameters as the real set (a).

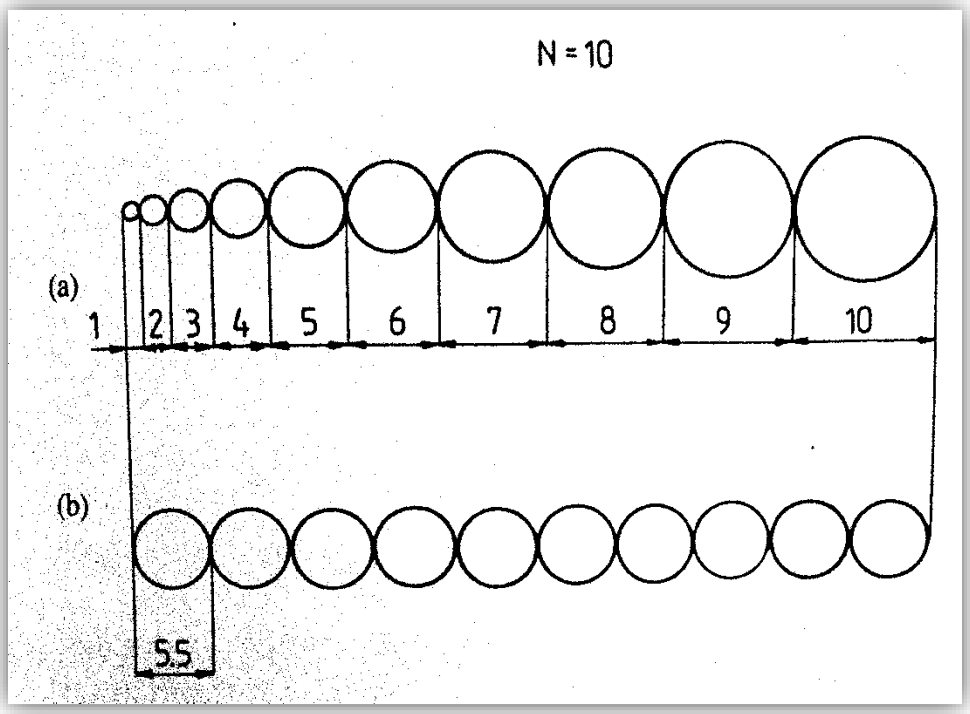


*Figure 14 showing sets of drops: (a) non-uniform set; (b) set equivalent with respect to drop number and size. [35]*

For heat and mass transfer applications, the volume-to-surface-area or Sauter mean diameter (SMD) $D_{32}$, is recommended [35] [34]. $D_{32}$ is the diameter of a uniform equivalent droplet set with the same total volume and same surface area of all droplets in the real set. For pressure swirl simplex atomizers, the complexities of the various physical phenomena involved during atomization have led to the use of empirical correlations to report expressions for the SMD. One such correlation was reported by Lefebvre and agrees well with experimental findings [34].

$$D_{32} = 2.25\sigma^{2.25}\mu_L^{0.25}m_L^{0.25}\Delta P_L^{-0.5}\rho_A^{-0.25} \tag{35}$$

Where $\Delta P_L$ is the pressure drop across the nozzle and $\rho_A$ is the density of the ambient gas into which the liquid is sprayed.

**Spray sheet thickness**

It had been mentioned that the liquid emerges from the discharge orifice of the pressure swirl simplex atomizer as a hollow cone which then breaks down due to various destabilising forces. The thickness of the conical sheet formed is an important characteristic that is used to calculate various aspects of the atomisation process such as the heat and mass transfer that may take place. As with the SMD, various empirical correlations have been reported to calculate this. Of note is the empirical relation reported by Rizk and Lefebvre [34];

$$t = 3.66\left(\frac{d_o \dot{m}_L \mu_L}{\rho_L \Delta P_L}\right)^{0.25} \tag{36}$$

Where $d_o$ is the nozzle discharge diameter.

**Cone angle**

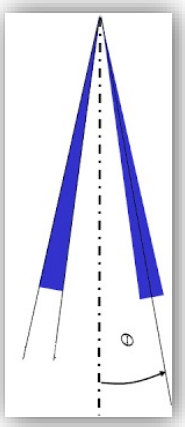


*Figure 15 showing the spray cone angle θ.*

The cone angle, sometimes referred to as the spray angle is the apex angle of the spray. As the distance from the discharge orifice is increased the spray narrows or curves inside due to the action of the ambient gas which starts to move as the liquid is ejected [35]. The spray angle can therefore only be uniquely determined in a vacuum. However, it has been observed through experiment that the cone angle is a function of the nozzle dimensions, physical properties of the liquid and the density of the medium in which it is sprayed. The individual effects of each of these has been studied and correlated. Of particular application in this work is the correlation reported by Rizk and Lefebvre [34] which represents the cone angle as a function of the nozzle discharge orifice diameter and sheet thickness.

$$\cos^2\theta = \frac{1-X}{1+X} \tag{37}$$

Where X denotes the ratio of the air core size and the nozzle discharge orifice diameter and is given by;

$$X = \frac{\left(d_o - 2t\right)^2}{d_o^2} \tag{38}$$

## 2.6.3 Spray devices used in Eskom

It was noted in section 2.3.4 that the deaerators used in Eskom power stations have different spray devices in the first deaeration stage. Table 2 shows each of the power stations visited together with the types of spray devices installed in the deaerators. These spray devices are briefly described in the following sections.

*Table 2: Eskom power stations visited and the respective spray devices in the deaerator types installed*

| ***Power Station*** | ***Deaerator type*** | ***Spray device*** |
|---|---|---|
| | | |
| *Plant 3* | *Tray type* | *Chinese head* |
| *Plant 4* | *Tray type* | *Simple pipe* |
| *Plant 5* | *Tray type* | *Perforated pipe* |
| *Plant 2* | *Stork type* | *Stork disc sprayer* |
| *Plant 1* | *Tray type* | *Spring loaded water distributor* |
| *Plant 6* | *Tray type* | *Spring loaded water distributor* |

From the six power stations visited, five types of spray devices were encountered. The spray devices can be categorised into two classes.

1. Fixed geometry spray devices
2. Variable geometry spray devices

**Fixed geometry spray devices**

The fixed geometry spray devices class contains those spray devices for which the geometry is fixed and is independent of the operating conditions. The Chinese head, simple and perforated pipe spray devices fall into this class. The Chinese head essentially consists of a pipe section attached to a plate on one end (Figure 16).

The main condensate passes through the pipe and hits against the plate before being introduced into the first deaerating stage. By so doing, the kinetic energy of the water is used to break up the water. The atomization quality achievable using this device is not clear and its occurrence in

literature is very limited. The device is also used to introduce high pressure feedwater drains into the feedwater tank.

*Figure 16: Chinese head spray device*

The simple pipe is strictly speaking not a spray device but merely a means of introducing water into the deaerator. Since no atomization can be achieved using this device, the main condensate is effectively introduced directly onto the deaerating trays without any atomization. It means therefore that in deaerators fitted with this technology, all the deaeration occurs in the second deaerating stage.

The perforated pipe spray device is fairly self-explanatory from its name and is simply a pipe with a multitude of holes on its outer surface. The main condensate is forced out of these holes and into the first deaeration stage. Depending on the size of the holes, the operating conditions and the thermodynamic properties of the water, an effect similar to that observed for jet atomizers may be achieved at each hole – thereby achieving an appreciable overall amount of atomization.

**Variable geometry spray devices**

The variable geometry spray devices class contains those devices whose geometry changes according to the operating conditions. This is probably done in order to keep the pressure drop across the device constant and perhaps low. The spring loaded water distributor and stork disc sprayer fall into this class.

The spring loaded water distributor consists of a shaft with a disc on one end and a spring on the other end (Figure 17). During operation the main condensate (blue arrows) pushes down the disc

and is introduced into the first deaerating stage via the annular orifice created. This forcing of the disc downwards compresses the lower spring and elongates the upper spring to which the shaft is connected. The resultant effect is that the springs oppose the movement of the disc and minimize the size of the orifice. The main condensate therefore forces itself out through the annular orifice as a conical sheet which later disintegrates as discussed in section 2.6.1.

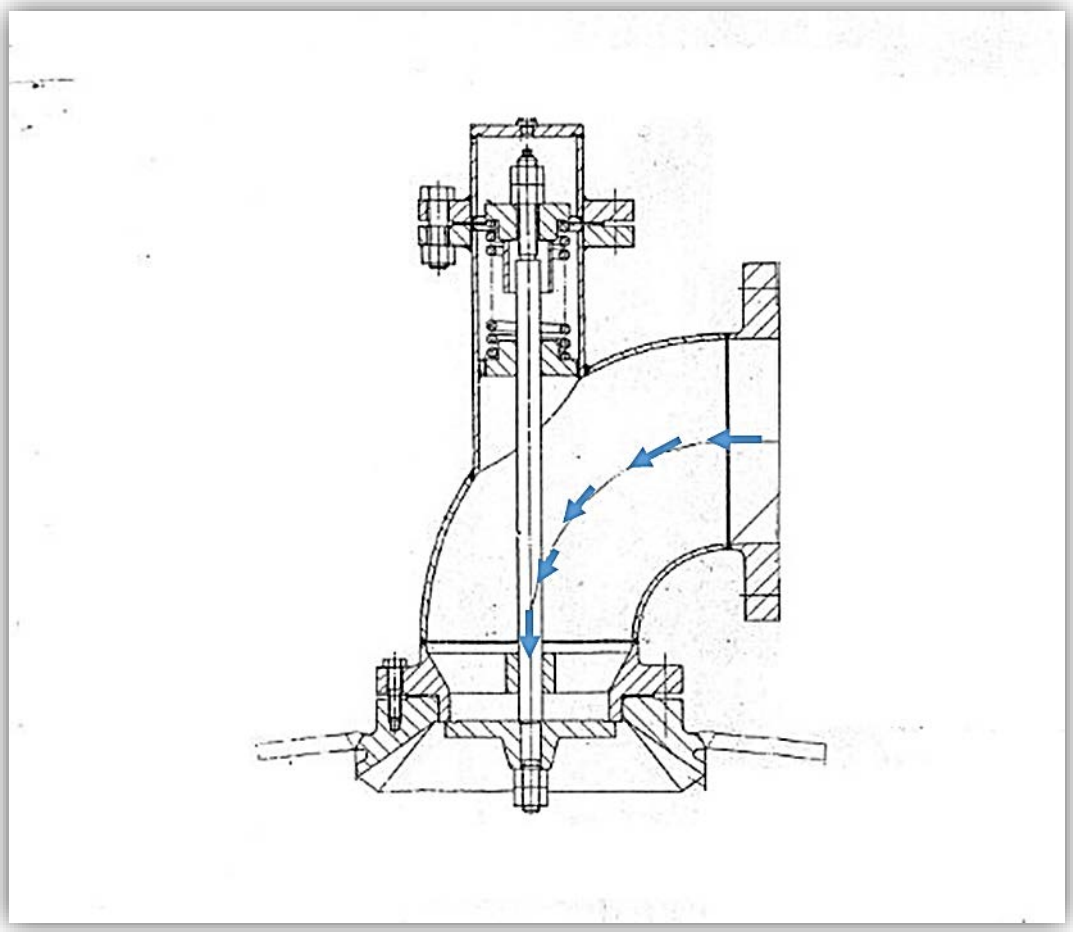

*Figure 17: Spring loaded water distributor [38]*

The stork disc sprayer is fitted in stork type deaerators and essentially consists of the following functional features;

- Spring discs
- Spacer rings
- Tie rods
- Flow distributors
- Outer casing

The sprayer is formed by installing a certain number of pairs of flexible spring discs on top of one another. The individual pairs of discs are clamped between perforated spacer rings such

that the edges of the two discs are pressed together at an initial stress when the system is in a state of rest. The discs and the spacer rings are braced together via tie rods to form a stack construction (Figure 18). A flow distributor is built into the sprayer and serves the task of evenly distributing the main condensate between the discs. This whole assembly is installed in a casing which is attached to the main condensate inlet, high pressure drains inlet, and to the deaerator vessel itself.

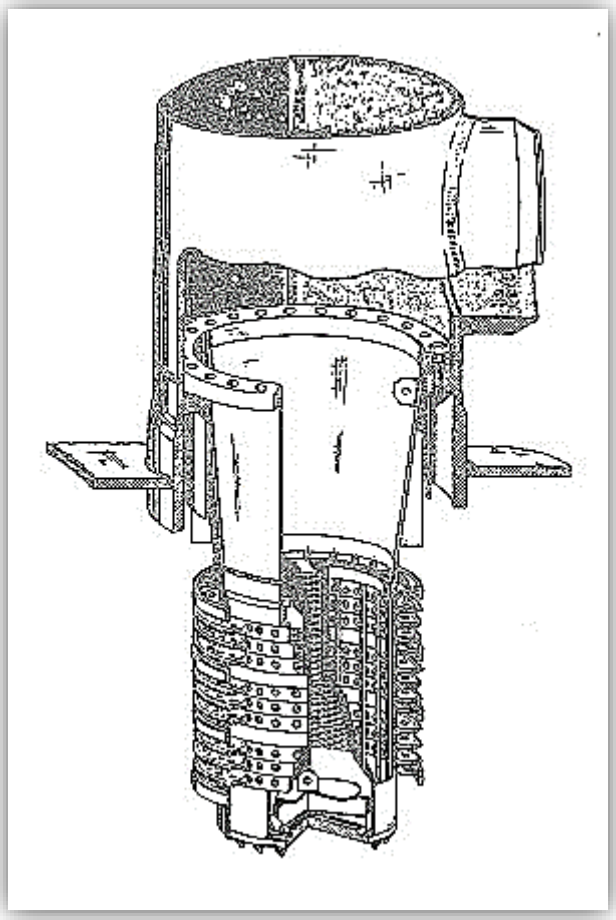

*Figure 18: Stork disc sprayer [39]*

During operation the main condensate and high pressure drains are introduced into the flow distributor through the casing. The water is then evenly distributed amongst the flexible disc pairs and forces a gap between the discs from which the water issues as a screen. Provided that the pairs are oriented correctly, a spray sheet of constant density is produced [39]. Through factors similar to those described for sheet disintegration is section 2.6.1, the sheet then breaks down into ligaments and finally into droplets.

Although there are many spray devices used in industry and in Eskom power stations, it was decided due to time and feasibility constraints to focus only on pressure swirl simplex atomizers as

these are commonly encountered in modern deaerators and the literature pertaining to their functionality and design is accessible. The types of spray devices described in this section will therefore not be considered any further.

## 2.7 Closing remarks

In this chapter the foundation of the material presented and used in the following sections is laid down. It was established that two types of deaerators are commonly used in industry and in Eskom power stations. These are the tray and spray type deaerators. The functionality and operating principles of the two deaerator types are similar and the first deaerating stage is identical.

It was established that the first deaeration stage plays the dominant role in the deaeration process and is responsible for over 90% of the heating and deaeration. A closer look into this first stage revealed that the main features of this stage are the spray devices or nozzles that are used to break down the water into small droplets in order to increase the rates of heat and mass transfer. Consequentially, the fundamental aspects of both heat and mass transfer and nozzle performance were explored and correlations pertaining to the transfer of mass from falling droplets, and nozzle characteristics and performance were presented.

These relationships and principles, together with others presented in the next chapter form the basis of the methodology that was finally adopted for the purpose of this work.

# 3. Literature Review

The purpose of this chapter is to present and review literature pertaining to the modelling of deaerators. The chapter begins by presenting and reviewing two mathematical deaerator models that were developed by Opris and Ferro et al respectively. Following that, two studies concerning heat and mass transfer in deaerators will be presented, after which the chapter will be concluded.

## 3.1 Previous mathematical models of deaerators

The general trend in deaerator modelling has been to treat the equipment as a simple direct contact heat exchanger and neglect the NCG extraction behaviour of the system. This might be due to the significant role played by the deaerator as a direct contact FWH and storage tank. It is possible that the performance of the deaerator in these processes is deemed more important than the removal of potentially harmful NCGs from the boiler feedwater. That being said, other researchers have included the NCG extraction behaviour of the devices in their models.

Two mathematical deaerator models are presented and reviewed in the following sections. It shall be observed that without alterations, neither modelling approaches was deemed satisfactory for use in this study due to inaccurate or missing NCG extraction information. However, the methodology finally used in the present study was inspired and drawn from a combination of different qualities adopted from the two studies in conjunction with the heat and mass transfer considerations presented at the end of this chapter.

### 3.1.1 The Opris model

Opris [1] developed a transient mathematical model of a deaerator in 2013 using the Advanced Continuous Simulation Language (ACSL). The model was successfully implemented by simulating a turbine shut down scenario for a 50MW power station.

The specific type of deaerator modelled was not stated in the work, “A deaerator model”, but images presented in the work suggest that it was a tray type deaerator with two inlet streams (main condensate and bled-steam) and one outlet stream (deaerated water). The mathematical background of the model was based on solving the conservation equations of mass and energy in one dimension together with some other relations that link the parameters.

**Model description**

The Opris model was developed in consideration of the following assumptions and simplifications;

- The liquid water and vapour phases exist in equilibrium inside the deaerator.

- There is the same pressure in the deaerating section and storage tank.
- The deaeration process is determined exclusively by the water heating process.
- There is variation in the water level in the tank as an effect of the varying input and output streams.

The following were neglected in the development of the model

- All effects of NCGs.
- The variation of the concentration of gases in the steam.
- The heat loss through the walls.

The inputs to the model were the mass-flow rates, temperatures and pressures of the inlet streams and the mass-flow rate of the deaerated water. The outputs of the model were the temperature and pressure of the outlet stream, together with the enthalpies of all the streams and the contents of the storage tank. The model also calculated the level inside the deaerator tank by assuming that the variation of the level is linearly related to the volume of the condensate. It is worth noting that this approach is only valid for vertical tanks and therefore it is assumed, contrary to the image presented in the literature, that the deaerator modelled was connected to a vertical storage tank. Figure 19 shows the algorithm used by Opris in developing the model.

**Critical review**

The general approach followed by Opris [1] in the development of the model stems from the fundamentals of thermal-fluid component modelling and is therefore valid and can be adopted as a starting point for the purpose of this study. However, there are a few areas in the model or model development that could be improved in order to make the methodology followed entirely applicable to this study;

- Firstly, the inputs to the Opris model do not represent inputs that the typical deaerator operator and users of the results of this study would possess. For example the bled steam mass flow rate. In actual fact, the bled steam mass flow rate is usually an output of the model dictated by various factors including the vent steam mass-flow rate [7].
- Secondly the model neglects the deaerator vent characteristics. Although this is a common practise even prescribed by some text book authors [5], it does mean that the deaerator model fails to capture an important characteristic of the equipment that can be used to optimise its performance and reduce operational costs [18]. Typical deaerator operators are in the habit of opening the deaerator vent valve to its maximum position in an attempt to rid the deaerating section of all NCGs [22]. Although this does indeed remove all NCGs from the deaerating dome, it also represents a waste in steam that could have otherwise been used to heat incoming feedwater and this inadvertently translates to financial loses

in the long run [22], especially if the steam is vented to the atmosphere instead of being recovered in a re-condensing device.

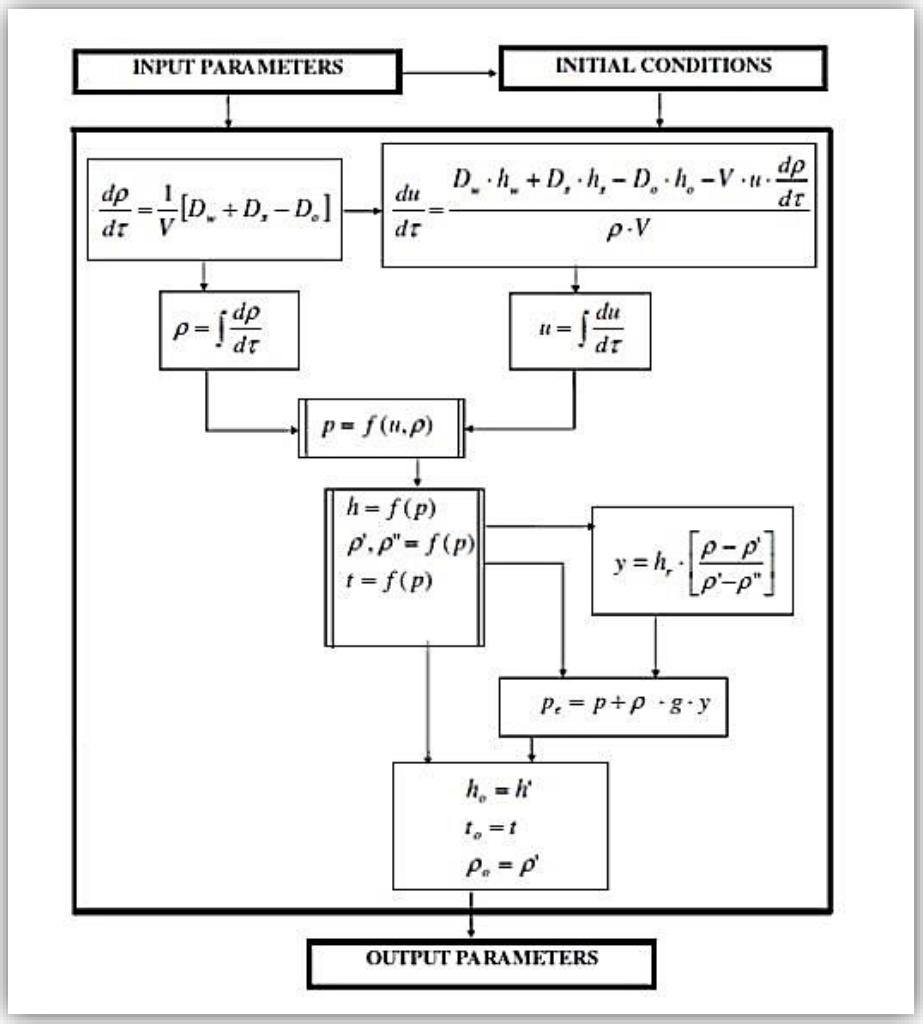


*Figure 19: Modelling algorithm for the Opris deaerator [1]*

- Thirdly the Opris deaerator model neglects the mass transfer characteristics of the equipment. Although the mass transfer characteristics of the equipment do not significantly affect the role of the deaerator as a water reservoir and FWH, it is after all what deaerators are designed and installed for. If a complete model of the equipment is to be developed, it is imperative therefore, that the major role for which the equipment is made for be captured. Accurately predicting the NCG extraction behaviour of the system has many advantages, including knowing exactly how much oxygen scavenger to use in order to avoid unnecessarily using too much scavenger and losing out financially.

## 3.1.2 The Ferro et al model

Ferro et al [4] developed a computer model of an Abu Dhabi National Oil Company (ADNOC) desalination plant deaerator using the FORTRAN software package. The model was developed in an attempt to seek an understanding of the flash and stripping phenomena inside the deaerator after a suspicion of an over design or non-optimised management of the deaerator. The model was run against the deaerators design specifications and the suspicions were confirmed.

The deaerator modelled, Figure 20, is a combination of the flash and vacuum type deaerators described in section 2.3.2. The deaerator consists of two deaerating sections. Water is sprayed through a sprinkler pipe into the first empty space. The expansion from a higher to a lower pressure guarantees flash separation [4]. The water then drops onto a corrugated plate which redistributes the liquid onto the packing. This is the second deaerating section. Stripping steam is fed from underneath the packing section and comes into contact with the falling liquid in a counter-current fashion and strips the water of the NCGs dissolved in it.

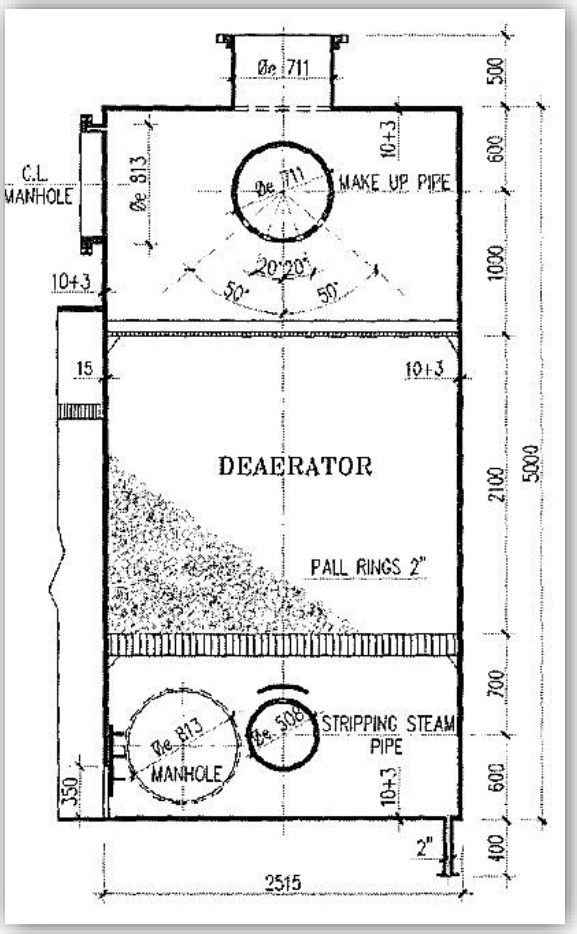


*Figure 20: Simplified schematic of the ADNOC plant deaerator [4]*

**Model description**

In terms of mass transfer equipment modelling, the deaerator was modelled as a stripping tower using the ideal-stage model type approach. The model is based on solving the conservation equations of mass, energy and momentum together with thermodynamic equilibrium relations for each stage. The principle assumptions made are;

- The stripping steam and feedwater are in thermodynamic phase equilibrium in the flash section of the deaerator.
- A "flash" efficiency of 0.986 has been included to account for the inaccuracy of the first assumption.

For the first part, the flash box, both Henry's and Raoult's laws were used to estimate the phase equilibrium whereas Henry's Law was used in the second part, which is the stripping section. Both these thermodynamic relations were presented in Chapter 2. The inputs to the model are the operating pressure of the deaerator, characteristics of the water (salinity, inlet temperature and total mass flow-rate) and stripping steam (inlet temperature and total flow rate) and geometric characteristics of the deaerator (length, width, total packing and ring size, theoretical stage efficiencies and numbers etc.). The outputs of the model are the water and steam temperatures and flow rates at the deaerator outlet, steam velocity, wetting flow rate, pressure drops and flash temperature, vapour pressure and the NCG concentration in the water and steam at the flash and stripping outlet sections.

**Critical review**

The model developed by Ferro et al is based on sound physics and mathematical principles and is highly detailed and fairly complex. The level of complexity achieved is made possible by the availability of the detailed design information of the deaerator e.g. theoretical stage efficiencies. It appears the model developed can capture most of the characteristics of the deaerator system modelled and can be applied usefully to the task that it was developed for. However, there are a two points that make the approach followed by Ferro et al difficult and perhaps impossible to apply to the current work. These are as follows.

- For a systems level model developed mainly from historical performance data, most of the inputs required for the development of this sort of model would be unavailable. It would require perhaps, detailed drawings of the deaerator, the type of which manufacturers are reluctant to share with deaerator users.
- It may have been noticed that this type of deaerator has no vent stream. This is because the stripping steam does not condense around the feedwater droplets as is the case with previously described deaerators. Instead, the steam-NGC mixture issues from the top of

the deaerator and is presumably used for other processes not documented in this literature. This makes it significantly simpler to implement an ideal-stage model type approach because the mass flow rates of the water and steam streams are generally constant. In the case were condensation of the steam around the water droplets takes place, many changes will have to be made to the way the concentrations have been evaluated and so this literature would require appreciable modifications in order to be applied to the current work.

The last point is not to discredit the usefulness of the literature as it plays the vital role of illustrating how the mass transfer models discussed in section 2.5.3 can be implemented in a deaerator type situation. It was unfortunate that the author did not find literature pertaining to the development of deaerator models using the mass transfer rate-based approach. The lack of design data pertaining to stage efficiencies of any kind for the deaerators modelled in this work made it necessary to follow the rate based approach.

## 3.2 Heat and mass transfer in deaerators

It was presented in section 2.3.1 that thermal deaeration is essentially a process of simultaneous heat and mass transfer. The current section deals with these two transport processes by considering previous works that have been done concerning heat and mass transfer in deaerators or similar devices. To start with, the treatment of heat transfer in spray condensers as prescribed by the VDI Heat Atlas [40] will be presented. This will be followed by a presentation of the work carried out by Sharma et al [41] [42] [43]concerning mass transfer in deaerators.

### 3.2.1 Heat transfer in deaerators

It has been stated that thermal deaerators consist of two deaerating stages, the first of which is called the preheater. Due to the very high rates of heat and mass transfer characterising this stage, it can be assumed for analysis purposes that the steam condensation and NCG desorption is complete once the droplets reach the second stage [6]. This means therefore that it is possible, without much error, to consider only the heat and mass transfer processes in the preheater section when analysing deaerators.

In light of this fact, the subject of mixing and spray condensation becomes useful in determining the heat transfer characteristics of deaerators, as it deals specifically with heat transfer involving spray droplets. This topic has been presented in the VDI Heat Atlas with a particular focus on spray condensers. By definition, spray condensers are condensers in which the steam to be condensed is

immediately brought into direct contact with the cooling medium [40]. This definition can be extended to the preheater stage of a thermal deaerator if the following idealisations are made;

- The “steam to be condensed” is the bled steam from the turbine and,
- The “cooling medium” is the feedwater flowing through the deaerator.

The remainder of this discussion will be tailored for deaerators subject to the above listed idealisations. The ideas are drawn directly from the VDI Heat Atlas for spray condensers and merely applied here to deaerators.

For large scale industrial applications the following assumptions can be made;

- The gas phase resistance to heat transfer is negligible compared to the liquid phase resistance i.e. the steam heat transfer coefficient is very high.
- The analysis of deaerators can be restricted to the consideration of heat transfer in the liquid phase only [40].
- The temperature on the phase boundary is equal to the saturation temperature of the bled steam once the feedwater and steam are brought into contact.
- The growth of the water droplets due to condensation can be neglected if the difference between the feedwater inlet temperature and the saturation temperature of the steam is less than 100K. (The most popular theories assume that the radius of the drops will be constant and the heat transfer in the resulting layer is negligible [40]).
- The spray droplets do not influence each other and there is no secondary atomization.

Subject to the assumptions detailed above, the heat transfer to the spray droplet is calculated in the same way as thermal conduction in a rigid ball. Only the important equations will be shown here.

The temperature of the ball is constant for time $t<0$ and the surface temperature is equal to the saturation temperature of the steam at $t>0$. In order to quantitatively describe the heat transfer, the dimensionless temperature is defined as;

$$\theta = \frac{T - T_{in}}{T_s - T_{in}} \tag{39}$$

Where

- $T$ is the bulk temperature in K.
- $T_{in}$ is the inlet temperature in K.
- $T_s$ is the saturation temperature in K.

If the droplet surface is in thermal equilibrium with the surrounding steam, the dimensionless mean temperature of the droplet can be expressed as;

$$\theta_m = 1 - \frac{6}{\pi^2}\sum_{n=1}^{\infty}\frac{1}{n^2}e^{-n^2\pi^2 Fo} \tag{40}$$

With the Fourier number

$$Fo = \frac{k \cdot t}{\rho c_p r^2} \tag{41}$$

Where

- $k$ is the liquid thermal conductivity in W/m$^2$ K.
- $c_p$ is the specific efficient heat capacity of the steam in J/kg K.
- $\rho$ is the liquid density.
- $r$ is the droplet radius.
- $t$ is the time, with t=0 as the droplet enters the steam space.

The sum in equation (40) converges rapidly but it is simpler in practical applications to use a proximity equation to determine the average temperature. This is given by;

$$\theta_m = \sqrt{1 - e^{-\pi^2 Fo}} \tag{42}$$

This proximity equation deviates from the exact solution according to (40) by less than 0.02. The relationships presented here will be used in the following chapter to determine the time taken to heat the FW inside the deaerator.

### 3.2.2 Mass transfer in deaerators

Most mass transfer equipment such as stripping columns, bubble tanks and packed columns have well established common relations that can be used to evaluate their mass transfer parameters. The same cannot be said for deaerators unfortunately. Some researchers have looked at mass transfer during deaeration from a rate-based perspective and the work of Sharma et al stands out as being the only validated resource available to the author. In their work, Sharma et al experimentally studied mass transfer of oxygen in the first and second stages of deaerators [42] [43], and the role of droplet diameters on the mass transfer inside the deaerator [41]. A summary of their studies is presented in the next section.

**Sharma et al study summary**

The researchers experimentally investigated different aspects of the deaeration process and compared their findings to analytical solutions. The deaerator studied was of the tray type with a pressure-swirl simplex atomizer producing a conical sheet of the geometry shown in Figure 21.

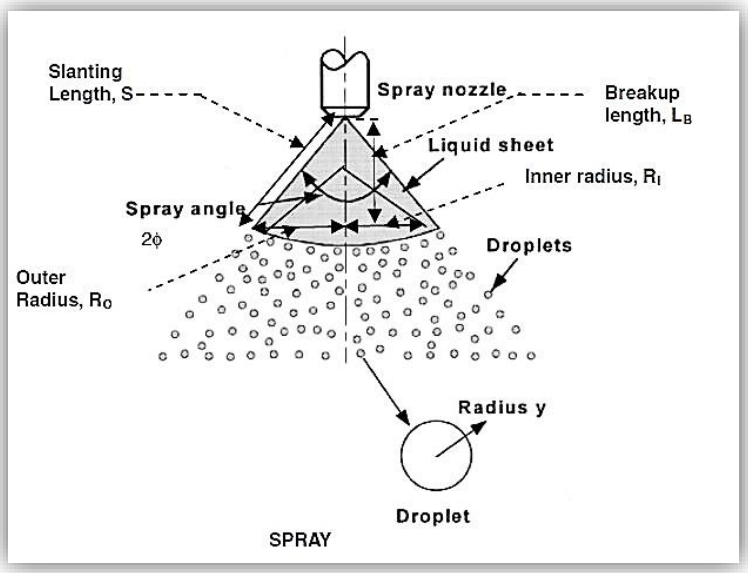


*Figure 21: Ensuing spray from a pressure swirl simplex nozzle in the first deaeration stage [43]*

The process of oxygen transfer from the feedwater to the steam was theoretically formulated as one related to the diffusion of oxygen from the centre of the water droplet to its surface subject to the following conditions and assumptions;

- The configuration of a droplet is a perfect sphere.
- The major resistance to diffusion is within the droplet and the resistance decreases as the temperature of the water droplets increases.
- The resistance for diffusion of the water-steam interface to the steam bulk phase is negligible.

Using the Two film theory, the MTC in the preheating section was evaluated from the Sherwood number using Treybal and Steinberger's equation reshown here for convenience. The low solubility of oxygen in water made it possible to equate the overall MTC to the liquid side MTC for reasons described in section 2.5.2.

$$Sh_d = Sh_0 + 0.347(\mathrm{Re}_d\, Sc_d^{0.5})^{0.62} \quad (43)$$

Where;

$$Sh_0 = 2 + 0.569(GrSc)^{0.25}, GrSc \leq 10^8 \quad (44)$$

$$Sh_0 = 2 + 0.0254(GrSc)^{0.25}\,\mathrm{Sc}^{0.244}, GrSc \geq 10^8 \quad (45)$$

To evaluate the droplet surface area and volume, the diameter was obtained from Domborowski and Munday's equation

$$d = 0.0134 \frac{FN^{0.209} \left(\frac{\mu_L}{\rho_L}\right)^{0.215}}{(-\Delta P)^{0.348}} \quad (46)$$

Where the flow number FN, for a hollow cone nozzle is given by;

$$FN = 2.08x10^6 \frac{m_L}{\rho_L \sqrt{P_{dea}/1000}} \quad (47)$$

Where;

- $m_L$ is the feedwater mass flow rate in kg/s.
- $\rho_L$ is the feedwater density in kg/m$^3$.
- $P_{dea}$ is the deaerator pressure in Pa.
- $\mu_L$ is the feedwater viscosity in kg/m s.
- $\Delta P$ is the pressure drop across the nozzle in Pa.

With the above quantities established, the oxygen continuity equation was solved on the liquid phase (FW).

The obtained results were successfully compared with those obtained from the experimental set up. In addition, the results reported also showed various trends between some parameters of interest e.g. the effect of increasing the feedwater mass-flow rate on the MTC. These results will be shown in the next chapter were they are used to validate the mass transfer characteristics of the model developed in this work.

## 3.3 Closing Remarks

In this chapter two mathematical models of deaerators were presented and reviewed. It was shown that neither modelling approaches followed could be implemented without modifications being made.

It was decided that the methodology applied by Opris [1] could be adopted for use in this study provided that appropriate modifications were made in order to in cooperate the NCG removal characteristics of the equipment. Such modifications would involve using the findings of Sharma et al [41] [42] [43] concerning mass transfer in deaerators, and the VDI heat atlas [40] concerning

heat transfer in spray condensers to formulate a methodology that can be used to calculate the NCG extraction characteristics of the deaerator system.

The methodology resulting from these modifications is presented in the following chapter.

# 4. Analytical Model Development and Validation

This chapter details the development and validation exercises performed on the analytical model. The chapter starts off by giving an outline of the model development, highlighting the mathematical relations and simplifications that make up the model. It then progresses to describing how key parameters and values needed to solve the mathematical relations are established or derived. This step then leads on to a summary of the model, which is followed by a detailed presentation of the validation exercises which were performed.

## 4.1 Model development

The analytical model is primarily based on solving the steady state mass and energy conservation equations using unidirectional geometry and concentrated parameters around the deaerator boundary as was done by Opris [1]. In addition, the continuity equation for oxygen diffusion from a falling droplet is solved as was demonstrated by Sharma et al [43] with the aid of some simplifications derived from the works presented by the VDI heat atlas [40]. As a means to allow for one more unknown to be solved for, the model also solves the one dimensional momentum equation for the vent pipe. For the purposes of this study, it was established that the most common and dominant NCG was oxygen, and it was therefore used as a representative gas for all NCGs. From a high level standpoint, the core of the model consists of three separate sections namely, the inputs, executions and outputs section. The three sections are described in turn below.

### 4.1.1 Inputs

The inputs to the analytical model can be further grouped into four classes depending on the nature of the information they provide. The four classes are presented below together with a brief description of the constituents of each class.

**Process inputs**

This class contains those inputs required to solve the mass and energy conservation equations for the bulk deaerator system. Functionally, these are;

- The mass flow rates of the main and return condensate streams and,
- The specific enthalpies of the main condensate, return condensate and bled steam streams.
- The bled steam inlet pressure.

Given that enthalpy values cannot be directly measured during normal operation and that more thermodynamic properties will be needed elsewhere in the model, any two thermodynamic properties can be defined for each stream. The two properties will then be used in the model to establish the enthalpy and other thermodynamic properties of the respective stream. The process inputs values must be at the physical boundary of the deaerator such that the effects of all connecting elements, such as pumps and valves, are eliminated as these are outside the scope of this work. Should the data available be at points other than the physical boundary of the deaerator, an appropriate pre-processing exercise should be performed to make the data usable. One example of such an approach will be shown in the case study performed to validate the analytical model.

**Chemical properties of water and oxygen**

This inputs class contains the chemical properties of both water and oxygen that are required to solve the continuity equation for oxygen diffusion from a falling droplet. These include the inlet oxygen concentration and are used to compute important characteristics of the mass transfer operation that governs deaeration.

**Deaerator design features**

These inputs provide information pertaining to the physical design of the deaerator system being modelled. One important aspect is the type of nozzle(s) used by the deaerator. This aspect determines the relations that will be used to solve the oxygen continuity equation. Although many different designs for spray atomizers are available, it was decided in this study, to use relations applicable to pressure swirl simplex atomizers. This choice was based on the fact that simplex atomizers are fairly widespread and have been sufficiently documented in literature. Other atomizer types are relatively new technologies and most of the information related to their design and performance is difficult to obtain. The minimal design features that need to be declared are;

- The length of the preheater section.
- The pressure loss characteristic for the vent pipe.
- The number and dimensions of the spray nozzles.
- The design spray angle of the nozzle.

The last feature is relatively difficult to declare as some nozzle specific calculations need to be performed beforehand. For the purposes of this study, it was chosen to use a constant spray angle of 60 degrees as it has been shown to be the most efficient for pressure swirl nozzles. If other types of nozzles are used, the required inputs might need adjustment.

**Miscellaneous inputs**

The rest of the inputs required to make the model work are defined under this class. These include ambient conditions of temperature and pressure along with ambient values for Henry's Law constant.

The outputs section of the model is discussed next. This is merely done for clarity and does not reflect on the sequence of the sections in the actual model.

### 4.1.2 Outputs

The functional goals of the analytical model are to;

1. Use analytical approaches to solve the steady state mass and energy conservation equations for the bulk system. In addition the model solves the momentum conservation equation for the vent pipe, and therefore fully defines every stream crossing the deaerator boundary in terms of its mass flow rate and thermodynamic properties (Figure 22) and to,
2. Determine the outlet concentration of oxygen in the deaerated water.

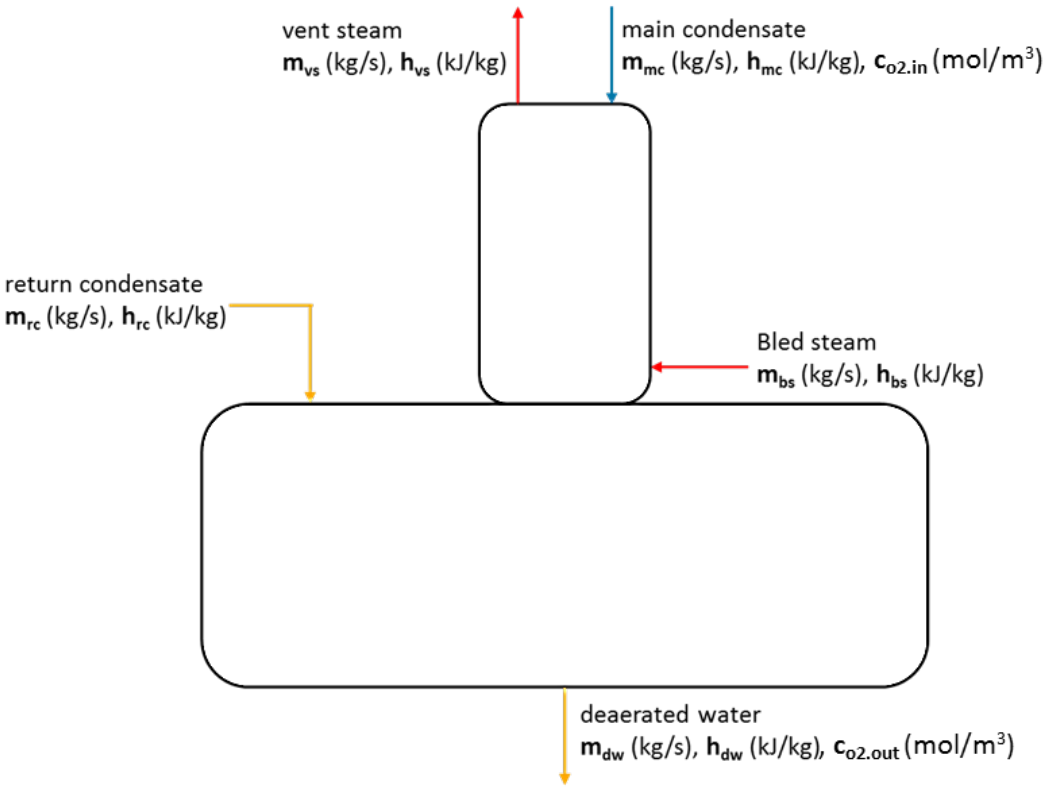


*Figure 22: Simple deaerator schematic showing the desired outputs of the analytical model.*

With regards to the first functional goal, only three output values can be calculated since only three conservation equations are solved. The vent steam mass flow $m_{vs}$ is determined using momentum conservation, the bled steam mass flow rate $m_{bs}$ using energy conservation, and the

deaerated water mass flow rate $m_{dw}$ using mass conservation. The enthalpy values for the vent steam and deaerated water streams are not inputs to the model but are needed in order to solve the conservation equations. These two values are calculated within the model based on assumptions that will be stated in the Execution section description.

### 4.1.3 Execution

**Solving the conservation equations**

The vent steam mass flow rate is calculated from momentum conservation, knowing the pressure drop characteristics of the vent outlet using equation(48).

$$m_{vs} = \sqrt{\frac{\Delta P_{vp} \cdot \rho_{vp}}{C_{K.vp}}} \tag{48}$$

Where $\Delta P_{vp}$ is the pressure drop across the vent pipe, i.e. the difference between the deaerator vessel pressure and the vent outlet pressure, which is very often simply the atmosphere. $C_{k.vp}$ is the pressure loss coefficient of the vent pipe, determined from the pressure drop characteristics of the vent.

Given that all necessary inputs are specified, the model rearranges and solves equations (49) and (50) simultaneously to find the two remaining unknowns.

$$m_{mc} + m_{drains} + m_{bs} = m_{dv} + m_{dw} \tag{49}$$

$$m_{mc}h_{mc} + m_{drains}h_{drains} + m_{bs}h_{bs} = m_{dv}h_{dv} + m_{dw}h_{dw} \tag{50}$$

The calculations are done subject to the following assumptions and simplifications in addition to those made by [1]:

1. There is a negligible pressure drop as the bled steam enters the deaerator such that the deaerator pressure is equal to the bled steam pressure.
2. The deaerating dome and feedwater tank are under similar thermodynamic conditions and can be treated as one vessel.
3. The vent steam enthalpy is the enthalpy of saturated vapour at the deaerator pressure. The energy contribution of the vented NCGs is thus assumed to be negligible.
4. The deaerated water enthalpy is the enthalpy of saturated liquid at the deaerator pressure.

Note that items (3) and (4) imply that the enthalpies of the vent stream and deaerated water streams need not be declared as inputs as they can be calculated internally in the executions section.

**Solving the oxygen continuity equation**

In order to determine the outlet oxygen concentration, the model solves the continuity equation for oxygen diffusion from a falling droplet. According to [43], assuming that there is no oxygen in the bled steam, the component continuity equation for oxygen diffusing from a spherical droplet can be written as;

$$\frac{d\omega_{o2}(t)}{dt} = -6\frac{Sh \cdot D_{o2.mc} \cdot \omega_{o2}(\mathrm{t})}{D_{32}^2} \tag{51}$$

Where $\omega_{o2}$ is the mass fraction or concentration of oxygen in ppb. In order to solve for the outlet concentration of oxygen after deaeration, equation (51) is rearranged and integrated to produce:

$$\omega_{o2}(t) = \omega_{o2.in} e^{-6\frac{Sh \cdot D_{o2.mc}}{D_{32}^2} \cdot t_{mt}} \tag{52}$$

From the above equation it is clear that the following parameters need to be known before a solution can be evaluated;

- Inlet concentration of oxygen $\omega_{o2.in}$
- The diffusivity of oxygen in water $D_{o2.water}$
- The droplet diameter $D_{32}$
- The time available for mass transfer $t_{mt}$ and,
- The Sherwood number *Sh*

The relations and processes used by the model to determine each of the above parameters are detailed below.

**Inlet oxygen concentration:** the inlet oxygen concentration is ideally an input to the model. However, should this value be unknown, the maximum possible concentration of oxygen in the incoming condensate can be computed using equation(53) . This is based on the assumption that the incoming condensate will be saturated with atmospheric oxygen.

$$\omega_{o2.in} = R_{con} \cdot M_{o2} \cdot mf_{o2.air} \cdot P_{mc} \cdot K_H(T_{mc}) \tag{53}$$

Where

$$R_{con} = 1 \times 10^6 \frac{m^3}{kg} \tag{54}$$

And Henry's law constant at any temperature is given by the following relationship [44].

$$K_H(T) = K_{H\theta} e^{\left[1700 \cdot K \cdot \left(\frac{1}{T} - \frac{1}{T_\theta}\right)\right]} \tag{55}$$

Where $K_{H\vartheta}$ represents Henry's law constant at ambient conditions and $T_{\vartheta}$ represents the temperature at ambient conditions.

**Oxygen diffusivity in water**: the following relation recommended by Wilke and Chang is used to evaluate the diffusivity of oxygen in water [28];

$$\frac{D_{o2.mc}\mu_{mc}}{T} = \frac{117.3x10^{-18}(\Phi_{mc}\cdot M_{mc})^{1/2}}{Vm_{o2}^{\ 0.6}} \tag{56}$$

Where

- $\Phi_{mc}$ is the solvent association parameter for the main condensate.
- $M_{mc}$ is the molecular weight of the main condensate in g/mol.
- $Vm_{o2}$ is the molal volume of oxygen at the normal boiling temperature in $cm^3$/mol.
- $\mu_{mc}$ is the viscosity of the main condensate in centipoises.
- $T$ is the temperature of the mixture in K.

**Droplet diameter:** The average droplet diameter used was the Sauter Mean Diameter, which according to Rizk and Lefebvre is recommended for mass transfer applications and for pressure swirl nozzles can be evaluated using the following experimentally corroborated correlation [34];

$$D_{32} = 2.25\sigma_{mc}^{2.25}\mu_{mc}^{0.25}\dot{m}_{mc}^{0.25}\Delta P_{mc}^{-0.5}\rho_{steam}^{-0.25} \tag{57}$$

**Time available for mass transfer:** The time available for mass transfer was computed based on the assumptions that;

1. Both heating and deaeration operations are completed in the preheater section of the deaerator, regardless of its type, as suggested by [6]. In other words, the contribution of the second section is insignificant. For deaerators with poorly performing nozzles, this assumption may be invalid.
2. The drops are of a constant diameter and do not influence each other as postulated by [40].
3. The water droplets are first heated to the saturation temperature at the deaerator pressure, then deaerated isothermally at that temperature.
4. The breakup length of the conical sheet is short such that the vertical distance travelled by a single droplet is equal to the preheater length.

The third assumption was an attempt to avoid the complicated mathematical manipulation that would be required if both the heat and mass transfer operations were dealt with simultaneously as they occur in real life during deaeration. Such an approach would call for solving a discretized mathematical problem, which is beyond the scope of this study. The assumption made has an

obvious effect on the final result as it over-estimates the effectiveness of the deaeration process. This over-estimation is offset by using a relatively shorter deaeration time as the model assumes that deaeration only starts after the heating is complete.

In order to evaluate the time required for deaeration, the total residence time of a water droplet inside the preheater is first evaluated using equation(58). The evaluation is performed subject to the assumption that the distance travelled by the droplet is very short relative to its speed such that any change in speed due to aerodynamic drag forces, buoyancy and gravity can be ignored.

$$t_{res} = \frac{L_{preheater}}{v_{droplet} \cdot \cos(\theta)} \tag{58}$$

Where;

$$v_{droplet} = \frac{\frac{m_{mc}}{N_{noz}}}{\rho_{noz} A_0 (1 - X)} \tag{59}$$

Based on the reasoning presented above, the residence time, $t_{res}$, is the summation of the time taken to heat the water droplets to saturation $t_{ht}$, and the time taken to deaerate the water $t_{mt}$. In order to evaluate $t_{ht}$, an approach similar to that prescribed by [40] for spray cooling and partly used by [6] on deaerators is followed. Using this approach, the time taken to heat the water to saturation is given by equation (60) subject to the assumptions and simplifications listed in section 3.2.1.

$$t_{ht} = \frac{Fo \cdot c_{p.mc.avg} D_{32}^2 \rho_{mc.avg}}{4 k_{mc.avg}} \tag{60}$$

Where;

$$Fo = -\frac{In\left(1 - \theta_m^2\right)}{\pi^2} \tag{61}$$

The time available for mass transfer is then evaluated by subtracting $t_{ht}$ from $t_{res}$.

**Sherwood number:** The Sherwood number can be evaluated using the correlation suggested by Steinberger and Treybal(62). The other parameters required to compute the dimensionless constants required in the Sherwood number correlations can be obtained from the property tables and the calculations detailed above.

$$Sh = Sh_0 + 0.347(\mathrm{ReSc}^{1/2})^{0.62} \tag{62}$$

Where

$$Sh_0 = 2 + 0.569(GrSc)^{0.25} \; for GrSc \le 10^8 \tag{63}$$

$$Sh_0 = 2 + 0.0254(GrSc)^{0.25} \, \mathrm{Sc}^{0.244} \; for GrSc \ge 10^8 \tag{64}$$

With the above relations defined and calculated, the model then solves equation(52) to determine the oxygen concentration in the deaerated water subject to the simplification that the water droplets are spherical and evenly distributed such that each one is a representation of the bulk water body.

The set of equations used to calculate the outlet oxygen concentration only applies to deaerator systems fitted with pressure swirl simplex atomizers. For any other nozzle type, an equivalent set of relations, specific to that nozzle type, must be used. Owing to the vast number and variations of atomizer designs in industry, no account of these different relations is given in this report. However, the equations likely to change are those concerning the average droplet diameter and the droplet velocity (equations (57) and (59) respectively).

## 4.2 Determination of unknown parameters

The processes reported in section 4.1 assume that all the inputs required for the model to work are available and can be declared in the inputs section. In most cases however, this is not case. Owing to the reluctance of manufacturers to divulge sensitive information about their products, most of the design features of deaerators will be unknown. This is especially true for internal features such as the nozzle dimensions and pressure loss characteristics of all inlets and outlets to the deaerator. In order to get over this hurdle, a calibration exercise may be required.

The calibration methods presented here are primarily targeted towards establishing two parameters of interest;

1. The vent pipe pressure loss coefficient
2. The nozzle discharge diameter

The methods suggested entail establishing the values of these parameters using the process conditions at the nominal load case under which the deaerator is designed to operate optimally. This is normally the 100% or full load case. The inherent requirement of these calibration methods is that all parameters of interest be known at this load condition so that additional relations can be derived and solved. The calibration methods to determine items (1) and (2) above are detailed below.

### 4.2.1 Determination of the vent pipe pressure loss coefficient

The vent pipe pressure loss coefficient should be declared as an input to the model and is used to calculate the vent steam mass flow rate. In the absence of detailed deaerator drawings, this value can be obtained by solving the steady state momentum conservation equation for the vent steam pipe at the 100% load case.

Assuming that the density and elevation differences are negligible and that the vent pipe is of a uniform geometry, the following can be written as a simplified form of the momentum conservation equation for the vent steam pipe;

$$\Delta P_{vp} = K_{vp} \frac{m_{vp}^{\ 2}}{2 \cdot \rho_{vp.avg} \cdot A_{vp}^{\ 2}} \tag{65}$$

Which can be further simplified to;

$$\Delta P_{vp} = C_{K.vp} \frac{m_{vs}^{\ 2}}{\rho_{vp.avg}} \tag{66}$$

Given that all other quantities in equation (66) are known, the pressure loss coefficient $C_{K.vp}$ can be evaluated by rearranging the equation. The value for $C_{K.vp}$ obtained using the 100% process conditions is then assumed to be a constant of the system since the vent pipe does not change, and can be used to determine the vent steam mass flow rate at any other load condition. Once the vent steam mass flow rate is determined, the model can then proceed to solving equations (49) and (50) to compute the bled steam and deaerated water mass flow rates.

### 4.2.2 Determination of the nozzle discharge diameter

The nozzle discharge diameter is an important parameter as it is used to determine the nozzle exit velocity, which in turn is used to compute the Reynolds number and droplet residence time. In order to determine its value from deaerator performance data, a backward calculation from equation (52) is first performed to determine the average droplet velocity. This velocity is then used to solve the continuity equation at the nozzle discharge and hence determine the nozzle dimensions. The equations of interest will be re-written here for convenience.

The principle reasoning behind the approach followed here is that a standard deaerating unit is designed to reduce the oxygen concentration in the feedwater to a maximum value of 7ppb during normal operation. This value is obtained from the deaerator performance test code [13] and is widely corroborated by other researchers and institutes. The idea therefore, is to establish the nozzle discharge diameter that results in the oxygen concentration being reduced to 7ppb at the

nominal load condition, if the inlet oxygen concentration in the main condensate stream is at the maximum possible value.

$$t_{mt} = \frac{D_{32}^2 In\left(\frac{\omega_{o2.out}}{\omega_{o2.in}}\right)}{6D_{o2.mc} \cdot Sh} \tag{67}$$

$$v_{droplet} = \frac{L_{preheater}}{t_{ht} + t_{mt}} \tag{68}$$

In order to find the droplet discharge velocity, equations (67) and (68) are solved simultaneously using a successive approximation iteration scheme. This step is based on the understanding that all other parameters in the two equations except $t_{mt}$ and $v_{droplet}$ are known. The velocity found will then be used in equation (69) to determine the discharge diameter of the nozzle.

$$d_0 = \sqrt{\frac{4}{\pi}\left(\frac{\frac{m_{mc}}{N_{noz}}}{\rho_{noz} v_{droplet}(1-X)}\right)} \tag{69}$$

Where;

$$\cos^2\theta = \frac{1-X}{1+X} \tag{70}$$

## 4.3 Analytical model summary

The processes detailed in sections 4.1 and 4.2 are combined to form the complete analytical model. This means that the model consists of one more section in addition to the three sections mentioned in the Model development. The extra section is called the pre-calculations section and is responsible for the calibration of the model using the 100% load case conditions as detailed in 4.2. For clarity, one may think of this additional section as a way of determining unknown parameters (vent pipe pressure loss coefficient and nozzle discharge diameter) that are needed as inputs to the core model. If all quantities required for the core model to be solved are known, there is no need to use this section at all and it can be ignored.

The pre-calculations section can be further split into sub-sections that are similar to the three sections that make up the core model. The key differences are;

- The inputs of the pre-calculations section are only the 100% load case process conditions as the model is calibrated at this load.

- The outputs of the pre-calculations section are only the vent steam pipe pressure loss coefficient and the nozzle discharge diameter. These outputs are then used as inputs to the core model.

In summary therefore, the model user first inputs the 100% load conditions into the pre-calculations section in order for the model to calibrate the system. The outputs of the calibration exercise are then sent to the core model, where they are combined with known user inputs for any off-design operating load. The new set of inputs is then used by the core model to execute and provide results corresponding to the new inputs. Figure 23 is a flow chart showing the structure of the model as summarised in the preceding section. The figures in brackets show where each particular section or process is described.

In order to establish whether the analytical model was accurate enough to be used as a verification tool for the Flownex model, a validation exercise was performed. The exercise involved running the model using data from a suitable reference deaerator system, and comparing the model predictions to the actual performance of that system. Ideally, all the information pertaining to the thermal-hydraulic and mass transfer characteristics of the reference system would be known. However, mass transfer information of existing deaerator systems was difficult to find and at the time of submission, was still unavailable. It was decided therefore, to split the validation exercise into two separate exercises; a thermal-hydraulic component validation exercise and a mass transfer component validation exercise.

The thermal-hydraulic component validation exercise demonstrated the model's ability to accurately predict the thermal-hydraulic characteristics of an actual deaerator system as originally planned. Specifically, this exercise demonstrated the model's ability to predict the mass flow rates and thermodynamic properties of all unknown streams crossing the deaerator boundary. This exercise was carried out through a case study of a known deaerator system and will be detailed in the following section. The mass transfer component validation exercise demonstrated the ability of the model to accurately predict the mass transfer characteristics of an actual deaerator system. Specifically, the exercise demonstrated the ability of the model to accurately predict the mass transfer coefficient for a given set of inputs. Due to lack of data from any existing operating unit, this exercise was carried out by comparing certain trends of interest to those found by Sharma et al [43] in their work "Oxygen stripping in deaerator feedwater: Condensation on spray droplets". The mass transfer component validation will be presented in the section that follows the thermal-hydraulic component validation.

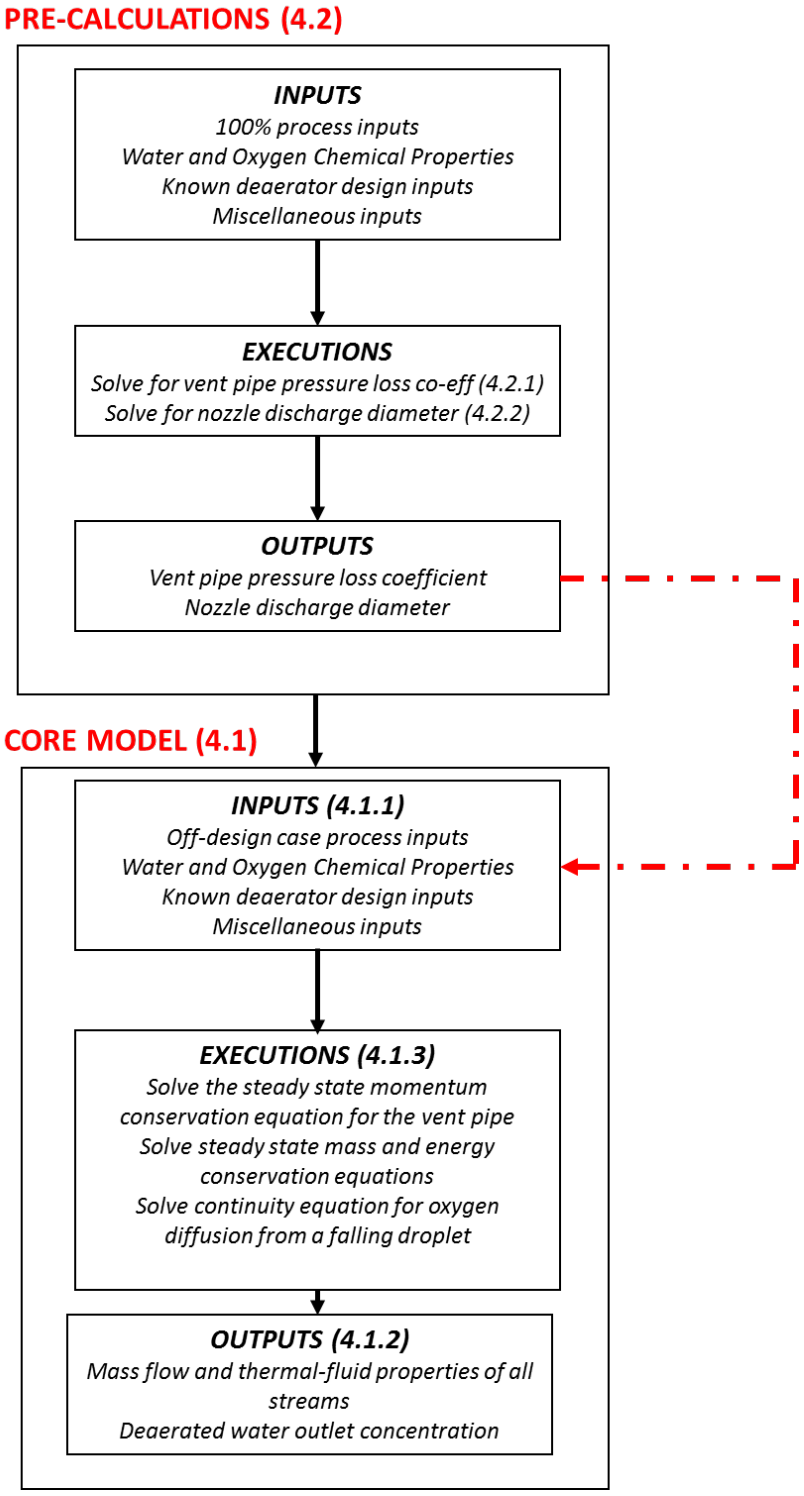


*Figure 23: Flow chart showing the key elements of each section of the analytical model*

## 4.4 Analytical model thermal-hydraulic performance validation

The case study used to validate the thermal-hydraulic component of the analytical model is detailed in this section.

### 4.4.1 Plant 1 Power Station overview

The plant chosen for the case study to validate the thermal hydraulic performance of the analytical model was Unit 2 of Plant 1 in Mpumalanga. The station was first synchronised onto the network on December 13, 1976. The deaerator system consists of two identical tray type deaerating units with the following main features:

- FWT volume 218.5m$^3$
- FWT diameter 4.5m
- Control level 3.34m
- Maximum condensate flow 678t/hr
- Preheater length 1m
- Number of nozzles 1

The two FWT's are connected by large diameter pipes and essentially operate as one system. The system is located between FWH 4 and FWH 6 (Figure 24) and receives steam from the intermediate pressure turbine during normal operation.

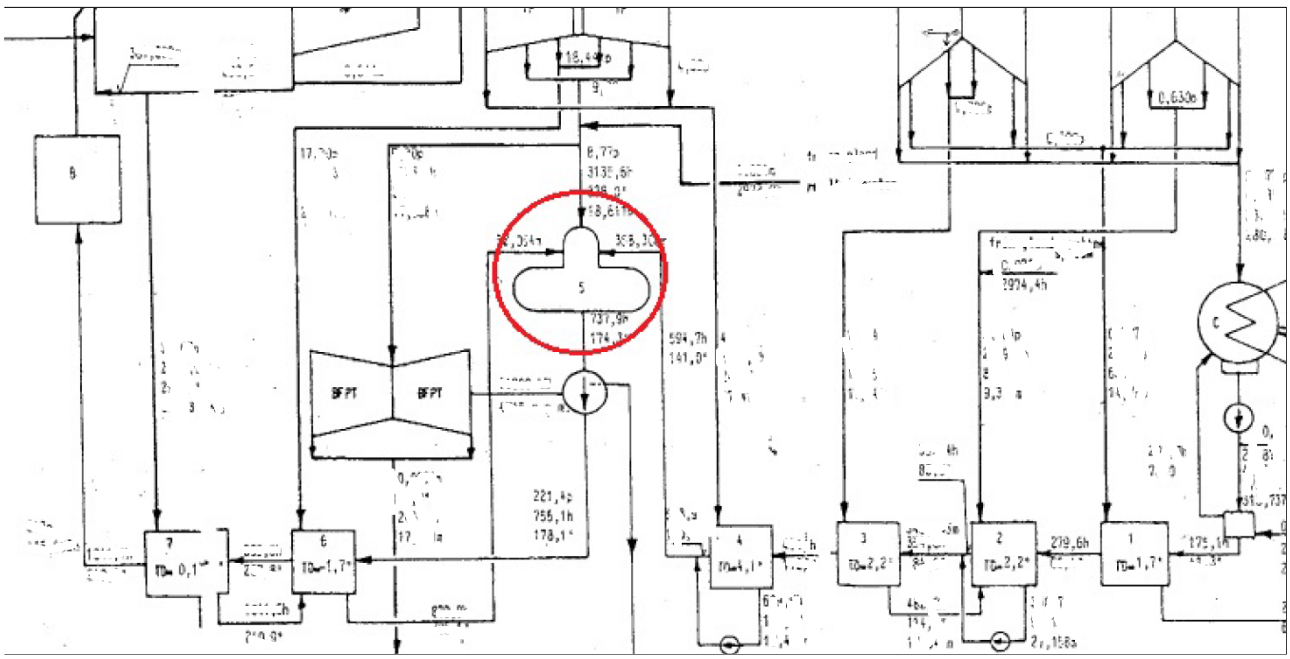


*Figure 24: Plant 1 Unit 2 deaerator system [45]*

The performance data available for the system could be directly read off heat balance diagrams or plant acceptance test reports. This data was in the form of mass flow rates and thermodynamic properties of all streams going into or coming out of the deaerator for different load conditions. The plant acceptance test report data was deemed more accurate and used in this study. Shown below is a table with the raw data obtained from the acceptance test report for the 100% load case. All nonspecific values were split in half as only one deaerator was modelled.

*Table 3: Raw data values for Plant 1 Unit 2 at 100% load*

| ***Parameter*** | ***Value*** | ***Unit*** |
|---|---|---|
| | | |
| *Bled steam mass flow rate ($m_{bs}$)* | *8.694* | *kg/s* |
| *Bled steam enthalpy ($h_{bs}$)* | *3144.2* | *kJ/kg* |
| *Bled steam pressure ($P_{bs}$)* | *0.8731* | *MPa* |
| *Main condensate mass flow rate ($m_{mc}$)* | *180.072* | *kg/s* |
| *Main condensate temperature ($T_{mc}$)* | *142.8* | *°C* |
| *Main condensate pressure ($P_{mc}$)* | *1.334* | *MPa* |
| *Return condensate mass flow rate ($m_{rc}$)* | *23.27* | *kg/s* |
| *Return condensate enthalpy ($h_{rc}$)* | *877.3* | *kJ/kg* |
| *Return condensate pressure ($P_{rc}$)* | *0.93932* | *MPa* |
| *Deaerated water mass flow rate ($m_{dw}$)* | *212.808* | *kg/s* |
| *Deaerated water temperature ($T_{dw}$)* | *174.072* | *°C* |
| *Deaerated water pressure ($P_{dw}$)* | *0.8731* | *MPa* |
| *Vent steam mass flow rate ($m_{vs}$)* | *0.332* | *kg/s* |
| *Vent steam temperature ($T_{vs}$)* | *174.072* | *°C* |
| *Vent steam pressure ($P_{vs}$)* | *0.8731* | *MPa* |

It can be noted from the above table that there is no mention of NCG gas concentrations. This is due to the fact that these concentrations are not part of the online measurements taken during normal operation or acceptance testing. In this case therefore, the maximum concentration of oxygen will be computed and used as discussed in section 4.1.3. As was mentioned in the Model development section, the performance data inputs to the model should be the properties of the streams at the physical boundary of the deaerator. For the Plant 1 deaerator system, some of the performance data was recorded at points that are far from the physical boundary of the deaerator. An appropriate pre-processing exercise was therefore performed in order to make the performance data usable. The exercise is described below.

## 4.4.2 Data pre-processing

Table 4 in conjunction with Figure 25 show the actual measuring points of the information extracted from the acceptance tests report, and whether or not it could be used without pre-processing. The column labelled “method of determination” shows the method that was used to

determine the value of the associated parameter. Values labelled as "measured" are those for which an actual physical measurement was taken and those labelled "calculated" are those for which a computation was done in order to determine the value in question and complete the acceptance test report.

*Table 4 showing measuring locations and methods used to determine values*

| ***Parameter*** | ***Method of Determination*** | ***Position*** | ***Suitable for use without further processing*** |
|---|---|---|---|
| | | | |
| *Main condensate mass flow rate ($m_{mc}$)* | *Calculated* | *A* | *Yes* |
| *Main condensate pressure ($P_{mc}$)* | *Measurement* | *B* | *Yes* |
| *Main condensate temperature ($T_{mc}$)* | *Measurement* | *C* | *Yes* |
| *Bled steam mass flow rate ($m_{bs}$)* | *Calculated* | *D* | *Yes* |
| *Bled steam pressure ($P_{bs}$)* | *Measurement* | *E* | *No* |
| *Bled steam temperature ($T_{bs}$)* | *Measurement* | *G* | *No* |
| *Return condensate mass flow rate ($m_{rc}$)* | *Measurement* | *H* | *Yes* |
| *Return condensate pressure ($P_{rc}$)* | *Measurement* | *I* | *No* |
| *Return condensate temperature ($T_{rc}$)* | *Calculated* | *J* | *No* |
| *Vent stream mass flow rate ($m_{vs}$)* | *Calculated* | *K* | *Yes* |
| *Vent steam pressure ($P_{vs}$)* | *Measurement* | *L* | *Yes* |
| *Deaerated water mass flow rate ($m_{dw}$)* | *Calculated* | *M* | *Yes* |
| *Deaerated water pressure ($P_{dw}$)* | *Calculated* | *N* | *Yes* |
| *Deaerator pressure ($P_{dea}$)* | *Measurement* | *O* | *Yes* |
| *Deaerator temperature ($T_{dea}$)* | *Measurement* | *P* | *Yes* |
| *Deaerator level* | *Measurement* | *Q* | *Yes* |

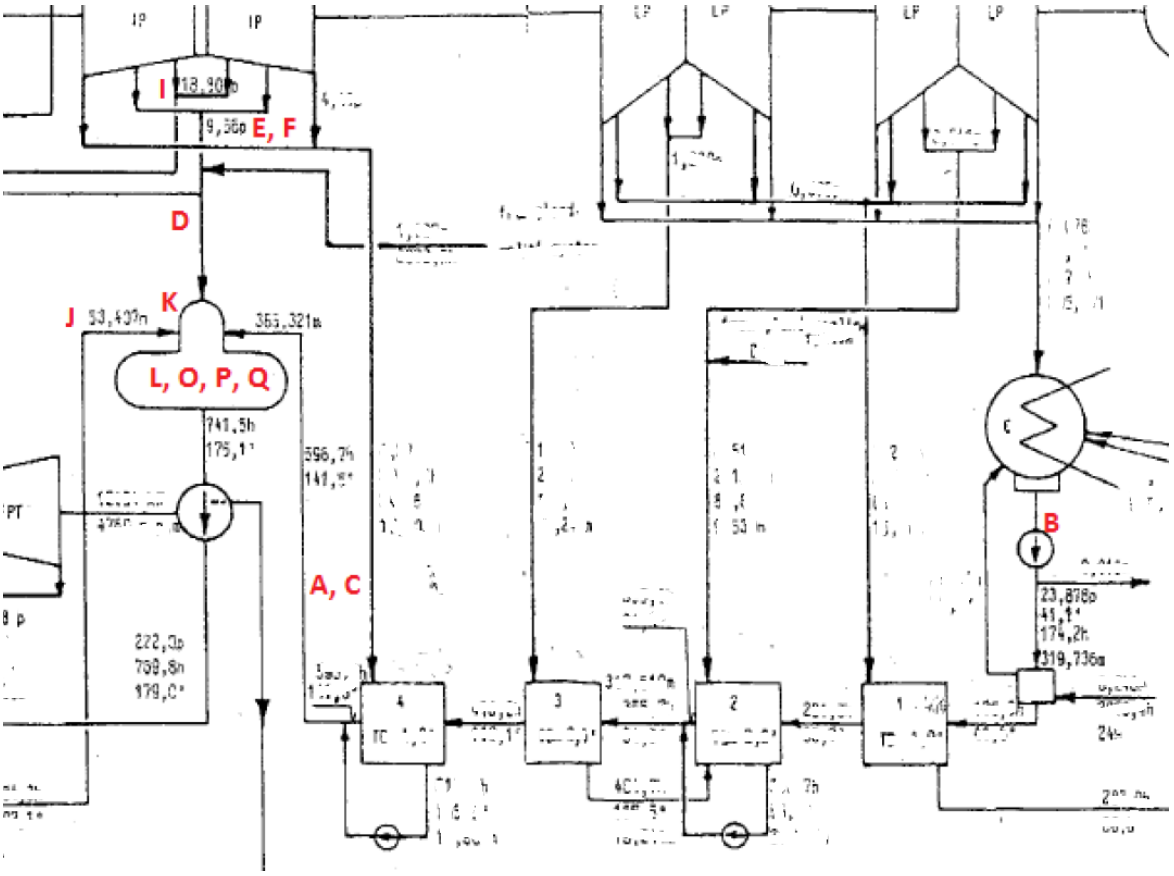


*Figure 25: Plant 1 Unit 2 heat balance showing acceptance test data measurement locations [45]*

Although most of the measuring points were not at the physical boundary of the deaerator, it was decided that using the values reported without alterations would not introduce any appreciable errors. The measuring points for the bled steam, and return condensate temperature and pressure however, were too far from the boundary and the recorded values needed pre-processing.

**Bled Steam properties data pre-processing**

The bled steam temperature and pressure measurements were taken at the extraction point of the intermediate pressure turbine (Figure 26). After this extraction point, the steam is linked to another channel and further split into two streams, one servicing the boiler feed pump turbine and the other servicing the deaerating unit. The connection and split in the piping introduce pressure drops that will change the thermodynamic properties of the steam that eventually ends up at the deaerator. In order to account for this pressure drop, one would need to know certain information about the piping and boiler feed pump turbine operation. This information was not readily available during the development of this work and such knowledge of the operation of other plant elements was beyond the scope of this study.

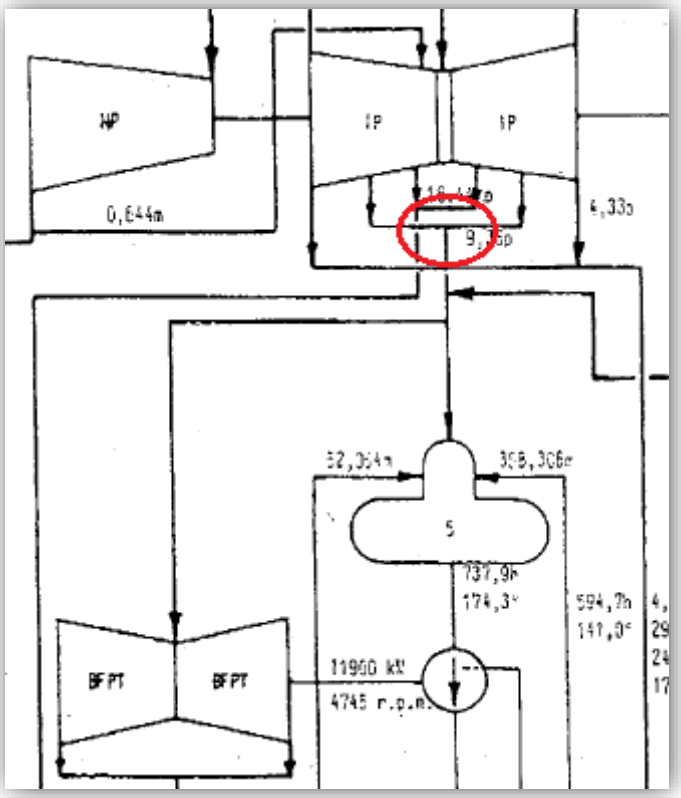


*Figure 26: Bled steam properties measuring point (circled in red) [45]*

From general knowledge of deaerating systems and judging from the large diameter pipes responsible for conveying the bled steam from the turbine extraction point to the deaerating unit, it was decided that the pressure drop of the steam upon entering the deaerator was negligible. This therefore means that the pressure of the steam just outside the deaerator dome is equal to the pressure inside. This assumption made it possible to define a new bled steam pressure at the inlet of the deaerator by equating it to a known trusted value (deaerator pressure).

The temperature at the measuring point was also subject to change as the steam progressed to the deaerator, but the enthalpy would stay constant assuming that the piping was adequately lagged and the flow process was adiabatic. This assumption made it possible to evaluate the enthalpy at the measuring point and equate it to the enthalpy at the deaerator inlet.

Through the process detailed above the bled steam temperature and pressure readings taken at the turbine extraction point were replaced by bled steam pressure and enthalpy readings at the deaerator physical boundary.

**Return condensate data pre-processing**

The return condensate pressure was originally calculated through assuming that there was no pressure drop across the shell side of FWH 6 and across the elements joining the FWH to the

deaerator. This allowed the authors of the acceptance test report to equate the return condensate pressure before the deaerator to the measured bled steam pressure before FWH 6. However, upon investigating the elements joining the deaerator system and FWH 6 (Figure 27), it became clear that this assumption was inaccurate as there was a flash box, geometry changes and a number of valves in between.

In order to account for the pressure drop across these elements, one would need detailed knowledge of each of the elements in between the two heaters. Such knowledge was not within the scope of this work. In order to determine the pressure of the return condensate just before the deaerator, a backward calculation based on knowledge of the geometry of the return condensate inlet, the return condensate mass flow rate and the pressure inside the deaerator was performed. The calculation can be summarised in the equation shown below.

$$P_{rc} - P_{dea} = \frac{K_{exit}}{2A_{rc.pipe}} \rho_{rc} Q_{rc}^2 \tag{71}$$

Where

- $A_{rc.pipe}$ is the area of the return condensate inlet pipe.
- $K_{exit}$ = 1 is the pipe exit loss factor associated with the return condensate inlet.

The temperature value reported for the return condensate before the deaerator was assumed to be equal to the saturation temperature corresponding to the shell side pressure of FWH 6. This temperature may have changed as the fluid interacted with the many elements shown in Figure 27. An approach similar to that described in the preceding section was used to replace this value with an enthalpy value at the deaerator inlet. As with the bled steam case, a new set of values was therefore produced to describe the characteristics of the return condensate at the deaerator interface.

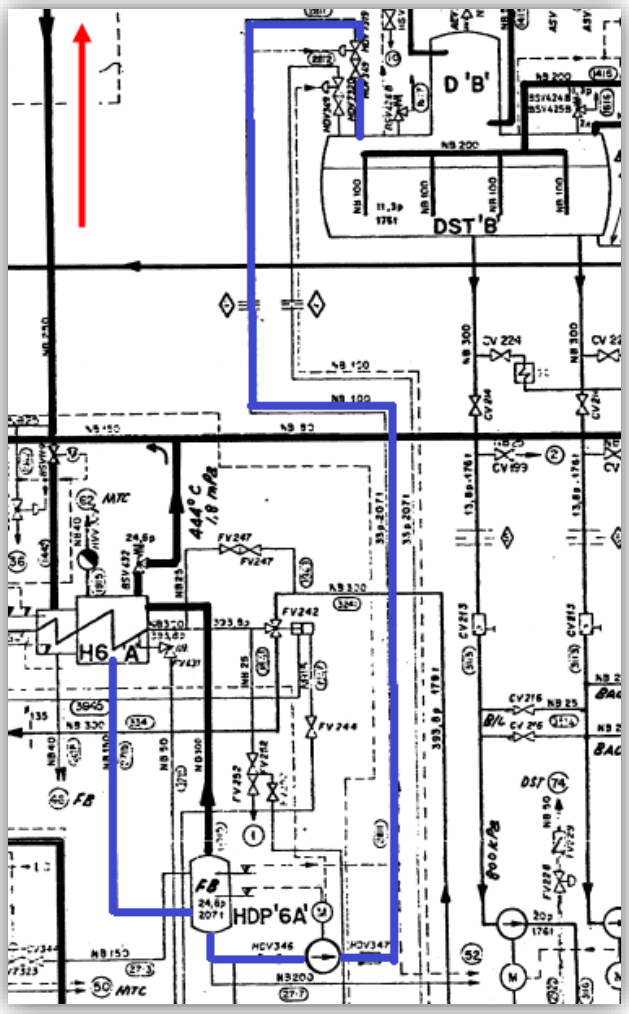


*Figure 27: Return condensate path (blue) from HPH 6 to deaerator.*

### 4.4.3 Data reconciliation

The changes detailed in the preceding sections gave rise to a new set of data points. To ensure that the new data set represented a true thermal-hydraulic system, a data reconciliation activity was performed. In summary, the activity involved first systematically testing for mass and energy balances around the deaerator system using the raw data values. If the mass and energy balances were not satisfied, each raw data value would then be adjusted in order to satisfy the balances. The magnitude of each adjustment was dependant on a user defined weighting factor, statistically called the variance, defined for each value. This weighting factor would then be used in a statistical procedure to find the minimum adjustment required for the corresponding value. The final data set after the pre-processing activity is shown in Table 5 against the raw data set for the 100% load case.

*Table 5: Raw and processed data values for Plant 1 Unit 2 at 100% load*

| *Parameter* | *Before Processing* | *After Processing* | *Unit* |
|---|---|---|---|
| | | | |
| *Bled steam mass flow rate ($m_{bs}$)* | *8.694* | *8.707* | *kg/s* |
| *Bled steam enthalpy ($h_{bs}$)* | *3144.2* | *3149.813* | *kJ/kg* |
| *Bled steam pressure ($P_{bs}$)* | *0.8731* | *0.873* | *MPa* |
| *Main condensate mass flow rate ($m_{mc}$)* | *180.072* | *180.360* | *kg/s* |
| *Main condensate temperature ($T_{mc}$)* | *142.8* | *143.829* | *°C* |
| *Main condensate pressure ($P_{mc}$)* | *1.334* | *1.334* | *MPa* |
| *Return condensate mass flow rate ($m_{rc}$)* | *23.27* | *23.270* | *kg/s* |
| *Return condensate enthalpy ($h_{rc}$)* | *877.3* | *877.300* | *kJ/kg* |
| *Return condensate pressure ($P_{rc}$)* | *0.93932* | *0.939* | *MPa* |
| *Deaerated water mass flow rate ($m_{dw}$)* | *212.808* | *212.005* | *kg/s* |
| *Deaerated water temperature ($T_{dw}$)* | *174.072* | *174.072* | *°C* |
| *Deaerated water pressure ($P_{dw}$)* | *0.8731* | *0.873* | *MPa* |
| *Vent steam mass flow rate ($m_{vs}$)* | *0.332* | *0.332* | *kg/s* |
| *Vent steam temperature ($T_{vs}$)* | *174.072* | *174.072* | *°C* |
| *Vent steam pressure ($P_{vs}$)* | *0.8731* | *0.873* | *MPa* |

### 4.4.4 Model implementation, results and discussion

Using the reconciled data and the known design inputs listed in section 4.4.1, the model was run for all load cases and the results recorded. This section details the inputs used, some intermediate results obtained and the final outputs of the model for the 100% load case.

**Pre-calculations section Inputs**

The reconciled values for the following parameters (Table 5) were used in the pre-calculations section in order to calibrate the model;

- Bled steam mass flow rate ($m_{bs}$)
- Bled steam enthalpy ($h_{bs}$)
- Bled steam pressure ($P_{bs}$)
- Main condensate mass flow rate ($m_{mc}$)
- Main condensate temperature ($T_{mc}$)
- Main condensate pressure ($P_{mc}$)
- Return condensate mass flow rate ($m_{rc}$)
- Return condensate enthalpy ($h_{rc}$)
- Return condensate pressure ($P_{rc}$)

After the calibration process, the model calculated the vent pipe pressure loss coefficient to be $1.745 \times 10^{7}$ $m^{-4}$. This value was then used as an input to the core model.

**Core model inputs**

The inputs used by the model for the 100% load case were therefore the reconciled values for;

- Bled steam enthalpy ($h_{bs}$)
- Bled steam pressure ($P_{bs}$)
- Main condensate mass flow rate ($m_{mc}$)
- Main condensate temperature ($T_{mc}$)
- Main condensate pressure ($P_{mc}$)
- Return condensate mass flow rate ($m_{rc}$)
- Return condensate enthalpy ($h_{rc}$)
- Return condensate pressure ($P_{rc}$)

And the calculated value for the vent pipe pressure loss coefficient ($Ck_{vp}$)

**Some intermediate results**

The following values were calculated by the model and used to solve the mass and energy conservation equations;

*Table 6: Intermediate results for the Plant 1 deaerator system at 100% load*

| ***Parameter*** | ***Value*** | ***Unit*** |
|---|---|---|
| *Deaerator pressure ($P_{dea}$)* | *8.73* | *bar* |
| *Main condensate enthalpy ($h_{mc}$)* | *606.248* | *kJ/kg* |
| *Deaerated water enthalpy ($h_{dw}$)* | *737.051* | *kJ/kg* |
| *Vent steam enthalpy ($h_{vs}$)* | *2772.829* | *kJ/kg* |
| *Vent steam mass flow rate ($m_{vs}$)* | *0.344* | *kg/s* |

**Results**

Table 7 shows the final output of the model;

*Table 7: Outputs from the analytical model for the Plant 1 deaerator system at 100% load*

| ***Parameter*** | ***Value*** | ***Unit*** |
|---|---|---|
| | | |
| *Bled steam mass flow rate ($m_{bs}$)* | *8.707* | *kJ/kg* |
| *Vent steam temperature ($T_{vs}$)* | *174.067* | *°C* |
| *Vent steam pressure ($P_{vs}$)* | *8.73* | *bar* |
| *Deaerated water mass flow rate ($m_{dw}$)* | *212.003* | *kJ/kg* |
| ***Parameter*** | ***Value*** | ***Unit*** |
| | | |
| *Deaerated water temperature ($T_{dw}$)* | *174.067* | *°C* |
| *Deaerated water pressure ($P_{dw}$)* | *8.73* | *bar* |

The results shown above confirm that the previously unknown thermodynamic properties of all streams crossing the deaerator boundary were defined. The next section shows the errors associated with each value and the discussion of the results based on that.

**Error calculation and discussion**

The error associated with each predicted value can be evaluated in a number of ways. A popular way is to express the difference between the predicted value and the actual value as a percentage of the actual value as shown in equation(72). It should be noted that for the purpose of this report, the error is defined as the deviation between the model output values and the acceptance test data values, which the model views as the raw or actual data.

$$error = \frac{acceptance\ test\ value - predicted\ value}{acceptance\ test\ value} \times 100 \tag{72}$$

Shown below are the errors computed using equation (72) for each parameter.

*Table 8: Analytical model errors for the Plant 1 deaerator system at 100% load*

| ***Parameter*** | ***Reconciled Data*** | ***Analytical Model*** | ***Analytical Model vs. Recon Data error (%)*** | ***Unit*** |
|---|---|---|---|---|
| | | | | |
| *Deaerator pressure ($P_{dea}$)* | 8.73 | 8.73 | 0.00 | *bar* |
| *Bled steam mass flow rate ($m_{bs}$)* | *8.707* | 8.707 | 0.00 | *kg/s* |
| *Vent steam mass flow rate ($m_{vs}$)* | *0.332* | 0.334 | 0.64 | *kg/s* |
| *Vent steam temperature ($T_{vs}$)* | *174.072* | 174.067 | 0.00 | *°C* |
| *Vent steam pressure ($P_{vs}$)* | *8.730* | 8.730 | 0.00 | *bar* |
| *Deaerated water mass flow rate ($m_{dw}$)* | *212.005* | 212.003 | 0.00 | *kg/s* |
| *Deaerated water temperature ($T_{dw}$)* | 174.072 | 174.067 | 0.00 | *°C* |
| *Deaerated water pressure ($P_{dw}$)* | 8.73 | 8.73 | 0.00 | *bar* |

The error values shown in Table 8 indicate that the model generally predicts the thermal-hydraulic characteristics of the Plant 1 deaerator system at the 100% load to a relatively high accuracy. This is the expected outcome as the model is calibrated at the 100% condition meaning that ideally, everything should be the same. The highest error is seen to be 0.64% for the vent steam mass flow rate. This error can be solely attributed to rounding errors as the model is calibrated at the 100% load case, leaving no room for much error.

The model was also run for the 46%, 60% and 80% load cases. The inputs and final results of each of these load cases are shown in Appendix A as they were here for the 100% load case. Here the results are only shown and discussed in graphic form.

Only the bled steam, vent steam and deaerated water mass flow rates errors will be shown here as the rest are not calculated in the model but either assumed or read off water-steam tables. For these parameters, the error is very small, ranging from 0.00% to 0.01% and is attributable to possible small variations in the water-steam tables.

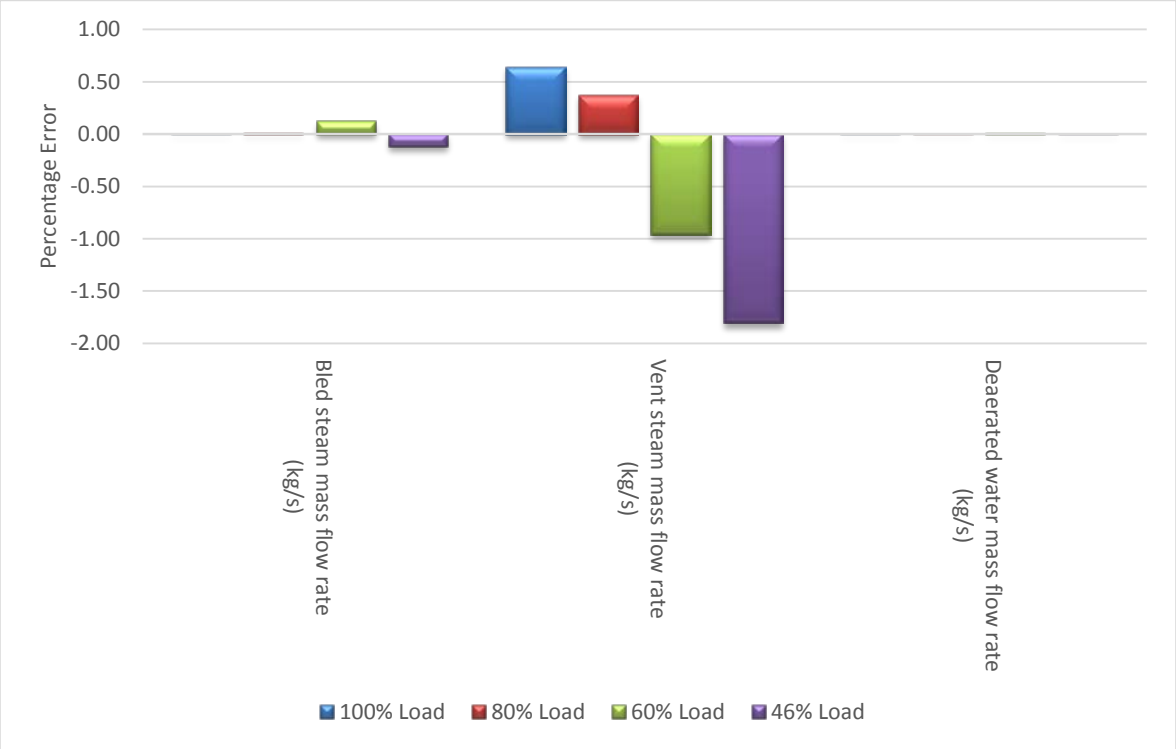


*Figure 28: Analytical model errors for the Plant 1 deaerator system at all loads*

From the results shown in Figure 28, it is clear that the model generally predicts the thermal-hydraulic characteristics of the Plant 1 deaerator system accurately at all loads. The magnitudes of the errors range between 0% and 1.81% with an average of 0.128%. The average error is raised by the relatively high errors associated with the vent steam mass flow rates. A closer look at the variation of the vent steam mass flow rate error with the load shows that the error steadily increases as the plant load is increased.

For the first two load cases the error is negative meaning that the model understates the vent steam mass flow rate. This changes for the 80% and 100% load cases as the error becomes positive, indicating an overestimation of the mass flow rate. A more useful graph is that of the absolute value of the error against the load case (Figure 30).

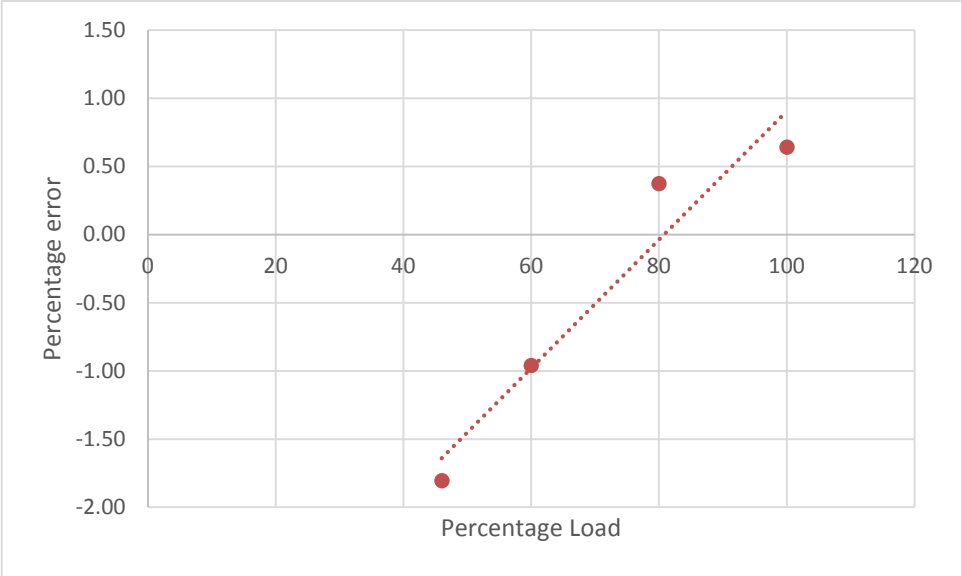


*Figure 29: Vent steam mass flow rate errors for the Plant 1 deaerator system at different loads*

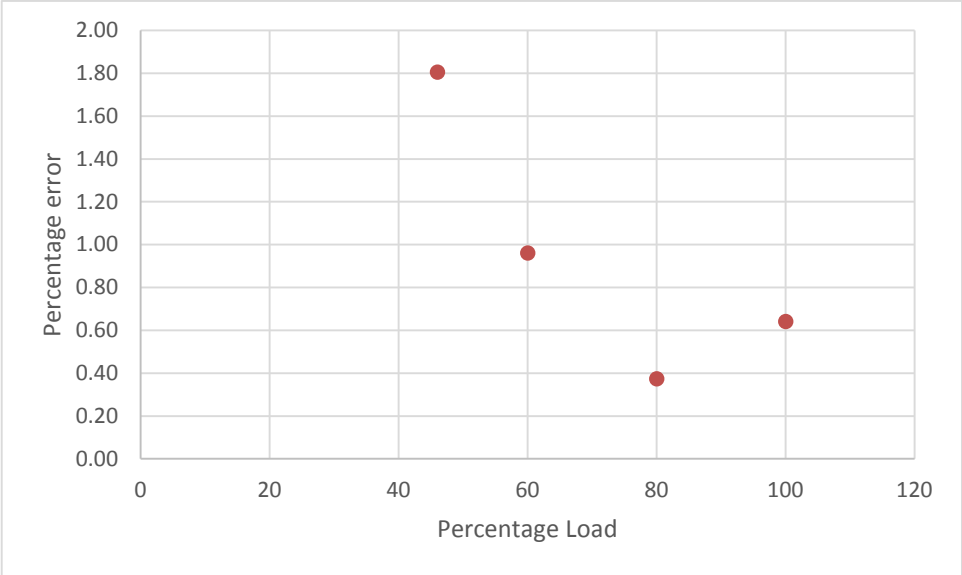


*Figure 30: Vent steam mass flow rate errors for the Plant 1 deaerator system at all loads. (Absolute values only)*

The absolute value of the vent steam mass flow rate error is generally seen to decrease with increasing load. This outcome may be due to the assumption made regarding the constancy of the vent pipe pressure loss characteristics. This assumption is based on the understanding that the vent pipe valve is unchanged for all load cases during operation. This might not be the case as it is standard procedure to control the vent pipe mass flow rate in order to minimise steam losses from the feedwater system. If this was the case during the acceptance testing, it may be used to explain the observed trends. However, the errors associated with assuming constant pressure loss characteristics are relatively small compared the total capacity of the deaerator and do not significantly affect the accuracy of the entire model significantly. It can be said therefore, that the

analytical model represents the Plant 1 deaerator system satisfactorily and was successfully validated.

## 4.5 Analytical model mass transfer component validation

The validation exercise for the mass transfer component of the analytical model involved comparing the model output to the results obtained by Sharma et al [43] in their work, "Oxygen stripping in deaerator feedwater: Condensation on spray droplets". However, the comparisons were only qualitative as the raw data used in the actual study was unavailable.

One way of qualitatively comparing the results was to plot graphs similar to those presented by Sharma et al [43] with the aim of observing and discussing the similarities and differences between the two sets of graphs. This was done for four graphs, all involving the mass transfer coefficient. The pairs of graphs and the discussion of each are presented below.

### 4.5.1 Variation of the mass transfer coefficient with main condensate mass flow rate at different deaerator pressures

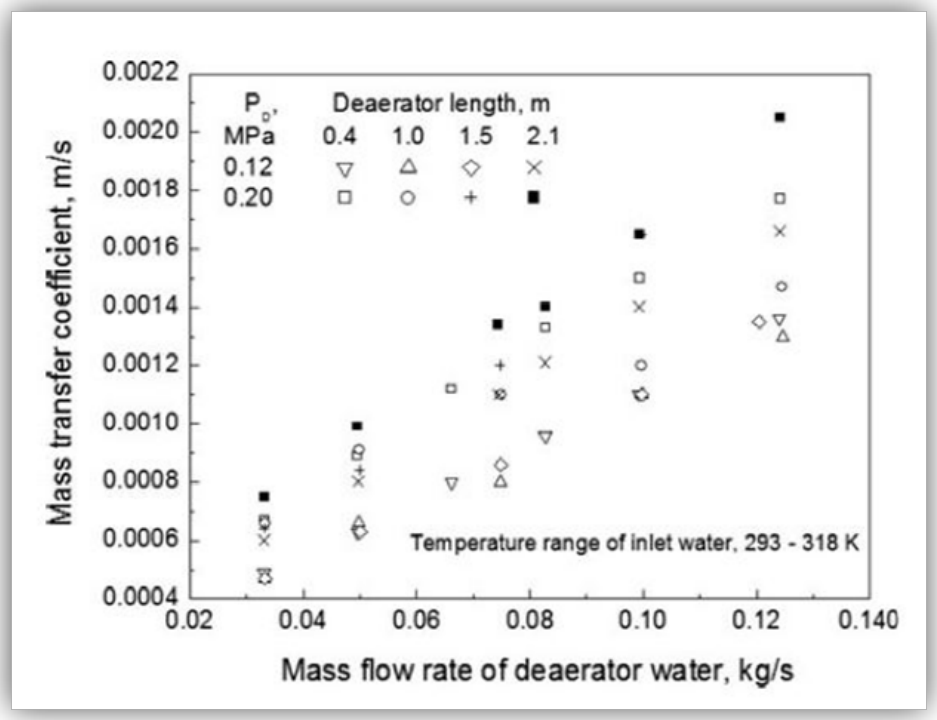


*Figure 31: Graph showing the variation of the mass transfer coefficient with the main condensate mass flow rate at different deaerator lengths and pressures [43].*

Figure 31 shows that the mass transfer coefficient increases with increasing main condensate mass flow rate in an approximately linear fashion. This observation was recorded from experiments conducted by Sharma et al [43] using a deaerator test rig and may be due to the dependence of the mass transfer coefficient on the velocity of the water droplets during deaeration. Increasing the mass flow rate results in an increased droplet velocity which in turn results in higher Reynolds and Sherwood numbers. It can also be observed that increasing the deaerator pressure results in an increased mass transfer coefficient for the same conditions. This is probably due to the higher temperatures associated with higher pressures which result in an increased oxygen diffusion rate.

A similar graph was constructed using the model results for the Plant 1 deaerator system. It was assumed, based on the shape of the ensuing spray, that the Plant 1 deaerator nozzle could be approximated by a fixed geometry pressure swirl simplex atomizer, making it a suitable system for comparison with Sharma's works. This assumption is not necessarily accurate but was only made in order to obtain a set of data points that could be used to demonstrate the mass transfer capabilities of the system.

The model was run at different bled steam pressures and a plot of the mass transfer coefficient against the mass flow rate was made. The length of the preheater was kept constant at 0.5m with a main condensate inlet temperature of 143.8 °C.

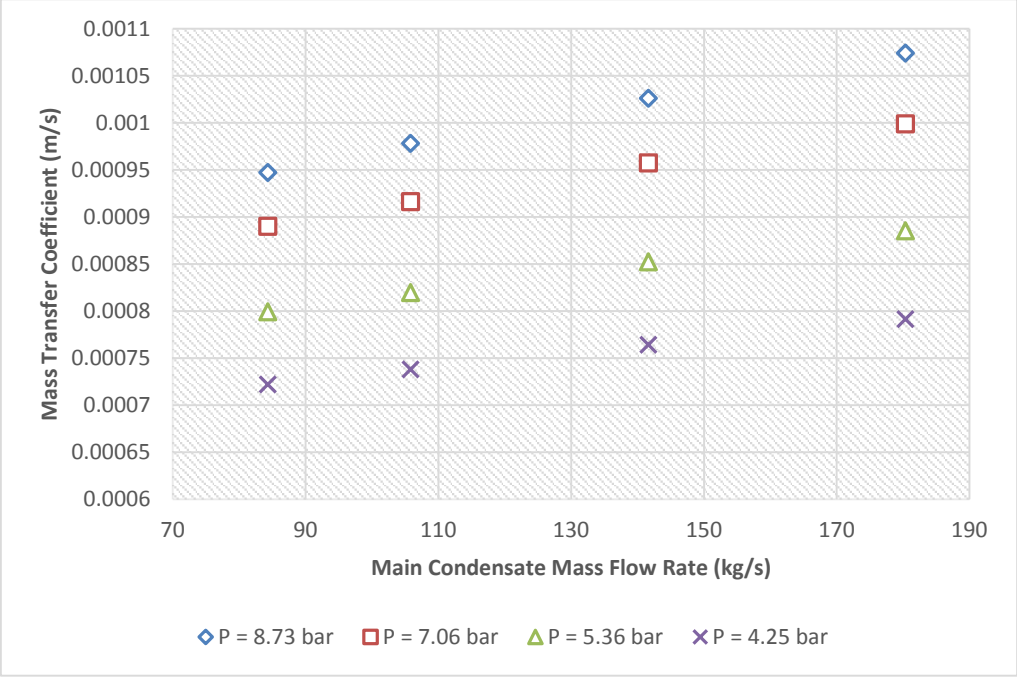


*Figure 32: Graph showing the model predictions of the variation of the mass transfer coefficient with the main condensate mass flow rate at different deaerator pressures.*

Figure 32 shows that the general linear trend observed in Figure 31 for the experimental results was satisfactorily predicted by the model. The variation of the mass transfer coefficient with deaerator pressure was also satisfactorily predicted as the model predicted consistently higher mass transfer coefficients at higher deaerator pressures. The differences in the gradients of the linear trends and the distances between points are a function of the quantitative differences between the Plant 1 deaerator system and the test rig used for the Sharma experiment.

### 4.5.2 Variation of the mass transfer coefficient with main condensate mass flow rate at different deaerator lengths

Figure 31 also shows that the mass transfer coefficient consistently increases with increasing deaerator lengths. This is the result of an increased residence time which in turn results in higher final temperatures for the same deaerating conditions. This variation is also satisfactorily predicted by the model (Figure 33), which predicts an increase similar to that observed from the experimental results.

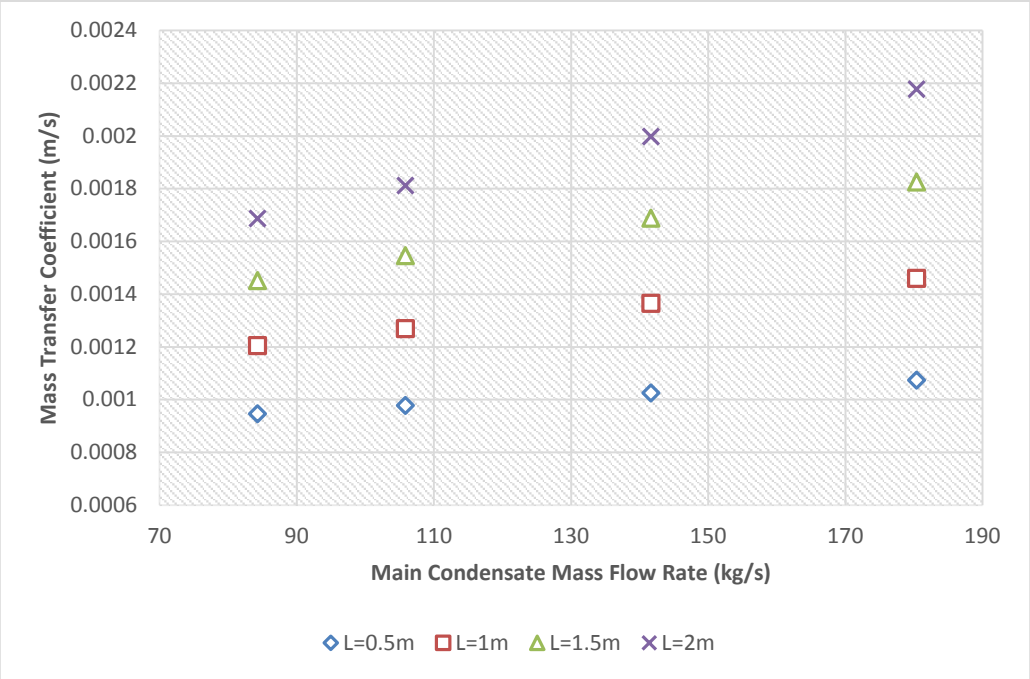


*Figure 33: Graph showing the model predictions of the variation of the mass transfer coefficient with the main condensate mass flow rate at different deaerator pressures.*

### 4.5.3 Variation of the mass transfer coefficient with main condensate temperature at different deaerator lengths

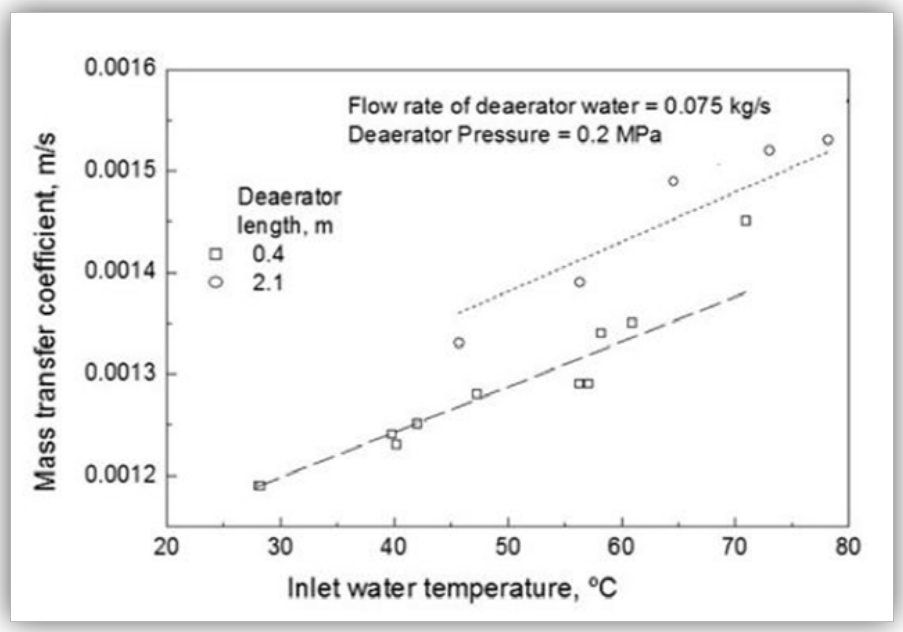


*Figure 34: Graph showing the variation of the mass transfer coefficient with the main condensate temperature at different deaerator lengths.*

Figure 34 shows a fairly linear relationship between the mass transfer coefficient and the main condensate temperature as observed from Sharma's experiment. The reason for this relationship stems from the fact that oxygen diffusion rates are increased at higher temperatures as the kinetic energy and therefore velocity of the diffusing species are increased. It can also be observed that the mass transfer coefficient consistently increases with increasing the deaerator length. This observation was noted and discussed in section 4.5.2.

Figure 35 shows a different relationship to that observed from the experimental set up. It appears from the figure, that the mass transfer coefficient is insensitive to the inlet temperature of the main condensate. This observation is the result of an assumption made in the development of the model, regarding the conditions under which deaeration occurs. It was assumed that deaeration only occurs after the water has been heated to saturation, and therefore under non-changing saturation conditions. This simplification is different from what happens in reality as stated in section 4.1.3. In reality, deaeration takes place under varying conditions as the main condensate is progressively heated inside the deaerator. The variations are such that the mass transfer coefficient steadily increases as the main condensate temperature is heated due to an increased

molecular mobility. The transfer coefficient is therefore lower at the main condensate incoming conditions than it is after the water is heated.

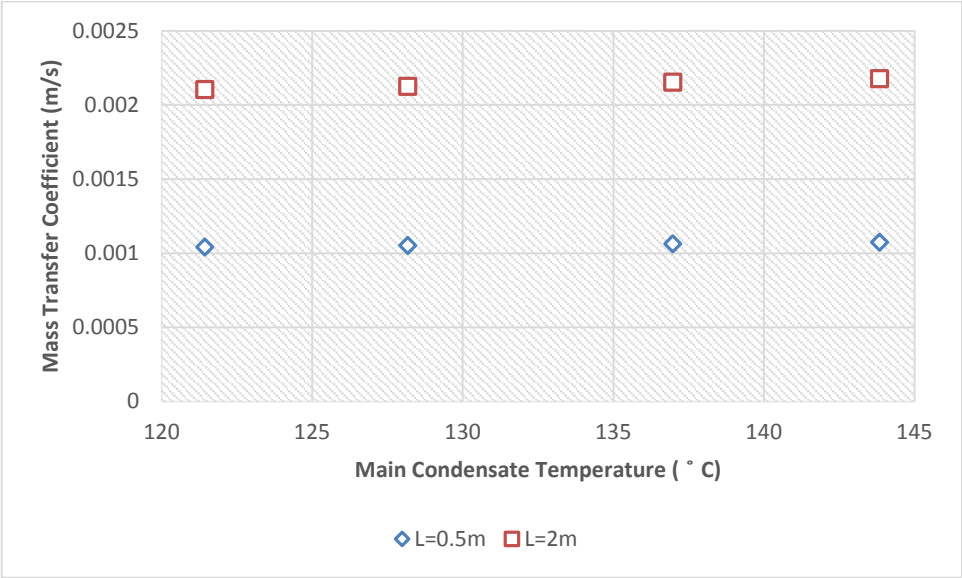


*Figure 35: Graph showing the model predictions of the variation of the mass transfer coefficient with the main condensate temperature rate at different deaerator lengths.*

The omission of this change in mass transfer coefficient with main condensate temperature is therefore responsible for the differences in the trends. The omission was not deemed to affect the accuracy of the model predictions significantly as the time for deaeration is much less according to the model. This reduction in the total time available for deaeration compensates for the overestimation of the mass transfer coefficient predicted by the model.

### 4.5.4 Variation of the mass transfer coefficient with main condensate oxygen concentration at different deaerator lengths

Figure 36 shows that the mass transfer coefficient decreases with increasing oxygen concentrations in the main condensate. The reason for this trend is unclear as the inlet concentration plays no significant part in changing the fluid properties of the main condensate, which ultimately determine the mass transfer coefficient. It is possible that the inclusion of very low inlet concentrations, between 0 – 500 ppb may have caused the distortion of what would have otherwise been a flat relationship showing no statistically significant link between the mass transfer coefficients and inlet concentrations. The consistent increase in the mass flow rate with increasing length and pressure has already been noted and discussed.

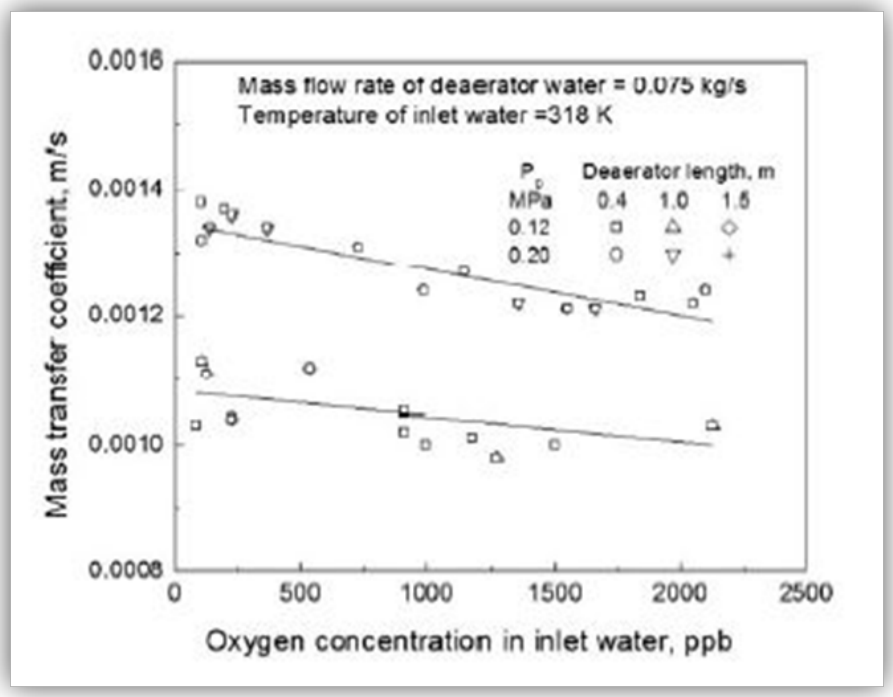


*Figure 36: Graph showing the variation of the mass transfer coefficient with the main condensate oxygen concentration at different deaerator lengths and pressures.*

Figure 37 and Figure 38 show that the model predicts no relationship between the mass transfer coefficient and the inlet oxygen concentration. From theoretical considerations, this result makes sense as it is not clear how such small concentrations of oxygen may affect the bulk mass transfer properties of the system.

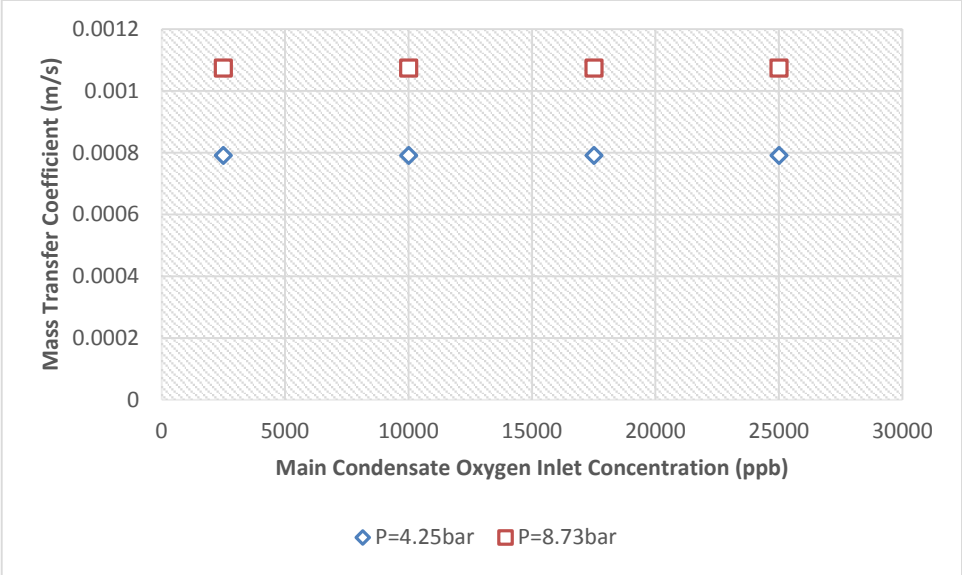


*Figure 37: Graph showing the model predictions of the variation of the mass transfer coefficient with the main condensate oxygen inlet concentration at different deaerator pressures.*

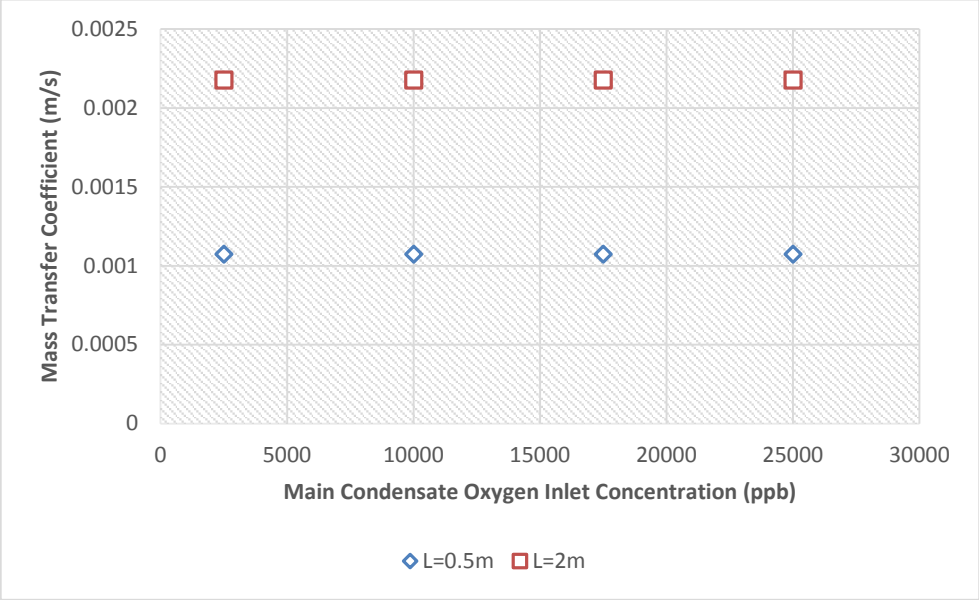


*Figure 38: Graph showing the model predictions of the variation of the mass transfer coefficient with the main condensate oxygen inlet concentration at different deaerator lengths.*

In summary, the model predicts the qualitative mass transfer characteristics of the Plant 1 deaerator system satisfactorily. The differences highlighted above have been noted and it was concluded that their effects on the accuracy of the model are minimal and relatively insignificant.

## 4.6 Closing remarks

The chapter detailed the development and validation exercises performed on the analytical model. The model was primarily based on solving the one dimensional mass and energy conservation equations together with the oxygen continuity equation for diffusion from falling droplets. The validation was carried out in two parts; one for the thermal-hydraulic performance of the model and the other for the mass transfer characteristics of the model. Both validation exercises produced satisfactory results which demonstrated the model's ability to faithfully predict the performance of a typical deaerator unit and therefore be used as a verification tool for the Flownex model.

# 5. Flownex Model Development, Verification and Validation

Upon the completion of the analytical model, the numerical deaerator model was developed in Flownex. This chapter details the development, verification and validation processes performed on the numerical model. The chapter commences by giving an overview of the Flownex SE software package before presenting the development activities performed. This is then followed by a summary of the verification and validation exercise done on the model.

## 5.1 Flownex SE overview

Flownex is a 1-dimensional thermal-hydraulic solver which can solve user defined networks using a numerical solution of the governing equations of fluid dynamics and heat transfer. "*It solves the partial differential equations of mass, momentum and energy conservation to obtain the mass flow rates, pressure and temperature distributions throughout the network*" [46]. The solver contains a library of standard industrial elements such as pipes, valves and tanks that can be linked together to form a network. The following section describes and discusses some Flownex elements, components and features relevant to this work.

**General Empirical Relationship Element**

The general empirical relationship element is found in the custom losses library and can be used to model pressure drops across valves, heat exchangers and experimental equipment. The component applies to gaseous, liquid and two phase flow and allows a fixed heat input to be specified for the fluid. The use and validity of this component is subject to the following assumptions and simplifications [47];

- One dimensional flow at the inlet and outlet.
- No work is done on or by the fluid except flow work.
- The flow is quasi-steady, i.e. the thermal and mass inertia are neglected.
- The volume contribution of the general empirical relationship is negligible compared to the volume of the system.

Figure 39 shows the element's input tab and the element icon;

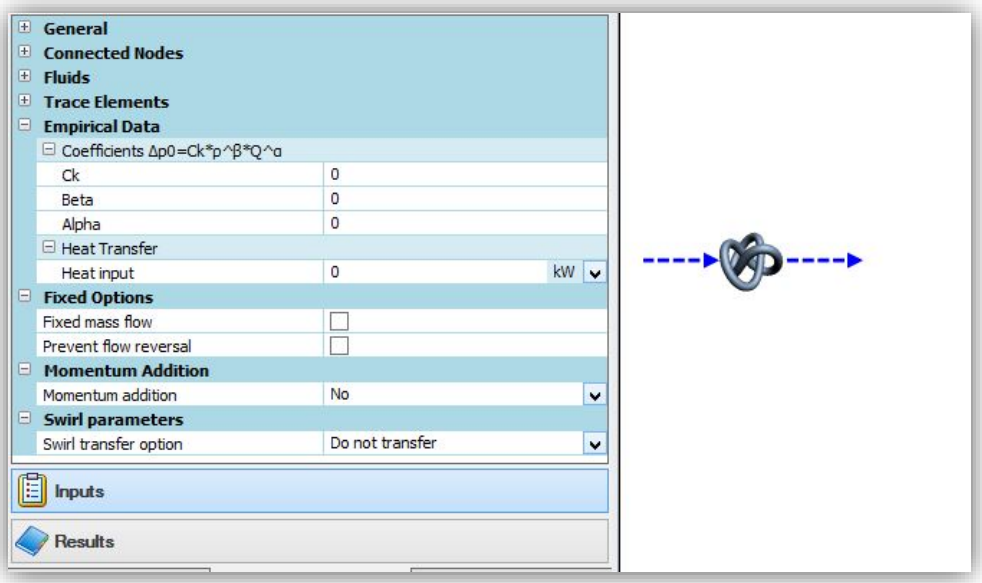


*Figure 39: General Empirical element* inputs dialogue box and element icon

The total pressure drop, *ΔP,* across the element is evaluated using the general empirical relationship shown below.

$$\Delta P = C_k \rho^{\beta} Q^{\alpha} \tag{73}$$

Where $\alpha$ and $\beta$ are geometry constants and $C_k$ is the pressure loss coefficient.

The main advantage of this component is that it allows the user to model pressure drops for systems with limited geometrical inputs by choosing values for $\alpha$, $\beta$ and $C_k$ using whichever method is convenient and applicable. For many fixed geometry pressure loss elements $\alpha$ and $\beta$ are normally 2 and 1 respectively.

**Flow Resistance**

The flow resistance element is also found under the custom losses library and can be used to model pressure drops across valves, heat exchangers, ducts and experimental equipment. Similar to the general empirical relationship element, the flow resistance component can be applied to gaseous, liquid and two phase flow and allows a fixed heat input to the fluid to be specified. The use and validity of this component is subject to the following assumptions and simplifications [47];

- One dimensional flow at the inlet and outlet
- No work is done on/by the fluid except flow work

Figure 40 shows the element's input tab and the element icon;

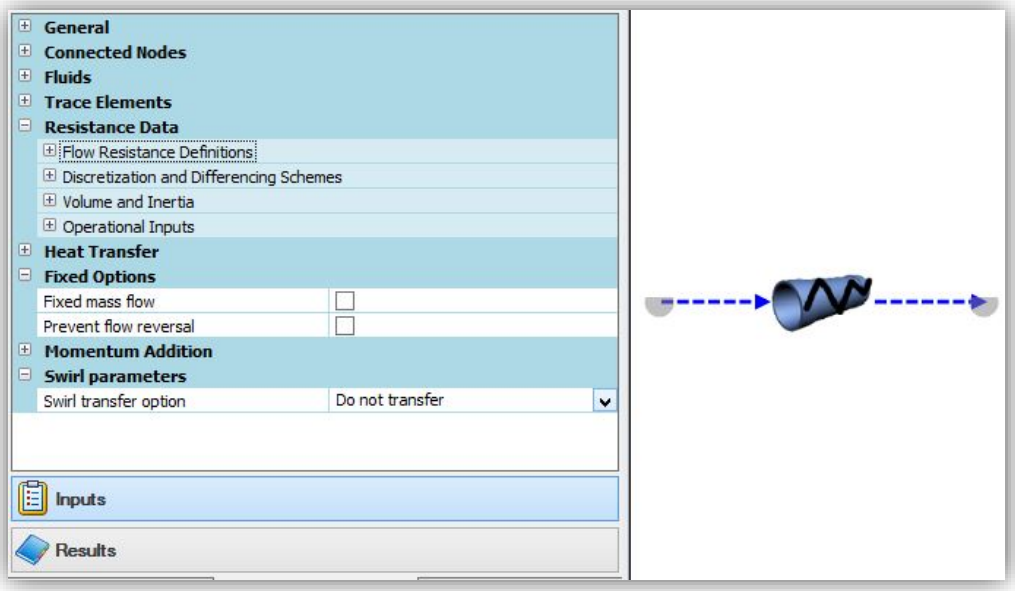


*Figure 40: Flow resistance inputs dialogue box and element icon*

The pressure drop across the flow resistance element is evaluated without considering secondary effects and can be calculated differently depending on the system being modelled. In cases with highly turbulent flow and density variations, the pressure drop is calculated using equation (74) shown below;

$$\Delta P = \frac{|\dot{m}|\dot{m}}{A_f \cdot A_{sf} \cdot A_0} + \rho g \Delta z \tag{74}$$

Where:

- $A_f$ is the flow admittance
- $A_{sf}$ is the admittance scaling factor
- $A_0$ is the opening

These parameters will have varying units depending on which options are being used.

In cases where the fluid density changes over the length of the flow resistance and the flow is still highly turbulent, the total pressure drop across the flow resistance element is given by;

$$\Delta P = \frac{|\dot{m}|\dot{m}}{\rho \cdot A_f \cdot A_{sf} \cdot A_0} + \rho g \Delta z \tag{75}$$

The pressure drops calculated using equations (74) and(75), together with the conditions associated with them, are simulated if the flow resistance element is using the “Quadratic Resistance Behaviour” option. This is the default option associated with this element, but in flow cases where the fluid density remains constant, and the flow is laminar or turbulent, the “Linear

Resistance Behaviour" option must be used. Using this option, the total pressure drop across the element is evaluated using equation(76).

$$\Delta P = \frac{\dot{m}}{A_f \cdot A_{sf} \cdot A_0} + \rho g \Delta z \tag{76}$$

The flow resistance component also has a fixed mass flow option. Using this option fixes the mass flow rate through the element in one of two ways;

1. By calculating the mass flow rate required across the element for a 0kg/s mass sources on a pressure boundary where the steady state continuity option of "Apply element fixed mass flow" is selected.
2. By fixing the mass flow to a user specified value.

An advantage of this component is that it allows linked components to be isolated from one another by becoming a low pressure drop link itself. This can be achieved by specifying a high admittance to the flow and it allows the separated components to be somewhat analysed separately without considering the direct impact of one component on the other. An additional advantage is that using the fixed flow option allows pressure boundaries to be designed for zero mass sources conveniently, without using the iterative designer.

**Two Phase Tank**

The two phase tank component can be used to model tanks containing two phase fluids with phase separation. In principle the two phase tank is a node with restricted functionality to allow the user to create an intuitive network on the drawing canvas using a unique icon to differentiate the two. Figure 41 shows the components inputs tab and icon.

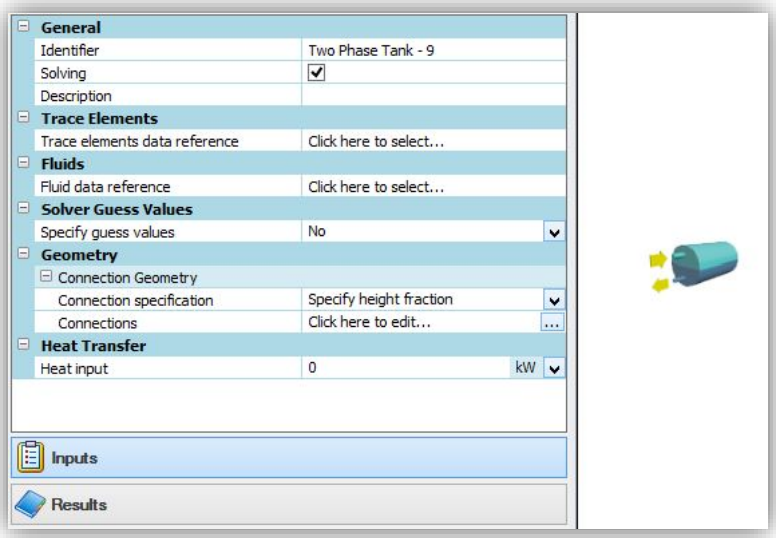

*Figure 41: Two phase tank component inputs dialogue box and component icon*

The component allows for the geometry of the tank to be modelled to be specified. In addition to this, it allows a volume or height fraction to be specified for each of the connections made between the tank and the external elements.

The two phase tank component contains steady state control options which can be used to achieve steady state mass balance of the component without using the iterative designer. The control options allow the user to specify a quality/level and starting pressure and the solver will calculate the appropriate mass flow(s) needed to achieve steady state balance. This mass flow will then be imposed onto the connecting element chosen as the “fixed mass flow element” as described in the preceding section for the flow resistance element. Depending on the options specified, Flownex can alter the design of the connected element to ensure that it produces the required mass flow rate even if the steady state control options are disabled.

**Trace elements**

Trace elements are used to represent elements suspended in a fluid with concentrations below 100 ppm. They can be traced around the network and are conserved in the same way that mass is conserved. Flownex reports the amount of trace elements anywhere in the network as a concentration, rather than the actual number of elements.

Trace elements are not automatically solved for by Flownex, the feature needs to be enabled. This is done by changing the “solve trace elements” option in the “Solvers/Utilities” window to “yes” (Figure 42).

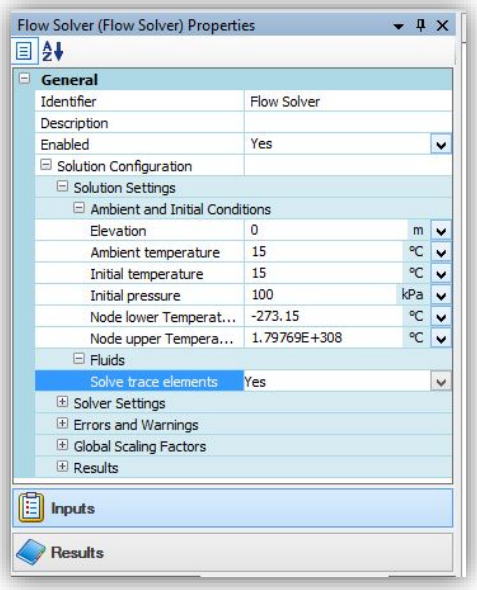


*Figure 42: Dialogue box showing the location of the "Solve trace elements" feature*

When the feature is activated, the user can then proceed to create trace elements that can be used to represent quantities or concentrations of interest around the Flownex network.

## 5.2 Model development

The development of the Flownex model consisted of the following four high level activities;

1. Library elements and components selection
2. Network set up and minimum input establishment
3. Excel component set up
4. Initiation and implementation

The four activities are described in the following sections.

### 5.2.1 Library elements and components selection

In order to develop a Flownex network representative of a typical deaerator system, the key components of a deaerator that affect its thermal-hydraulic behaviour had to be identified. These are;

- The deaerator and storage tank.
- The main condensate inlet to the deaerator – nozzle.
- The bled steam inlet to the deaerator.
- The return condensate inlet to the deaerator.
- The vent steam outlet.
- The deaerated water outlet.

The next step was to select suitable Flownex library element and components that represent, as close and as generic as possible, the six components listed above. The components and the library elements selected to represent them are discussed next.

**Deaerator and storage tank**

The deaerator is normally located on top of a storage or feedwater tank which is normally a horizontally oriented cylindrical tank with a plural of connections to the various streams entering and/or leaving the system. The volume of the actual deaerator is normally very small compared to that of the storage tank and because it does not maintain any level, it was neglected for this study and treated as part of the storage tank. During normal operation, the tank contains two phases with the liquid level being controlled by a level control system as described in section 2.3.3. It was decided that the tank will be represented by a two phase tank with the qualities described in section 5.1.

**Main condensate inlet - nozzle**

The main condensate inlet is usually a nozzle or atomizer. The nozzle may be of the fixed geometry (as described extensively in section 2.6) or variable geometry type. Regardless of the type, the atomizer can be adequately represented by a general empirical relationship element with an appropriate pressure loss coefficient. For the variable geometry type of atomizer, the pressure loss coefficient has to be presented as a function of the operating conditions in order to ensure that the element still simulates the actual atomizer operation. This is not necessary for the fixed geometry type as the pressure loss coefficient is constant.

**Bled steam inlet**

The bled steam inlet is normally a relatively large diameter pipe connected to the deaerating dome. The pressure drop across the connecting section is very low compared to pressure drops elsewhere in the system such that it was neglected in this study. The connection was therefore represented using a flow resistance element with a relatively high admittance, $A_f$.

**Return condensate inlet**

The return condensate inlet connection is usually a pipe section directly connected to the feedwater tank. The pipe diameter is significantly smaller than the feedwater tank and so there are significant pipe exit losses experienced at this point. In order to capture the losses adequately, a general empirical pressure loss element with a constant pressure loss coefficient was selected to represent the return condensate inlet connection.

**Vent steam outlet**

The vent steam normally exits the deaerator dome through a pipe either connected to a lower pressure vessel, like the condenser, or discharging the steam-NCG mixture directly to the atmosphere. The pipe normally has a valve that can be adjusted and therefore its pressure drop characteristics can be varied. The element selected to represent the vent pipe was the general empirical pressure loss element for reasons similar to that given for the return condensate inlet.

**Deaerated water outlet**

The deaerated water outlet is normally a large diameter pipe section connected to the tank. In some cases, the connection may be a vortex breaker. However, in order to obtain steady state balance on the two phase tank (deaerator), it was decided that the deaerator outlet be represented by a flow resistance element for which the “fixed mass flow option” is activated.

**Oxygen gas**

The oxygen gas concentration is represented using trace elements. Although strictly speaking, dissolved oxygen cannot be described as “particles suspended in a fluid”, it was decided that using trace elements was the most convenient and sensible approach to follow.

## 5.2.2 Model network set up and minimum inputs

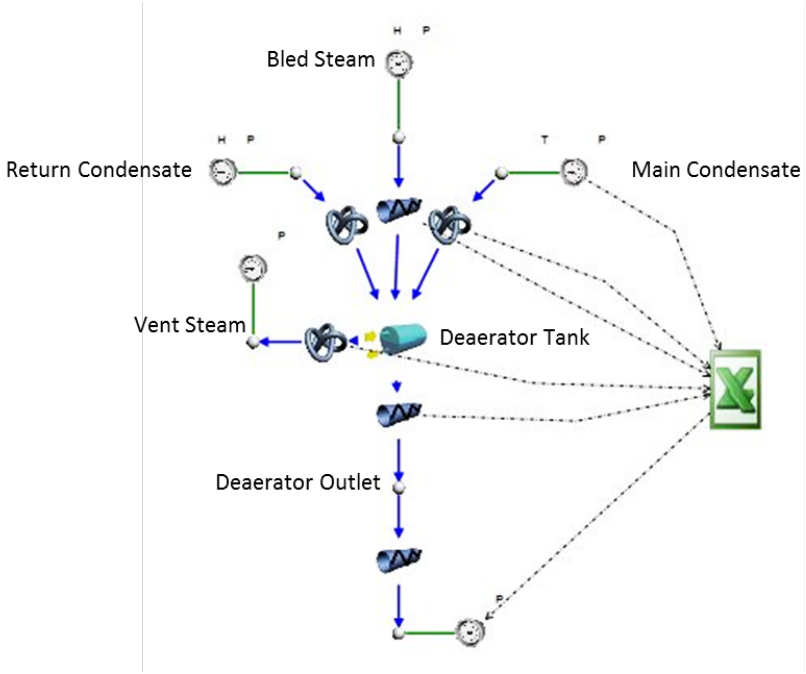


*Figure 43 : Deaerator model network*

The elements selected above were linked together as shown in Figure 43 to form the deaerator model network. In addition to the library elements and components, a Microsoft Excel component was also included. The main function of the Excel component is to calculate the concentration of oxygen in the deaerated water and relate it to the trace elements concentration at the deaerator outlet. An external component is required for this task as Flownex is not designed to perform mass transfer simulations. The Excel component determines the outlet oxygen concentration by solving the continuity equation for oxygen diffusion from a falling droplet in the same way as that detailed in the Execution section of the Analytical Model Development and Validation. The final concentration is then imposed as a boundary condition on the deaerated water outlet using the “data transfer links” feature. More about this feature will be presented shortly.

The minimum inputs required for each element are presented next.

**Boundary conditions**

The boundary conditions required for the Flownex model are quite different to those required for the analytical model. The primary reason for this is that the Flownex model also solves the momentum conservation equation for the bulk deaerator system, meaning that it can take a larger number of unknowns. The secondary reason is that the Flownex model was developed with the intended global power plant model in mind, therefore the parameters chosen as inputs are those which would result in minimal difficulties during the integration phase. The following boundary conditions should be specified;

- Pressure values at the deaerator boundary for all streams.
- The enthalpy values of the bled steam and return condensate streams.
- The temperature and oxygen concentration of the main condensate stream.

**Deaerator tank**

The minimum inputs for the deaerator tank are;

- The tank volume.
- The tank diameter.
- A volume fraction of 1 for the vent steam pipe.
- A volume fraction of 0 for the deaerated water outlet.

If the volume fractions of the other connections to the tank are known, they can be specified too. However, caution should be exercised when doing so since Flownex will include hydraulic heights based on the understanding that all boundary conditions are on the “0 elevation level”.

For this model, only the vent pipe and deaerated water outlet locations (volume fractions) are compulsory inputs as they are located in the same areas regardless of the deaerator system being modelled. For streams were volume fractions are not specified, Flownex will treat the two phase tank as one with homogenous properties with respect to those streams, and ignore the effects of the hydraulic pressure associated with the level inside the tank.

**Main condensate inlet-nozzle**

The minimum inputs required for the main condensate inlet are;

- A value for, or a script to calculate, the pressure loss coefficient $C_k$.
- A value of 1 for $\beta$ and 2 for $\alpha$.

Depending on the nozzle type, the pressure loss coefficient could be a constant or a function of the operating conditions. If the coefficient varies with operating conditions, an appropriate script should be written to update the value.

For this model, the value of the pressure loss coefficient is assumed to vary as a function of the pressure drop across the nozzle. In order to update the value for each different pressure drop, the "data transfer links" feature is used. This feature allows external software packages, such as Microsoft Excel for this study, to exchange information with the Flownex model and update certain fields if required. The transfer link used to update the pressure loss coefficient obtains a value for the pressure drop across the nozzle and uses that to calculate the pressure loss coefficient required for that set of conditions. The updated value is then sent back to the Flownex network using a second data transfer link, and used in the simulation.

The pressure drop is defined via the feedwater inlet pressure boundary, as well as the bled steam pressure boundary. The consequence is that the mass flow will be "adjusted" based on these conditions by means of the changing loss coefficient such that the appropriate feedwater mass flow is introduced into the deaerator.

**Bled steam inlet**

The minimum inputs for the bled steam inlet are;

- Flow resistance behaviour: Linear.
- Flow admittance: 0.01.

It is assumed that the density variations at the bled steam inlet are negligible and therefore the linear option for the flow resistance behaviour is chosen for improved accuracy. The flow admittance used could be larger but this would result in very small pressure drops across the flow resistance element, which may cause solver instabilities especially during transient simulations.

**Return condensate inlet and vent steam pipe**

The minimum inputs for these two streams are;

- A value for, or a script to calculate, the pressure loss coefficient $C_k$.
- A value of 1 for $\beta$ and 2 for $\alpha$.

The reason for two options to calculate the pressure loss coefficient have already been discussed under the minimum inputs section for the main condensate inlet. For this model, the pressure loss coefficient for the return condensate inlet and the vent steam pipe were set as a constants by default.

**Deaerated water outlet**

The deaerated water outlet is represented by two flow resistance elements connected in series. If one flow resistance element is used, it will effectively become a fixed mass flow element located between two pressure boundaries. This situation will cause an error and Flownex will not solve the

network. To overcome this, a second flow resistance element is connected in series with the first one.

The minimum inputs for the deaerated water outlet are;

- "Fixed mass flow" option enabled for the first flow resistance element.
- A flow admittance value for the first flow resistance.
- A flow admittance of 250 000 for the second flow resistance element.

The flow admittance value for the first flow resistance is not specified quantitatively here because it depends on the load case being simulated. When running the model in steady state, any high flow admittance value can be used, provided the "Fixed mass flow" option is enabled. However, during transient simulations, the option is disabled and the mass flow through the deaerator outlet will be calculated based on the flow admittance specified for the two flow resistances. In these cases, to ensure that the mass flow rates calculated are correct and do not result in untrue mass sources or sinks in the two phase tank, an appropriate flow admittance value for the first flow resistance element should be used to start with. The effect of varying this admittance essentially simulates the role of the boiler feed pump during standard deaerator operation. The speed of the pump varies with load and controls the mass flow rate drawn from the deaerator. In the global power plant model, a boiler feed pump will be present and used to control the mass flow rate drawn from the deaerator therefore inputting a load specific flow admittance becomes unnecessary.

### 5.2.3 Microsoft excel component set up

The Microsoft Excel component is responsible for solving the component continuity equation for oxygen diffusion from a falling droplet and establishing the outlet oxygen concentration. In cases where deaerators with variable geometry nozzles ae used, the component is also responsible for the updating of the pressure loss coefficient for the nozzle as it is dependent on the conditions under which the deaerator operates. The component is made up of three main sections and has a structure similar to that of the core analytical model. The sections are;

1. Inputs section
2. Execution section
3. Outputs section

The sections are briefly described below. It should be noted that the assumptions made in the Excel component calculations are exactly the same as those made in the analytical model and described in section 4.1. This section will therefore focus only on the constituents of the three

sections with the aim of making it possible to understand how the component works, and will not restate all the assumptions made.

**Inputs**

The inputs to the analytical component can be grouped into three classes according to the nature of information they provide and to their source. The constituents of each class will be described with the aid of screen shots from the component itself. Note that the input classes do not necessarily correspond to those of the analytical model although some of the class names may be identical.

*Process inputs*

This inputs class contains the thermal-hydraulic properties required to determine the dimensionless groups and other parameters required to solve the oxygen component continuity equation. The inputs are all obtained from the Flownex model through the use of data transfer links. Figure 44 is a screen shot showing the constituents of this class and their respective sources.

| PROCESS INPUTS FROM FLOWNEX | | | |
|---|---|---|---|
| **Description** | **Units** | **Symbol** | **Source** |
| Oxygen concentration at deaerator inlet | ppb | $c_{o2.in}$ | Trace element amount at GE representing nozzle |
| Main condensate mass flow rate | kg/s | $m_{mc}$ | Mass flow rate across GE representing nozzle |
| Main condensate temperature at deaerator inlet | K | $T_{dea.in}$ | Downstream temperature of GE representing nozzle |
| Deaerated water temperature at deaerator outlet | K | $T_{dea.out}$ | Upstream temperature of FR representing deaerator outlet |
| Main condensate density at deaerator inlet | $kg/m^3$ | $\rho_{dea.in}$ | Downstream density of GE representing nozzle |
| Main condensate density at deaerator outlet | $kg/m^3$ | $\rho_{dea.out}$ | Upstream density of FR representing deaerator outlet |
| Bled steam density at deaerator inlet | $kg/m^3$ | $\rho_{s.dea.in}$ | Dowstream density of FR representing bled steam inlet pipe |
| Bled steam density at deaerator outlet | $kg/m^3$ | $\rho_{s.dea.out}$ | Upstream density of GE representing vent pipe |
| Main condensate viscosity at deaerator outlet | kg/ms | $\mu_{dea.out}$ | Average viscosity across FR representing deaerator outlet |
| Bled steam viscosity at deaerator inlet | kg/ms | $\mu_{s.dea.in}$ | Average viscosity across FR representing the bs inlet pipe |
| Bled steam viscosity at deaerator outlet | kg/ms | $\mu_{s.dea.out}$ | Average viscosity across GE representing the vent pipe |
| Main condensate conductivity at deaerator inlet | W/mk | $k_{dea.in}$ | Average conductivity across GE representing nozzle |
| Main condensate conductivity at deaerator outlet | W/mk | $k_{dea.out}$ | Average condusctivity across FR representing deaerator outlet |
| Main condensate isobaric specific heat at deaerator inlet | J/kgK | $Cp_{dea.in}$ | Average specific heat across GE representing nozzle |
| Main condensate isobaric specific heat at deaerator outlet | J/kgK | $Cp_{dea.out}$ | Average specific heat across FR representing deaerator outlet |
| Main condensate pressure drop across deaerator nozzle | Pa | $\Delta P_{noz}$ | Pressure drop across general GE representing the nozzle |
| Main condensate pressure at nozzle inlet | Pa | $P_{mc}$ | Upstrem pressure of GE representing nozzle |
| Main condensate temperature at nozzle outlet | K | $T_{noz.in}$ | Upstream temperature of GE representing nozzle |
| Average main condensate density across nozzle | $kg/m^3$ | $\rho_{noz}$ | Average density across GE element representing the nozzle |
| Average main condensate viscosity across nozzle | kg/ms | $\mu_{noz}$ | Average viscosity across GE element representing the nozzle |

*Figure 44: Screenshot of the process inputs section of the Excel component*

Most of the inputs shown in Figure 44 are further processed later on in the Excel component. This is done because the values required to solve the oxygen component continuity equation are mainly those pertaining to the average properties across an element, or the saturated conditions

inside the tank. As these cannot be directly extracted from the Flownex model, the upstream and downstream values of certain elements of interest are extracted and then further processed to determine the actual average values required. For cases where variable geometry nozzles are used, the pressure drop across the general empirical element representing the nozzle is also extracted from Flownex model as an input to the Excel component. The reasons for this are explained in section 5.3.1 which is concerned with the determination of the nozzle pressure loss characteristics.

*Design specification inputs*

This inputs class contains those inputs that describe the physical design parameters of the deaerator being modelled. As with the analytical model, the inputs specified here are mainly those pertaining to the design characteristics of the nozzle in the first deaerating stage. Figure 45 is a screen shot showing the constituents of this class and their respective sources.

| DESIGN SPECIFICATION INPUTS | | | |
|---|---|---|---|
| **Description** | **Units** | **Symbol** | **Source** |
| Number of Nozzles | - | $N_{noz}$ | Design Specification or calibaration |
| Nozzle discharge diameter | m | $d_0$ | Design Specification or calibaration |
| Nozzle X factor | - | $X$ | Design Specification or calibaration |
| Deaerator preheater length | m | $L_{preheater}$ | Design Specification or calibaration |

*Figure 45: Screenshot of the design specification inputs section of the Excel component*

Unlike with the analytical model, the Flownex model is not self-calibrating and therefore the parameters required in this input class need to be known before the model is used. Calibration exercises similar to those described for the analytical model can be used to obtain the required values.

*Miscellaneous inputs*

This input class contains the chemical properties of both oxygen and water required to solve the component continuity equation for oxygen diffusion from a falling droplet, and the rest of the inputs required to make the model work. These include the nozzle spray angle and the Henry's law constant information.

The outputs section of the Excel component is discussed next. This is merely done for clarity and does not reflect on the actual sequence of the sections in the Excel component.

| MISCELLANEOUS INPUTS | | | |
|---|---|---|---|
| **Description** | **Units** | **Symbol** | **Source** |
| Ambient Tempertaure | K | $T_{\vartheta}$ | Miscellaneous input |
| Ambient Pressure | kPa | $P_{\vartheta}$ | Miscellaneous input |
| Ideal gas constant | J/molK | $R_{ideal}$ | Miscellaneous input |
| Henry's Law Constant at ambient conditions | $kmol/m^3 atm$ | $K_{H\vartheta}$ | Miscellaneous input |
| Association parameter for solvent water | - | $\varphi_{water}$ | Miscellaneous input |
| Molecular weight of solvent water | g/mol | $M_{water}$ | Miscellaneous input |
| Molal volume of oxygen at normal boiling point | $cm^3/mol$ | $V_{oxygen}$ | Miscellaneous input |
| Molar mass of oxygen | g/mol | $M_{oxygen}$ | |
| Oxygen mole fraction in air | - | $mf_{02.air}$ | Miscellaneous input |
| Unit conversion factor | $mol/m^3$ | **ppb to M** | Miscellaneous input |
| Gravitational acceleration | $m/s^2$ | **g** | Miscellaneous input |
| Critical temperature of water | K | $T_{lim.up}$ | Miscellaneous input |
| Dimensionless temperature limiting check (for transients only) | | | |
| Resolution of temperature measuring equipment | K | **ΔK** | User specified input |
| Spray angle | deg | $\vartheta$ | User specified input |

*Figure 46: Screenshot of the miscellaneous inputs section of the Excel component*

**Outputs section**

The outputs of the Excel component are;

- The nozzle pressure loss coefficient which is sent back to the model via a data transfer link connected to the general empirical element representing the nozzle (only for cases where variable geometry nozzles are used).
- The outlet oxygen concentration which is sent back to the model via a data transfer link connected to the boundary condition at the deaerator outlet.
- The overall mass transfer coefficient.

The last output is not sent back to the model and exists as an additional output for cases were the user may want further insight into the NCG extraction capabilities of the system.

The processes followed to convert the inputs into outputs are presented next.

**Execution section**

In the execution section the model essentially determines;

- The nozzle pressure loss coefficient (only for cases where variable geometry nozzles are used).
- The outlet oxygen concentration.

*Determination of the nozzle pressure loss coefficient*

The nozzle pressure loss coefficient is determined using the pressure drop across the nozzle (obtained from the Flownex model). This is done using a pre-defined relationship that links the two parameters. The nature of the relationship is described in section 5.3.1.

*Determination of the outlet oxygen concentration*

The first step taken in determining the outlet oxygen concentration is that of preparing the process inputs obtained from the Flownex model. The preparation uses the process inputs to calculate the average conditions that will be used to determine the parameters required to solve the oxygen component continuity equation. Figure 47 shows the description of the resulting average values, their symbols and the equations used to compute the average values.

| FLOWNEX DATA PREPARATION | | | |
|---|---|---|---|
| **Description** | **Units** | **Symbol** | **Equation** |
| Average main condensate density in deaerator | $kg/m^3$ | $\rho_{dea}$ | $\rho_{dea} = \frac{\rho_{dea.in} + \rho_{dea.out}}{2}$ |
| Average steam density in deaerator | $kg/m^3$ | $\rho_{s.dea}$ | $\rho_{s.dea} = \frac{\rho_{s.dea.in} + \rho_{s.dea.out}}{2}$ |
| Average steam viscosity in deaerator | $kg/ms$ | $\mu_{s.dea}$ | $\mu_{s.dea} = \frac{\mu_{s.dea.in} + \mu_{s.dea.out}}{2}$ |
| Average main condensate surface tension across nozzle | $N/m$ | $\sigma_{noz}$ | $\sigma_{noz} = \frac{\sigma_{noz.in} + \sigma_{noz.out}}{2}$ |
| Average main condensate conductivity in deaerator | $W/mk$ | $k_{dea}$ | $k_{dea} = \frac{k_{dea.in} + k_{dea.out}}{2}$ |
| Average main condensate isobaric specific heat | $J/kgK$ | $Cp_{dea}$ | $c_{p.dea} = \frac{c_{p.dea.in} + c_{p.dea.out}}{2}$ |
| Target temperature | $K$ | $T_{target}$ | $T_{target} = T_{dea.out} - \Delta K$ |

*Figure 47: Screenshot showing the results of the Flownex data preparations section of the Excel component*

The target temperature represents the temperature at which deaeration is expected to start happening. It is offset from the saturation temperature by 0.05°C to avoid getting a dimensionless temperature of 1 which would represent a mathematical discontinuity and hence make it impossible to obtain the time required for heat transfer. The value of 0.05°C is specified as $\Delta K$ in the inputs and represents what was termed “the resolution of the temperature measuring device”. In principle this should not affect the accuracy of the model since deaerators normally only heat the water to within a degree or two of the saturation temperature.

The second step is the determination of the nozzle specific parameters that are required to determine some of the parameters needed to solve the oxygen component continuity equation.

These are the parameters expected to change if any other nozzle type is used in the model as explained in the Execution section of the analytical model. The key outputs of this section, used directly in the oxygen component continuity equation, are the SMD $D_{32}$ and the droplet velocity $U_{droplet}$. Figure 48 shows the description of the determined parameters, their symbols and the equations used to compute them.

| NOZZLE SPECIFIC PREPARATION | | | |
|---|---|---|---|
| **Description** | **Units** | **Symbol** | **Equation** |
| Sauter Mean Diameter (SMD) | m | $D_{32}$ | $D_{32} = 2.25\sigma^{2.25}\mu_L^{0.25}m_L^{0.25}\Delta P_L^{-0.5}\rho_A^{-0.25}$ |
| Nozzle discharge area | $m^2$ | $A_0$ | $A_o = \frac{\pi d_o^2}{4}$ |
| Droplet velocity | m/s | $U_{droplet}$ | $U_{droplet} = \frac{\frac{m_{mc}}{N_{noz}}}{\rho_{noz}A_0(1-X)}$ |

*Figure 48: Screenshot showing the results of the nozzle specific preparations section of the Excel component*

The third step in determining the outlet oxygen concentration is determining the heat and mass transfer characteristics that eventually provide the final parameters that are required to solve the oxygen component continuity equation. It is in this section that the rest of the parameters used directly in the oxygen component continuity equation are determined. These are;

- The diffusivity of oxygen in water.
- The time available for mass transfer.
- The Sherwood number.

Figure 49 is a screenshot of this third step, which is labelled under Mass Transfer Preparation. The red arrows show where each calculated value is used. The equations used to calculate each value are also shown.

The last parameter is the maximum oxygen concentration that can exist in the feedwater. This value is based on the thermodynamic properties of the main condensate at the deaerator inlet (as explained in section 4.1.3) and should be used only when the inlet concentration of oxygen is unknown.

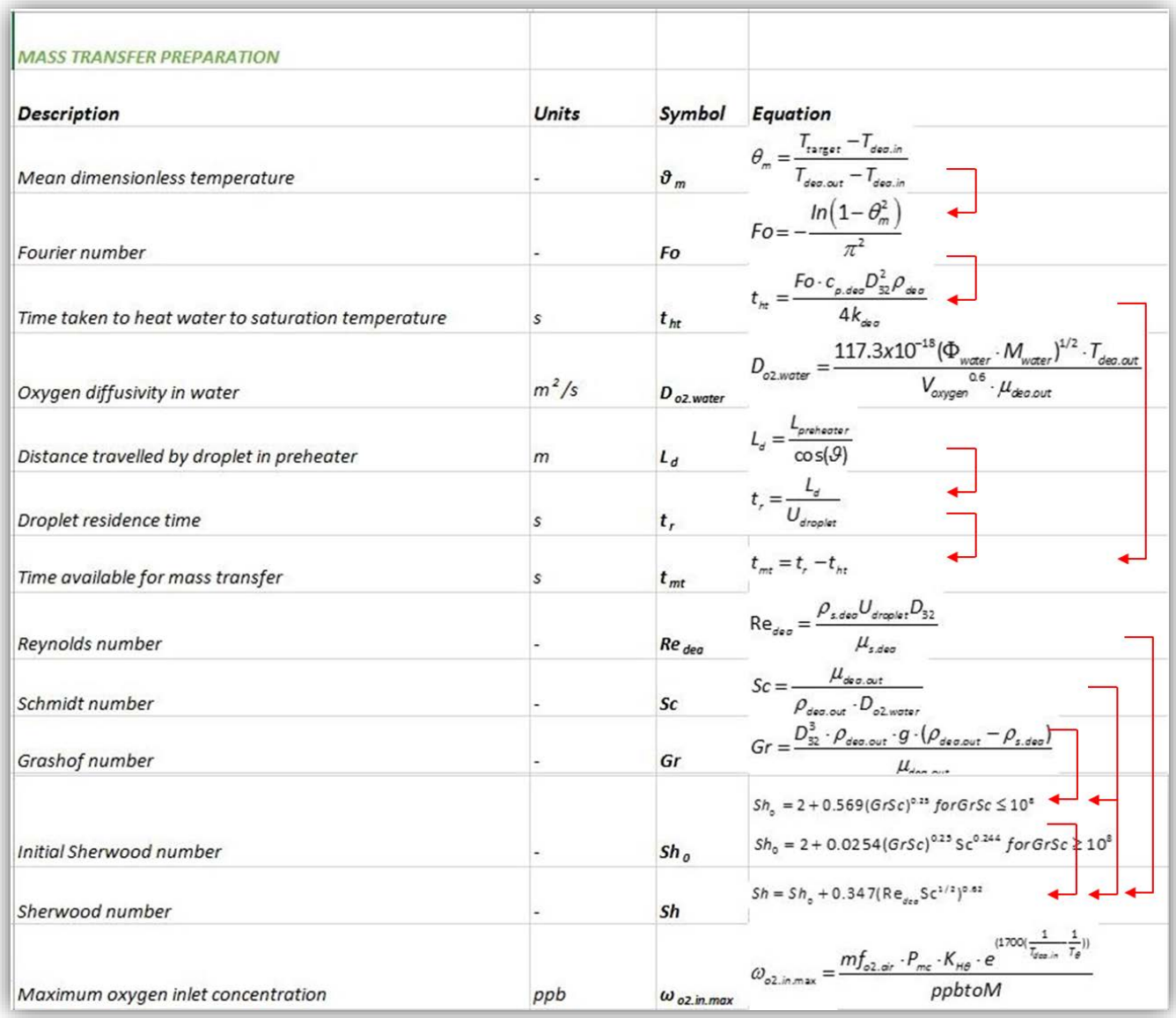

MASS TRANSFER PREPARATION

| Description | Units | Symbol | Equation |
|---|---|---|---|
| Mean dimensionless temperature | - | $\vartheta_m$ | $\theta_m = \frac{T_{target} - T_{dea.in}}{T_{dea.out} - T_{dea.in}}$ |
| Fourier number | - | $Fo$ | $Fo = -\frac{In(1-\theta_m^2)}{\pi^2}$ |
| Time taken to heat water to saturation temperature | s | $t_{ht}$ | $t_{ht} = \frac{Fo \cdot c_{p.dea} D_{32}^2 \rho_{dea}}{4k_{dea}}$ |
| Oxygen diffusivity in water | $m^2/s$ | $D_{o2.water}$ | $D_{o2.water} = \frac{117.3x10^{-18}(\Phi_{water} \cdot M_{water})^{1/2} \cdot T_{dea.out}}{V_{oxygen}^{0.6} \cdot \mu_{dea.out}}$ |
| Distance travelled by droplet in preheater | m | $L_d$ | $L_d = \frac{L_{preheater}}{\cos(\vartheta)}$ |
| Droplet residence time | s | $t_r$ | $t_r = \frac{L_d}{U_{droplet}}$ |
| Time available for mass transfer | s | $t_{mt}$ | $t_{mt} = t_r - t_{ht}$ |
| Reynolds number | - | $Re_{dea}$ | $Re_{dea} = \frac{\rho_{s.dea} U_{droplet} D_{32}}{\mu_{s.dea}}$ |
| Schmidt number | - | $Sc$ | $Sc = \frac{\mu_{dea.out}}{\rho_{dea.out} \cdot D_{o2.water}}$ |
| Grashof number | - | $Gr$ | $Gr = \frac{D_{32}^3 \cdot \rho_{dea.out} \cdot g \cdot (\rho_{dea.out} - \rho_{s.dea})}{\mu_{dea.out}}$ |
| Initial Sherwood number | - | $Sh_0$ | $Sh_0 = 2 + 0.569(GrSc)^{0.25}$ for $GrSc \leq 10^8$<br>$Sh_0 = 2 + 0.0254(GrSc)^{0.25} Sc^{0.244}$ for $GrSc \geq 10^8$ |
| Sherwood number | - | $Sh$ | $Sh = Sh_0 + 0.347(Re_{dea} Sc^{1/2})^{0.62}$ |
| Maximum oxygen inlet concentration | ppb | $\omega_{o2.in.max}$ | $\omega_{o2.in.max} = \frac{mf_{o2.air} \cdot P_{mc} \cdot K_{H\theta} \cdot e^{(1700(\frac{1}{T_{dea.in}} - \frac{1}{T_\theta}))}}{ppbtoM}$ |

*Figure 49: Annotated screenshot of the mass transfer preparations section*

The last step in determining the outlet oxygen concentration is that of actually solving the oxygen component continuity equation. This is carried out in the calculations section of the executions section in the Excel component. Figure 50 is a screenshot showing the calculations section and the equations used to arrive at the desired values.

The outlet oxygen concentration is then sent back to the Flownex model through the use of a data transfer link. The mass transfer coefficient is not sent anywhere but is calculated as an additional parameter to provide further insight into the mass transfer characteristics of the deaerator being modelled.

| CALCULATION | | | |
|---|---|---|---|
| **Description** | **Units** | **Symbol** | **Equation** |
| Oxygen concentration at deaerator outlet | ppb | $\omega_{o2.out}$ | $\omega_{o2.out} = \omega_{o2.in} e^{-6\frac{Sh \cdot D_{o2.water}}{D_{32}^2} \cdot t_{mt}}$ |
| Mass transfer coefficient | m/s | $k_L$ | $k_L = \frac{Sh \cdot D_{o2.water}}{D_{32}}$ |

*Figure 50: Screenshot of the calculations section of the Excel component*

## 5.2.4 Network initialization and implementation

Once the model is set up correctly and all minimum inputs have been declared, the steady state control options need to be initialized.

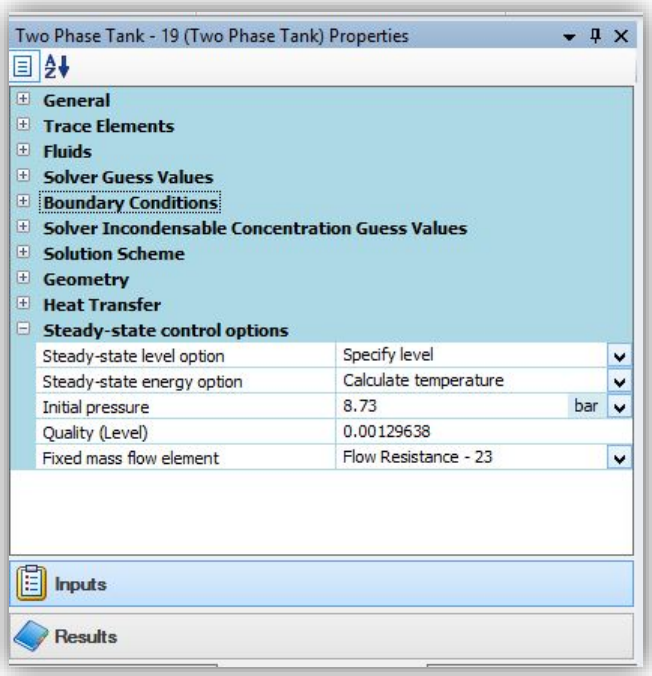


*Figure 51: Steady-state control options dialogue box.*

The initiation is achieved by choosing the “Specify level” and “Calculate temperature” options for the two phase tank as shown in Figure 51. The initial pressure used should correspond to the deaerator pressure required for the load case being simulated. For this study, this pressure is equal to the bled steam pressure at the deaerator entrance. The quality specified should correspond to the control level inside the deaerator during normal operation at the load case being simulated. The conversion from level to quality can be done using equations shown below.

$$x = \frac{\rho_{gas} \cdot \left(V_{dt} - V_{liquid}\right)}{\rho_{gas} \cdot \left(V_{dt} - V_{liquid}\right) + \rho_{liquid} \cdot V_{liquid}} \tag{77}$$

With,

$$V_{liquid} = L_{dt}\left[R_{dt}^2 \cos^{-1}\left(\frac{R_{dt} - h_L}{R_{dt}}\right) - \left(R_{dt} - h_L\right) \cdot \sqrt{2 \cdot R_{dt} \cdot h_L - h_L^2}\right] \tag{78}$$

Where;

- $L_{dt}$ is the deaerator tank length.
- $R_{dt}$ is the deaerator tank radius.
- $h_L$ is the liquid level inside the deaerator tank (3.44m for Plant 1).
- $\rho_{gas}$ is the density of saturated vapour at the deaerator pressure.
- $\rho_{liquid}$ is the density of saturated liquid at the deaerator pressure.
- $V_{dt}$ is the total deaerator tank volume.

The "fixed mass flow element" should be chosen as the first flow resistance element representing the deaerator outlet.

Having specified all boundary values and performed the initialization steps, the model can be run in steady state. If the user wishes to perform a transient simulation, the steady state control option should be disabled to enable the level changes inside the tank to be simulated and tracked correctly. Disabling the steady state control options is achieved through unfixing the mass flow rate flowing out of the deaerator by setting a transient action to calculate the required mass flow rate. This ensures that the mass flow rate flowing out of the deaerator is not constant and allows the level changes inside the deaerator to be correctly simulated.

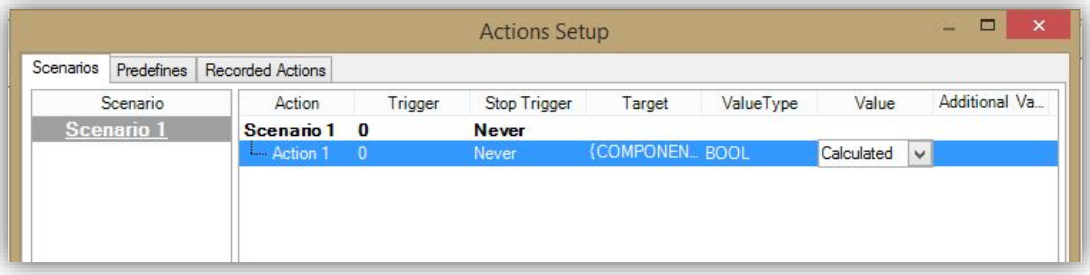


*Figure 52: Actions set up dialogue box showing the "calculated" option for the deaerator outlet mass flow rate*

## 5.3 Determination of design specific parameters

The Flownex model clearly requires much more design information compared to the analytical model, and has no self-calibration abilities, meaning that the information needs to be known

before using the model. The preceding discussions on how to set up and run the model assume that the user of the model will know all of the information required. This is rarely the case and this section is dedicated to illustrating some methods that can be used to determine the pressure loss characteristics of the nozzle and return condensate streams together with the flow admittance for the deaerator outlet stream.

Although the nozzle dimensions and pressure loss characteristics of the vent pipe are also required to run the model, they were discussed in section 4.2 and will not be covered here.

### 5.3.1 Determination of the nozzle pressure loss characteristics

The technique used to establish the nozzle pressure loss characteristics is very similar to that used to find the vent pipe pressure loss characteristics as detailed in the preceding chapter. The difference is that the process is carried out for all load cases until a set of pressure loss coefficients corresponding to known pressure drops across the nozzle is obtained. The pressure loss coefficients are then plotted against the pressure drops and an appropriate curve fitted. The equation corresponding to this curve can take any form depending on the nozzle type, but has to be explicitly expressible in the form shown by equation (79)

$$C_{K.mc} = f(\Delta P_{mc}) \tag{79}$$

The obtained equation can then be used in the Excel component to update the pressure loss coefficient for each simulation. For constant geometry nozzles, the pressure loss coefficient need only be determined for the nominal load case and kept constant.

It is important to note that the method suggested here is for use in instances where the process conditions of the deaerator at different loads are known, but the design information pertaining to the nozzle is not known or is inadequate. Some nozzle manufacturers provide performance curves which can be digitized and represented in equation form as well. In cases were better information is present, it should be used for improved accuracies.

### 5.3.2 Determination of the return condensate inlet pressure loss coefficient

The return condensate pressure loss characteristics are obtained in the exact same way as the vent pipe pressure loss coefficient described in section 4.2.1. The inlet connection to the tank is of a constant geometry and so the loss characteristics do not change with load and need only be established at the nominal load case.

In instances were detailed drawings of the deaerator are available, the pressure loss coefficient for the return condensate stream can be easily obtained by inspecting the exact geometry and using standard thermal-fluids approaches and loss factors. In these cases, it is advised to do this for improved accuracy.

### 5.3.3 Determination of deaerator outlet admittance

The determination of the admittance value for the first flow resistance element representing the deaerator outlet is slightly different and makes use of the Flownex model itself. In order to use Flownex to calculate the admittance values, the model described above is run with the "Change design" option enabled for the flow resistance element in question (Figure 53).

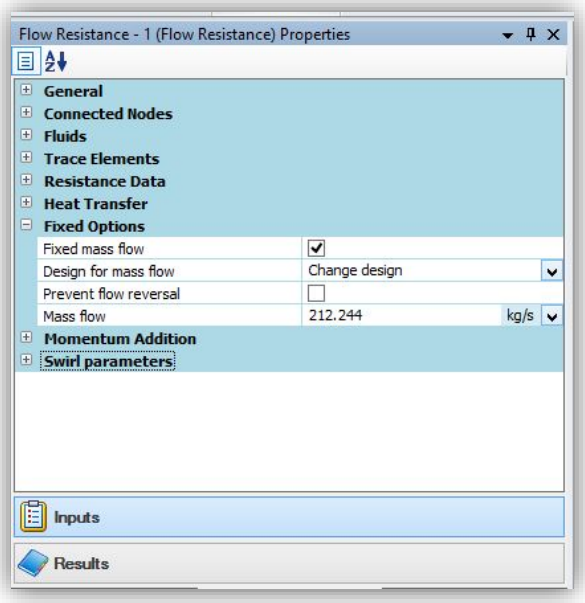


*Figure 53: Inputs tab for the first flow resistance element representing the deaerator outlet*

Flownex then calculates the flow admittance value required to allow that same mass flow rate through the flow resistance element even if the steady state control options on the two phase tank were disabled, as they are in transient simulations. The result of this process is the flow admittance for flow resistance corresponding the load case being simulated. The same can be done for all load cases and a plot similar to that suggested for the nozzle pressure loss coefficient plotted.

In instances were better information about the variation of the mass flow rate at the deaerator outlet is known, it should be used for improved accuracy.

## 5.4 Flownex model verification

The Flownex model was verified by running it for the Plant 1 deaerator system described in section 4.4.1 and comparing its results to that of the analytical model. The specifics of the system and the data pre-processing exercises performed will not be re-written here as they are reported in the previous chapter. Here only the inputs to the model and the results for the 100% load case are presented and discussed.

**Inputs**

Shown in Table 9 are the inputs to the Flownex model for the Plant 1 deaerator system at 100% load.

*Table 9: Inputs to the Flownex model for the Plant 1 deaerator system at 100% load.*

| ***Parameter*** | ***Value*** | ***Unit*** |
|---|---|---|
| | | |
| *Main condensate pressure ($P_{mc}$)* | *13.34* | *bar* |
| *Main condensate temperature ($T_{mc}$)* | *143.829* | *°C* |
| *Main condensate pressure loss coefficient ($C_{k.mc}$)* | *13081.5* | *$m^4$* |
| *Bled steam pressure ($P_{bs}$)* | *8.73* | *bar* |
| *Bled steam enthalpy ($h_{bs}$)* | *3149.81* | *kJ/kg* |
| *Return condensate pressure ($P_{rc}$)* | *9.39* | *bar* |
| *Return condensate enthalpy ($h_{rc}$)* | *877.3* | *kJ/kg* |
| *Return condensate pressure loss coefficient ($C_{k.rc}$)* | *8106.51* | *$m^4$* |
| *Vent steam pressure ($P_{vs}$)* | *1.013* | *bar* |
| *Vent steam pressure loss coefficient ($C_{k.vs}$)* | *$1.77 \times 10^7$* | *$m^4$* |
| *Deaerated water pressure ($P_{dw}$)* | *8.73* | *bar* |
| *Deaerated water outlet admittance ($Af_{.dw}$)* | *7.69* | *-* |
| *Deaerator tank volume ($V_{dt}$)* | *218* | *$m^3$* |
| *Deaerator tank diameter ($D_{dt}$)* | *4.5* | *m* |
| *Deaerator tank initial pressure ($P_{dea.in}$)* | *8.73* | *bar* |
| *Deaerator tank quality (x)* | *0.001296377* | *-* |
| *Oxygen inlet concentration ($\omega_{o2}$)* | *22650.286* | *ppb* |

The Plant 1 deaerator system is fitted with a variable geometry nozzle of the type described in section 2.6.3. In order to determine the pressure loss characteristics of this nozzle at different operating conditions, the excel component is used as described in section 5.2.3. Figure 54 shows the variation of the pressure loss coefficient with the pressure drop across the model. The equation representing the shown relationship is shown below.

$$C_{k.mc} = -416416.321545 \cdot \Delta P_{noz}^3 + 5397591.36223 \cdot \Delta P_{noz}^2 - 23311137.0325 \cdot \Delta P_{noz} + 33564487.0541$$

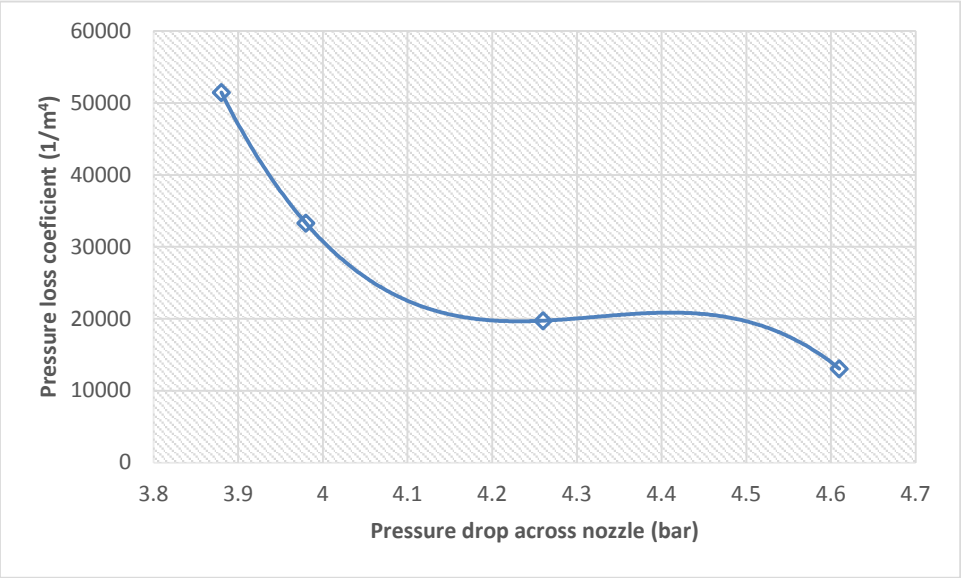


*Figure 54: Pressure loss coefficient variation with nozzle pressure drop for the Plant 1 deaerator system*

**Results**

The Flownex model result consists of the mass flow rates, and the temperature and pressure conditions throughout the network. This is significantly more detailed than the analytical model result and therefore only a few parameters could compared. These were:

- The mass flow rates of all streams crossing the deaerator boundary.
- Deaerator pressure.
- Deaerated water temperature.
- Oxygen concentration in the deaerated water

The values of these parameters for the 100% load case as predicted by the Flownex model are shown in Table 10.

*Table 10: Outputs from the Flownex model for the Plant 1 deaerator system at 100% load.*

| ***Parameter*** | ***Value*** | ***Unit*** |
|---|---|---|
| | | |
| *Main condensate mass flow rate ($m_{mc}$)* | *180.526* | *kg/s* |
| *Bled steam mass flow rate ($m_{bs}$)* | *8.68* | *kg/s* |
| *Return condensate mass flow rate ($m_{rc}$)* | *23.3657* | *kg/s* |
| *Vent steam mass flow rate ($m_{vs}$)* | *0.332* | *kg/s* |

| | | |
|---|---|---|
| *Deaerated water mass flow rate ($m_{dw}$)* | *212.244* | *kg/s* |
| *Deaerator pressure ($P_{dea}$)* | *8.72* | *bar* |
| *Deaerated water temperature ($T_{dea}$)* | *174.02* | *°C* |
| *Oxygen concentration in deaerated water ($\omega_{o2}$)* | *6.82* | *ppb* |

**Error calculation and discussion**

The comparison between the analytical and Flownex model predictions was achieved by determining the error associated with the Flownex model predictions. In this context, the error is defined as a representation of the difference between the predictions of the two models, and is calculated using equation (80) below.

$$error = \frac{Flownex\,\mathrm{mod}el\ prediction - Analytical\,\mathrm{mod}el\ prediction}{Analytical\,\mathrm{mod}el\ prediction} \times 100 \tag{80}$$

*Table 11: Flownex model errors for the Plant 1 deaerator system at 100% load*

| ***Parameter*** | ***Analytical Model Prediction*** | ***Numerical Model Prediction*** | ***Units*** | ***Error (%)*** |
|---|---|---|---|---|
| | | | | |
| *Main condensate mass flow rate (mmc)* | 180.36 | *180.526* | *kg/s* | *-0.09* |
| *Bled steam mass flow rate (mbs)* | 8.71 | *8.68* | *kg/s* | *0.31* |
| *Return condensate mass flow rate (mrc)* | 23.27 | *23.3657* | *kg/s* | *-0.41* |
| *Vent steam mass flow rate (mvs)* | 0.33 | *0.332* | *kg/s* | *0.63* |
| *Deaerated water mass flow rate (mdw)* | 212.00 | *212.244* | *kg/s* | *-0.11* |
| *Deaerator pressure (Pdea)* | 8.73 | *8.72* | *bar* | *0.11* |
| *Deaerated water temperature (Tdea)* | 174.07 | *174.02* | *°C* | *0.03* |
| *Oxygen concentration in deaerated water ($\omega_{o2}$)* | 7.00 | *6.82* | *ppb* | *2.57* |

Table 11 shows the errors associated with the Flownex model predictions. From the Error column, it is clear that the errors associated with most of the values are small, with most of them being less than 0.5%. These errors are attributable to the minor differences between the steam properties tables used, rounding errors and the deaerator pressure differences caused by the slight pressure drop over the bled steam inlet. The model was also run for the 46%, 60% and 80% load cases and the results are presented in graphical form (Figure 55). The inputs and actual results for each of these load cases can be found in Appendix A.

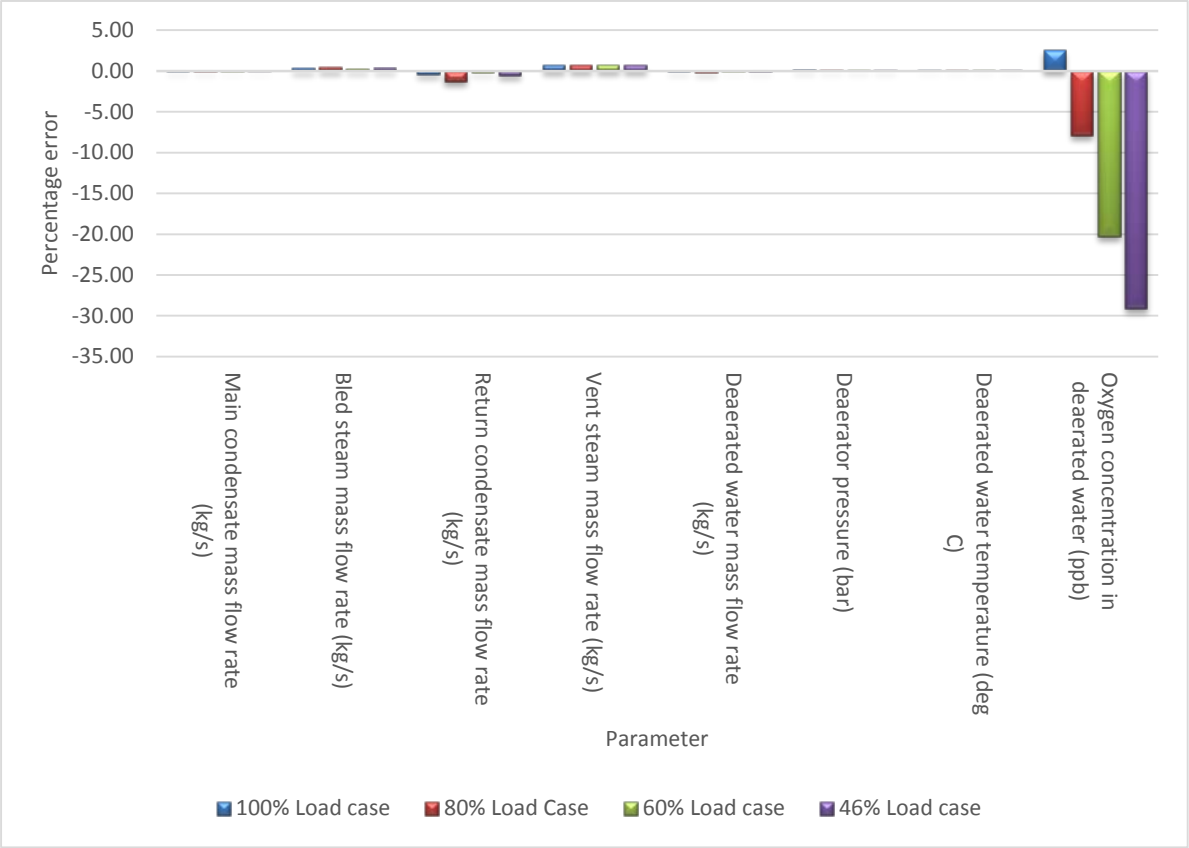


*Figure 55: Flownex model errors for the Plant 1 deaerator system at all loads*

Figure 55 shows that the differences between the Flownex and analytical model results are generally small (between 0.02% and 0.67%) except for the outlet oxygen concentration (between 2.57% and 29.17%). The errors observed can be attributed to the minor differences between the steam properties tables used, rounding errors and the differences in the deaerator pressure values used by the two models. In the analytical model, the deaerator pressure is set to be equal to the bled steam pressure at the deaerator inlet. On the other hand, the Flownex model calculates a deaerator pressure that is slightly lower than the bled steam pressure. This is a result of the small pressure drop experienced as the steam passes through the flow resistance element representing the bled steam inlet. This lower pressure then causes slight changes in the mass flow rates of all streams and a difference in the conditions inside the deaerator. The most affected parameter is the mass transfer computation as this is affected by the saturation temperature inside the deaerator.

That being said, Figure 55 somewhat exaggerates the errors associated with the outlet oxygen concentration. The method used to calculate the error inherently gives large error values for small differences if the parameter in question is of a small magnitude. To illustrate this point, Table 12 shows the actual differences between the Flownex and analytical model results for the oxygen concentrations. It is clear that the values are not as far apart as suggested by Figure 55.

*Table 12: Flownex model errors for the oxygen outlet concentration*

| ***Parameter*** | ***Analytical Model Prediction (ppb)*** | ***Numerical Model Prediction (ppb)*** | ***Difference (ppb)*** |
|---|---|---|---|
| | | | |
| *Oxygen concentration in deaerated water (ppb) 100% Load* | 7.000 | *6.820* | *0.18* |
| *Oxygen concentration in deaerated water (ppb) 80% Load* | 4.182 | *4.514* | *-0.33* |
| *Oxygen concentration in deaerated water (ppb) 60% Load* | 2.116 | *2.546* | *-0.43* |
| *Oxygen concentration in deaerated water (ppb) 46% Load* | 0.999 | *1.290* | *-0.29* |

In summary, the verification exercise was successful and showed that the Flownex deaerator model was a true representation of the analytical model, which itself was validated against actual reconciled plant data and shown to be a true representation of the Plant 1 deaerator system.

## 5.5 Flownex model validation

Following the verification exercise detailed in the preceding section, the Flownex model was validated by comparing its steady-state predictions to actual performance data for two different deaerator units. In addition, a transient case study was also performed. The validation exercises and results are presented in this section.

### 5.5.1 Plant 1 case study

The first validation exercise performed on the Flownex model consisted of comparing the steady-state model predictions for all load cases at Plant 1, with the actual reconciled data obtained from the system. The errors associated with the predictions were computed using equation(72), which is re-written here for convenience. The errors are shown represented in Figure 56.

$$\frac{actual\,value - predicted\,value}{actual\,value} \times 100 \tag{81}$$

The error values shown in Figure 56 are relatively small, ranging from 0% for the deaerated water temperature at the 60% load case, to 2.32% for the vent steam mass flow rate at the 46% load case. As observed for the analytical model validation in the previous chapter, the vent steam mass flow rates represent the highest errors with a combined average of 1.03%. In addition, it can be observed that the vent steam mass flow rate error steadily increases with decreasing load and is smallest at the 100% load case. These observations can be attributed to the fact that the pressure loss coefficient for the vent pipe was calculated at the 100% load case and assumed to stay constant throughout. As highlighted in the previous chapter, this is not always the case as a vent pipe valve may have been used to control and minimise the steam loss from the system.

In general, the results show good agreement between the model predictions and the actual results.

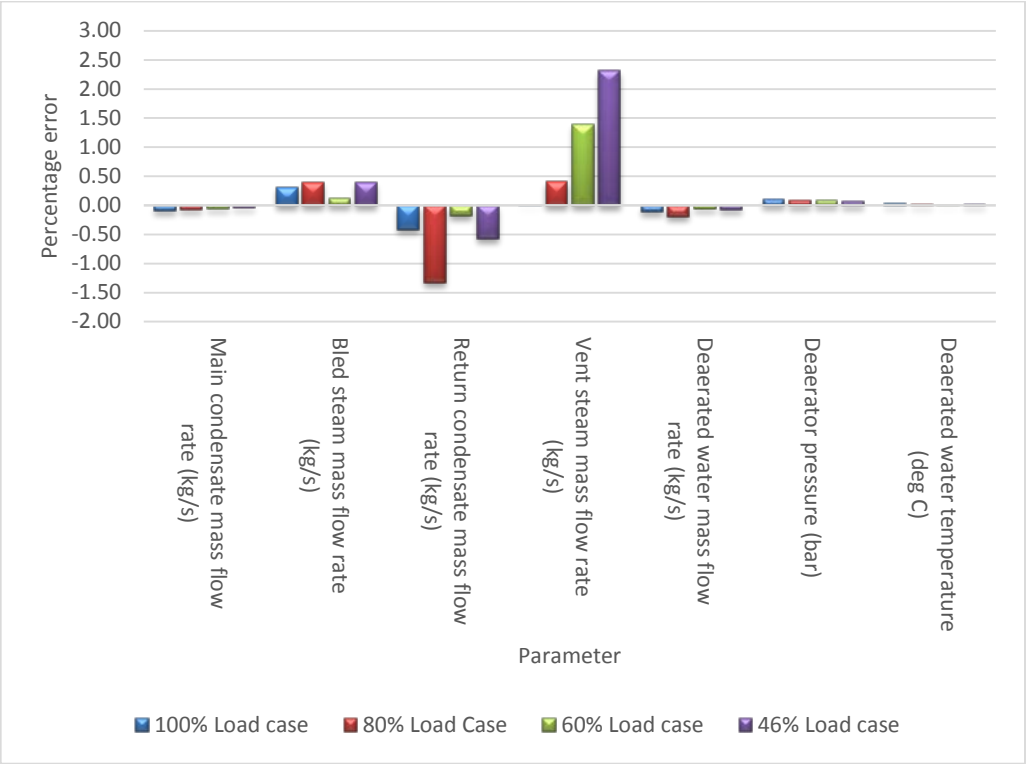


*Figure 56: Flownex model errors for the Plant 1 deaerator system at all loads*

A notable omission from Figure 56 are the error values associated with the outlet oxygen concentration predictions. There was no NCG concentration data available for the Plant 1 deaerator system and therefore no values to compare the model predictions to. However, the trends reported in the Analytical model mass transfer component validation section are also true for this model and it can therefore be said that its mass transfer characteristics are qualitatively valid, provided the system being modelled has a pressure swirl simplex atomizer.

A second case study was performed in order to demonstrate the performance of the model on a different deaerator system. The plant chosen for this exercise was Unit 3 of Plant 2 in Mpumalanga.

## 5.5.2 Plant 2 case study

Plant 2 has a stork type deaerator with the following properties;

- FWT volume 450m$^3$
- FWT diameter 4.5m
- Control level 2.9m
- Maximum condensate flow 500kg/s

The deaerator system consists of one deaerating tank fitted with two stork sprayers. It is located between FWH 4 and FWH 6 (Figure 57) and receives steam from the Intermediate pressure turbine during normal operation. The performance data of the system was obtained from heat balance diagrams and pre-processed in the exact same way as that described in sections 4.4.2 and 4.4.3.

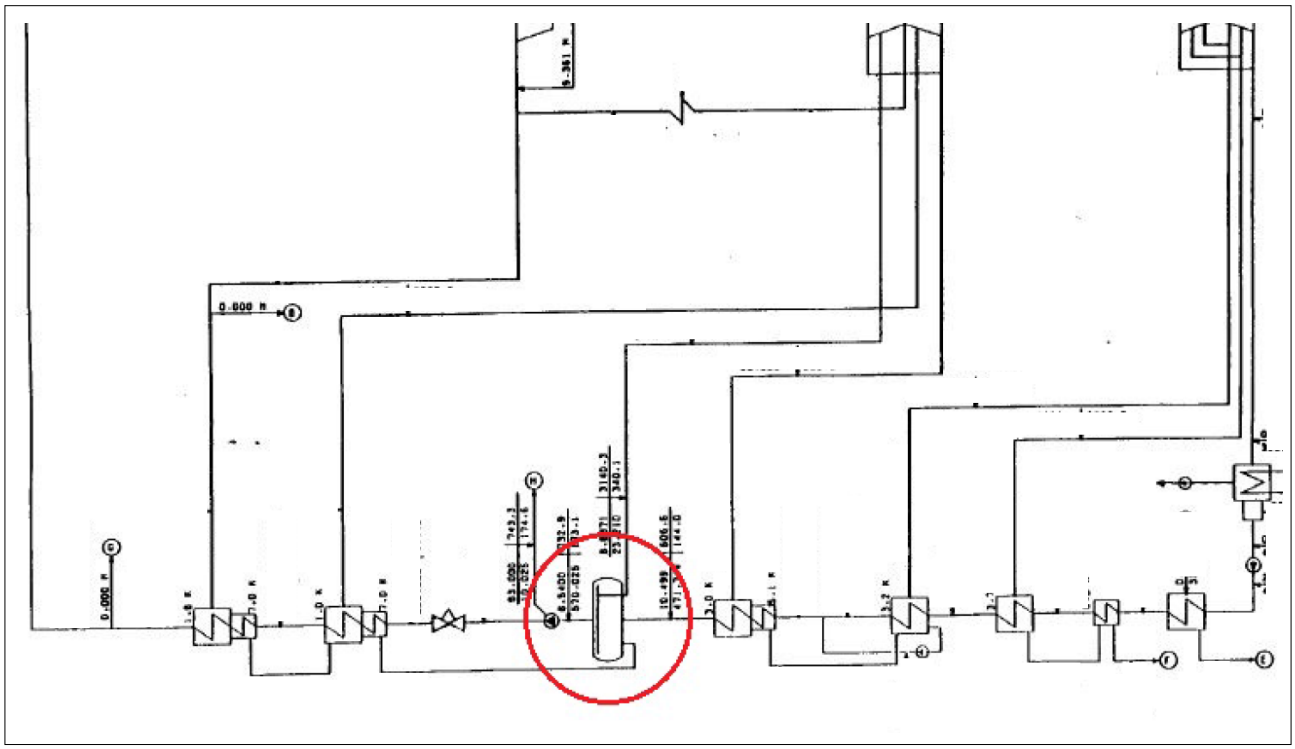

*Figure 57: Plant 2 Unit 3 deaerator system*

The model was set up and run in steady-state at all loads and the results obtained were compared to the performance data from the heat balance diagram. The errors associated with each value, as defined by equation (81) are shown in Figure 58 in graphical form. For the numerical input and output values related to each load case, the reader is directed to Appendix A.

Figure 58 shows that the Flownex model generally predicts the performance of the Plant 2 deaerator system well. The errors associated with the compared parameters range from 0% for a number of parameters, to -5.97% for the return condensate mass flow rate at the 40% load case. This large spike in the return condensate mass flow rate is attributable to the constant pressure loss characteristics assumed for the general empirical relationship element representing the return condensate inlet. It is possible that other elements e.g. downstream valves, may have been changed at the 40% load case. This would affect the pressure loss characteristics of the general empirical element but was not captured in the model.

Apart from the large spike in the return condensate mass flow rate error, the errors are generally high for the vent steam mass flow rate. This was also observed for the Plant 1 case study and the reasons for its occurrence are similar. In addition to the reasons stated before, it should be noted that the vent steam mass flow rate is very small compared to the total mass flowing through the deaerator such that small errors in the vent steam mass flow rate will not significantly affect the accuracy of the overall model. In general, Figure 58 shows good agreement between the Flownex model prediction and the actual reconciled data from Plant 2 as was observed for the Plant 1 case study.

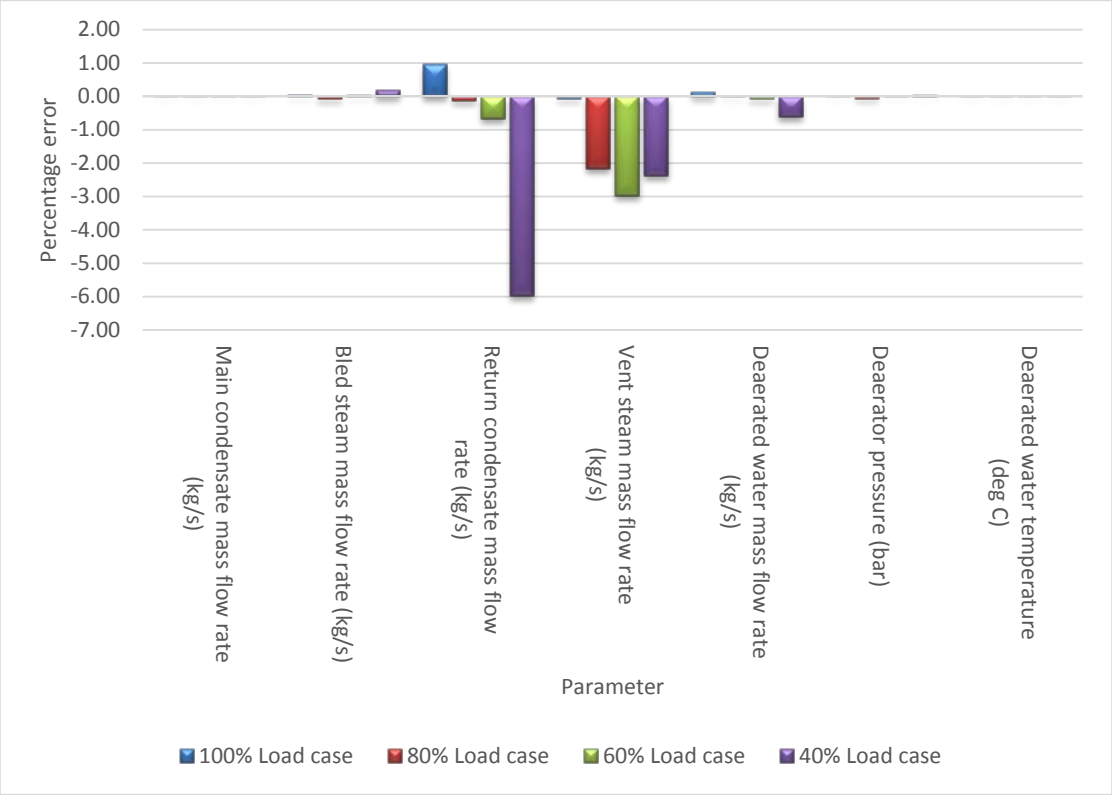


*Figure 58: Flownex model errors for the Plant 2 deaerator system at all loads*

The case studies presented so far have been limited to steady state simulations. This has been driven by the relative dominance of the steady state regime during normal power plant operation. However, the Flownex model can be used to simulate transient scenarios and the remainder of this section is devoted to demonstrating the transient performance of the model.

## 5.5.3 Transient model implementation, results and discussion

When any one, or a combination of the boundary conditions associated with normal steady-state operation is altered, the system conditions change in order to settle at a new steady-state regime. The operation between the two steady-state regimes is termed transient operation and is characterised by a change in the system conditions with time.

One key parameter that is bound to change during most transient operations concerning the deaerator is the condensate level inside the tank. Normally, this level is maintained at some pre-set value by a level control system as described in section 2.3.3. Such a control system links the deaerator to other plant components and its design was not within the scope of this study. Its omission made it impossible to compare the Flownex model transient response with any actual data as there are no deaerators in industry operating without level control systems. The transient validation exercise reported here is therefore limited to studying uncontrolled trends and evaluating whether or not they are expected and make sense.

The transient scenario simulated is one corresponding to a turbine trip at Plant 2 after 20s of steady state operation. During a turbine trip the following events take place: (Note that only those events directly affecting the deaerator are listed here).

1. The steam supply to the deaerator and FWHs is cut off and the turbine train pressure drops to the condenser pressure. To avoid rapid loss of deaerator pressure, which might lead to boiler feed pump cavitation or an implosion (although very unlikely), auxiliary steam is immediately supplied to the deaerator. This is normally at a slightly lower pressure and the source varies depending on the actual plant being simulated, but is often from the hot reheat line.
2. The bled steam and return condensate non-return valves are immediately shut in order to prevent the contents of the deaerator unit from flowing back into the turbine.
3. The inlet conditions of the main condensate, particularly the temperature and enthalpy, begin to change as the downstream feedwater heaters are also starved of heating steam.

**Model set up**

In order to simulate the above mentioned events, the following activities were performed. Each activity is numbered in accordance to the corresponding event.

1. A transient action was set to change the pressure boundaries corresponding to bled steam inlet to 7.4bar (auxiliary steam pressure), and the return condensate inlet to 0.136bar (condenser pressure) at 20s.
2. The “prevent flow reversal” option is enabled in order to simulate the closure of the valves. This option essentially provides an effect similar to that of a non-return valve.
3. A simplified network of the low pressure FWHs is developed in order to simulate the changes to the main condensate conditions at the deaerator inlet. The network is developed using operating manuals and heat balance diagrams from Plant 2. More of this is presented next.

In order to develop a simplified network of the low pressure FWHs at Plant 2, the following assumptions and simplifications were made;

- The same amount of condensate flows through all the FWHs between the condenser and the deaerator i.e. there are no additions or removals of condensate between the condenser and deaerator.
- The heater tubes and water boxes are full of water and therefore their design volume is representative of the total volume of water between the condenser and the deaerator.

Based on these assumptions and simplifications, each FWH was represented as a combination of one general empirical pressure loss element, one node and one composite heat transfer element (Figure 59). The general empirical pressure loss element was responsible for capturing the pressure loss characteristics of each FWH. The volumes of the water body and the metal associated with each heater were captured in the node and the composite heat transfer elements respectively. This was done in order to capture the thermal inertia of both the water body and the metal associated with the heaters and connecting pipes as accurately as possible. The areas available for heat transfer and the metal volumes were all obtained from the operator's manual of each of the FWHs.

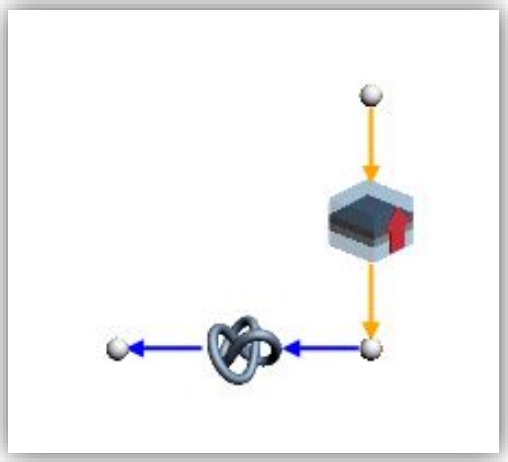

*Figure 59: Simplified network of a low pressure feedwater heater.*

The composite heat transfer element caters for the heat transfer operations that occur in a FWH viz. convection on the outside of the tubes, conduction through the tube material, and then convection on the inside of the tube. At 20s, an action is set up to disable the convective heat transfer on the outside of the tube. This is done by making the upstream heat transfer coefficient equal to 0, and has the same effect as stopping the bled steam flow to the respective feedwater heater. The complete network, with all FWHs connected together and to the deaerator is shown in Figure 60

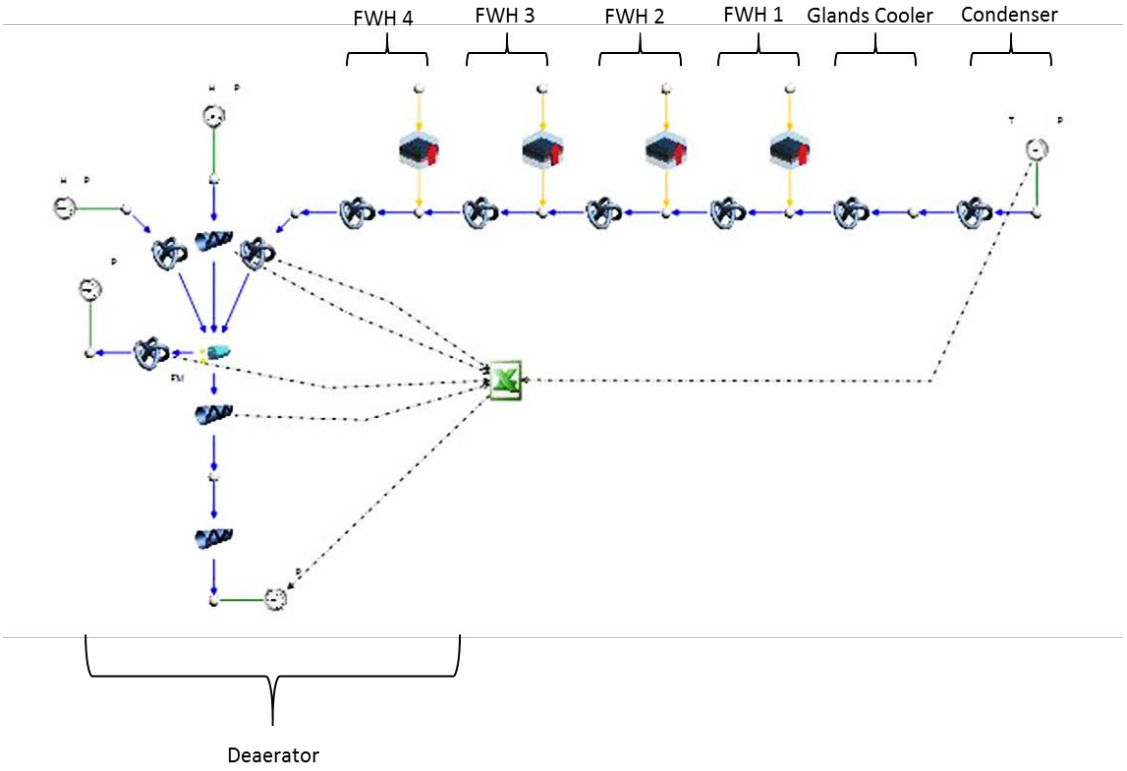


*Figure 60: Network representing the deaerator and simplified Low Pressure FWH train.*

Figure 60 shows that the first node is not connected to a composite heat transfer element. This node represents the glands cooler and so is modelled simply as a volume of water without a heat source. The Flownex designer function was used to calibrate the loss characteristics of the general empirical pressure loss elements to ensure that the correct mass flow rate flows through each FWH was captured. The same function was used to determine the bled steam temperatures that would ensure the expected outlet temperatures from each feedwater heater. An account of the design values used in this simulation is given in [39].

**Model implementation, results and discussion**

The model was initialised at the 100% load case for Plant 2. The transient actions described in the preceding section were implemented and the model was run for 200s. Five trends were analysed and discussed with the aid of theoretical considerations and literature references. These are;

- The variation of the low pressure FWH outlet temperatures and the main condensate inlet temperature with time during the transient scenario.
- The variation of the deaerator pressure with time during the transient scenario.
- The variation of the deaerator temperature with time during the transient scenario.
- The variation of the deaerator outlet oxygen concentration with time during the transient scenario.

- The variation of the condensate level inside the feedwater tank with time during the transient scenario.

The results obtained are shown and discussed below in that order.

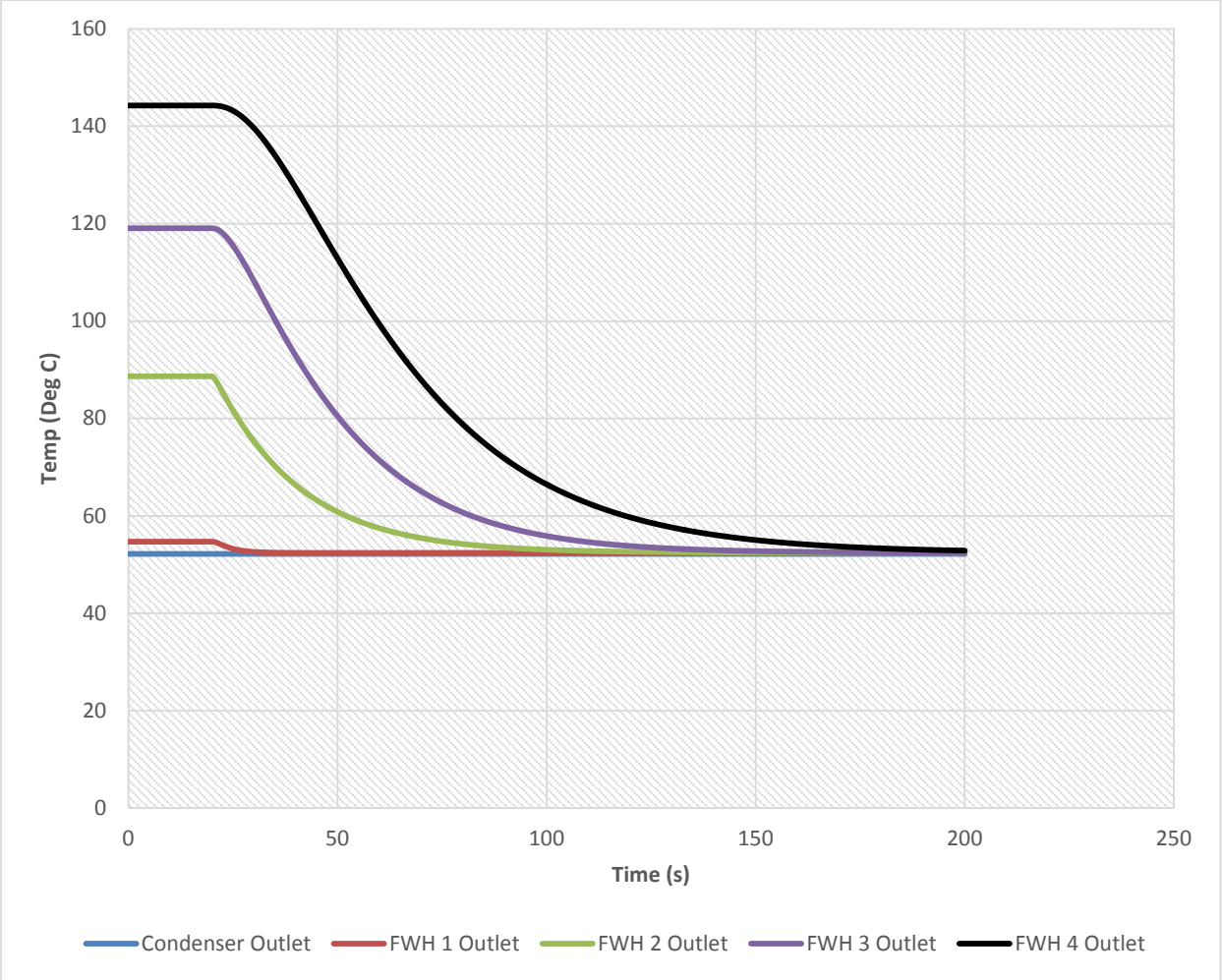


*Figure 61: Variation of Low Pressure FWH outlet temperatures with time during turbine trip.*

Figure 61 shows the variation of the outlet temperatures of the low pressure FWHs with time. The black trend represents the variation of the main condensate temperature with time during the transient. It is clear from the figure that the outlet temperatures from all the FWHs sharply decrease towards the condenser temperature once the bled steam supply is cut off (at 20s). This is due to the fact that the water is no longer being heated and therefore the temperature at the condenser outlet will eventually become the same temperature throughout the low pressure FWH train. Such a trend is expected and corroborated by [6]. With this, it can be said that the simplified low pressure FWH network is behaving accordingly and the results of the transient exercise are sensible.

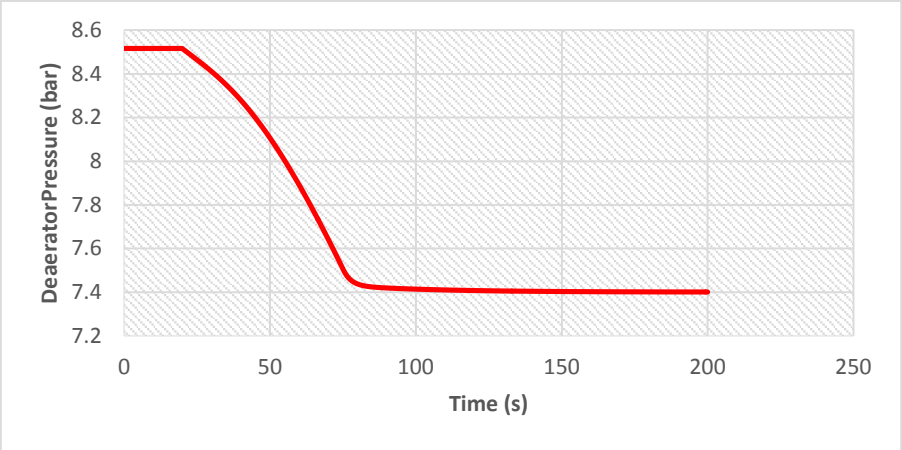


*Figure 62: Variation of deaerator pressure with time during turbine trip.*

Figure 62 shows the variation of the deaerator pressure with time during the transient. The graph shows a rapid decay of the pressure from its initial value of 8.52bar at the 100% load case. The pressure then settles at a new steady state value that corresponds to the pressure of the support steam (7.4bar). This decay is the result of the quenching of the steam by the cooling main condensate [6]. If no support steam is used, or if the control system does not respond quickly enough, the feedwater pumps might experience a low NPSH situation and trip because of the protection system [6]. This trend is also expected and increases confidence in the transient integrity of the model.

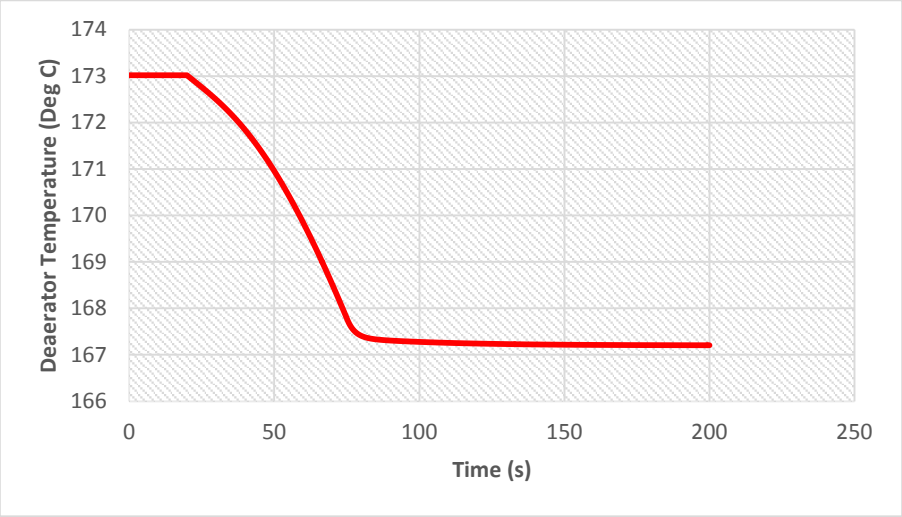


*Figure 63: Variation of deaerator temperature with time during turbine trip.*

Figure 63 shows the variation of the deaerator temperature with time during the turbine trip. The graph shows a rapid decay of the temperature from its initial value of 173 °C at the 100% load case. The temperature then settles at a new steady state value, of 167.21 °C, which corresponds to the saturation temperature at the pressure of the support steam. The general decrease is a result

of the effect of the incoming cool water, which cannot be heated to saturation by the reduced amount of steam. The general shape of the graph is similar to that shown in Figure 62 for the deaerator pressure variation. This is an expected outcome and stems from the fact that the contents of the deaerator are always under saturation conditions at all points between the two transient regimes.

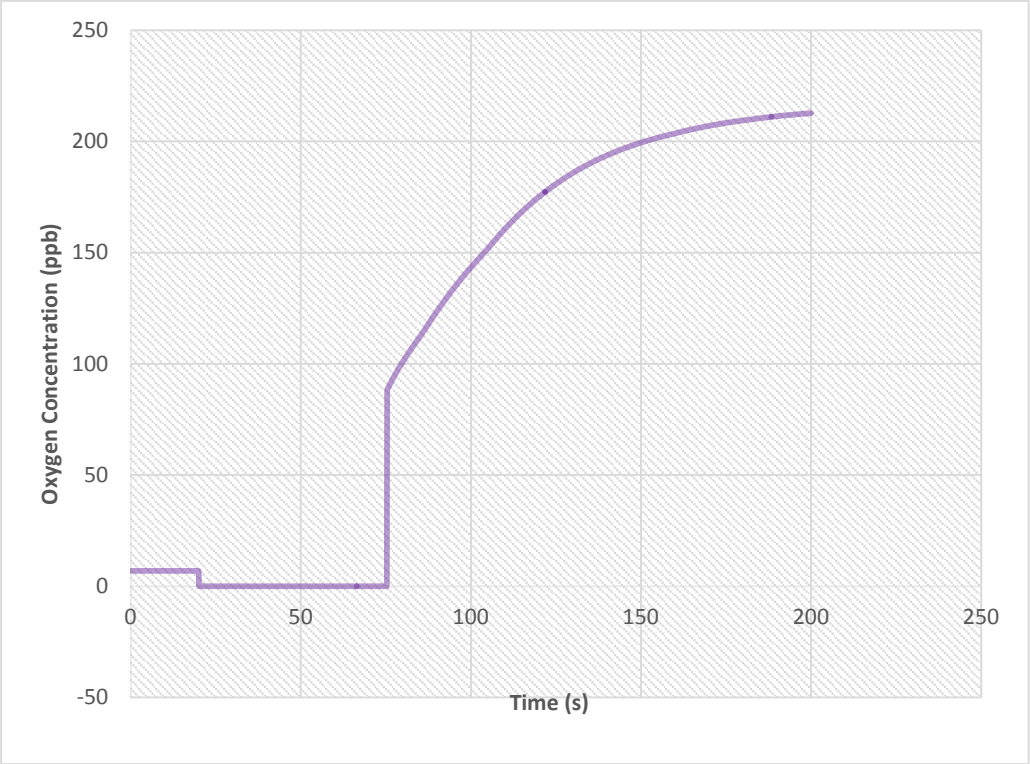


*Figure 64: Variation of deaerator oxygen outlet concentration with time during the turbine trip*

Figure 64 shows the variation of the outlet oxygen concentration with time. It should be noted that this graph does not strictly apply to the Plant 2 deaerator system as it is not fitted with a pressure swirl simplex nozzle system. The variation of the outlet oxygen concentration is only shown here for the sake of completeness, and to demonstrate that the Flownex model solves the oxygen component continuity equation, and determines the outlet oxygen concentrations during transient simulations as well. In order to better understand the following description concerning Figure 64, consider Figure 65.

Figure 65 shows that the mass flow rate of the main condensate into the deaerator sharply decreases at the 20s mark corresponding to the point at which the turbine trips. This decrease in mass flow rate is somewhat unexpected considering that the main condensate pressure drop across the nozzle increases due to the decrease in the deaerator pressure – meaning the mass flow rate across the nozzle should increase. The observed dip is a consequence of the pressure pulse created by the sudden pressure drop inside the deaerator.

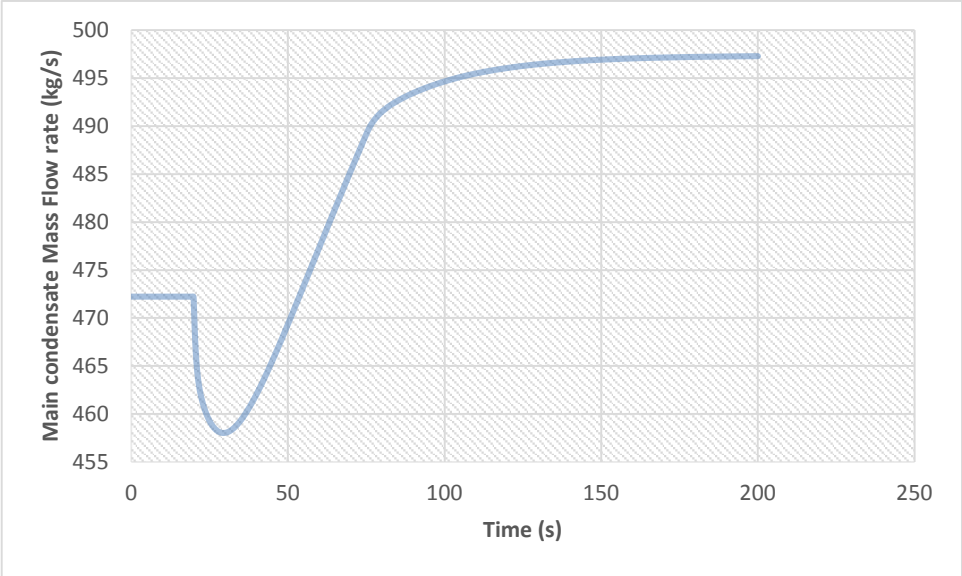


*Figure 65: Variation of main condensate mass flow rate with time during the turbine trip*

The pulse traverses towards the condenser extraction pump and temporarily increases the resistance to the mass flow thereby causing the mass flow rate to temporarily decrease. A similar effect was encountered by O'Kelly [6] during a similar simulation of a turbine trip.

Figure 64 shows that the outlet oxygen concentration suddenly drops to values very close to zero at the 20s mark. This decrease in concentration is the result of two key factors. The first is the increased residence time inside the deaerator caused by the temporary dip in the main condensate mass flow rate. According to equation(58), the residence time of the droplet inside the deaerator is a function of the droplet velocity which itself is a function of the mass flow rate of the main condensate across the nozzle. As the mass flow rate decreases, the nozzle discharge velocity also decreases meaning that the time spent by a droplet inside the deaerator is increased, leading to an increase in the time available to deaerate that droplet. The second factor is the reduced average diameter of the droplet due to the increased pressure drop across the nozzle. Although the effect of the increased pressure drop is countered by the decrease in the mass flow rate of the main condensate across the nozzle (equation(57)), the effect of the increased pressure drop appears to dominate and cause a net decrease in the average diameter. This decrease in turn means that the oxygen molecules have less distance to travel in order to leave a single droplet and therefore the deaeration effect is increased.

From 75.2s the oxygen concentration sharply and then gradually increases towards a new steady value of 213 ppb corresponding to the new steady state regime under which the deaerator will be operating. The increase begins at a point corresponding to the point at which the new deaerator pressure is reached (auxiliary steam pressure) and steady state operation is restored. This may be due to the fact that the deaeration process is now being carried out under lower temperature and

pressure conditions which correspond to relatively lower mass transfer coefficients as observed in section 4.5.1.

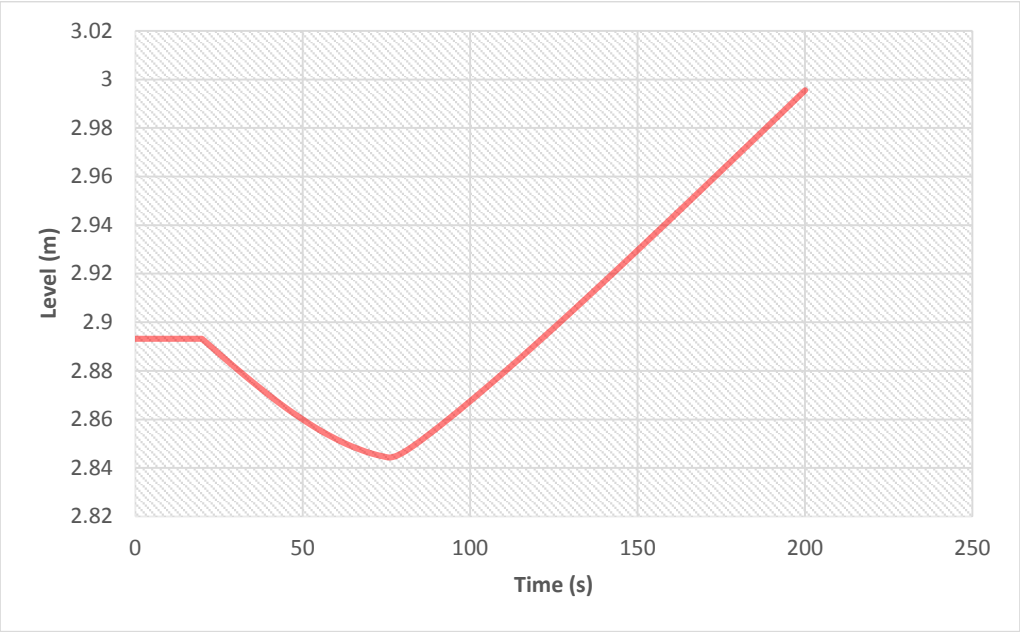


*Figure 66: Variation of deaerator condensate level with time during turbine trip.*

Figure 66 shows the variation of the condensate level inside the deaerator tank with time. Normally this level is kept constant by the level control system so this trend does not represent a real life scenario. The sudden drop of level at the 20s mark is caused by the abrupt stoppage of the deaerating steam flow. This, compounded with the temporary dip in the main condensate mass flow rate, causes a sudden decrease in the inflowing quantities and therefore a decrease in the deaerator level since the outlet mass flow rate is still fairly constant. The pressure decay inside the deaerator however causes the main condensate flow rate into the deaerator to eventually increase, since there is a larger pressure difference between the condensate extraction pump outlet and the deaerator. This increase in mass flow rate is responsible for the increase in level observed around the 78s mark. Had there been a level control system in place, the main condensate mass flow rate would have been altered to change the amount of water flowing into the tank in order to keep the level constant.

Although the transient validation exercise was limited to analysing and discussing trends based on theoretical considerations, it was deemed to be successful because of the good agreement between the expected outcomes and the model predictions. It can be said therefore that the transient operation of the model is satisfactory and the model overall is of a satisfactory standard.

## 5.6 Closing remarks

In this chapter the Flownex model was described, verified and validated. The key components used in the model were described in detail together with the network set up and the exercises that need to be performed before the model is used. The verification exercise showed satisfactory agreement between the predictions of the analytical and Flownex model, raising the confidence in the steady state integrity of the model. The steady state integrity of the model was further demonstrated through two case studies, both of which showed good agreement between the model predictions and actual plant values. Lastly, the transient integrity of the model was tested through running a turbine trip simulation. Although the results obtained could not be compared to any actual results or trends, they could be explained satisfactorily using theoretical considerations and it was concluded that the model was performing as intended and desired.

# 6. Conclusions, Limitations and Recommendations

## 6.1 Conclusions

The primary objective of this study was to develop a thermal-hydraulic model of a deaerator in Flownex. The model is primarily intended to serve as a building block for the coal fired power plant model that the EPPEI Center for Energy Efficiency intends to develop, but can also be used as a standalone model to study the behaviour of deaerating systems independently. The primary objective was successfully met through achieving the three secondary objectives listed in section 1.2.2 and reshown here for convenience.

1. Establishment of the types and operating principles of the deaerators used in in industry, particularly in Eskom power stations.
2. Development and validation of an analytical model of a deaerator in Mathcad.
3. Development, verification and validation of the Flownex model using the analytical model as a reference.

An account of how each of these objectives was met is presented in the following sections.

### 6.1.1 Establishment of the types and operating principles of the deaerators used in industry and in Eskom power stations

**Establishment of the types of deaerators used in industry and Eskom power stations**

This objective was achieved through performing a thorough literature search based on both theoretical considerations and information pertaining to assets owned by Eskom, and by visiting six Eskom power stations. It was established that the two main types of deaerators used in industry are the tray-spray type deaerator and the spray-scrubber type deaerator. The two are more commonly called the tray and spray type deaerators respectively. It was also established that a third deaerator type, called a stork type deaerator is also used in industry and installed in some Eskom power stations. The stork type deaerator is essentially a spray type deaerator but is often considered separately because of its markedly different design and external features.

**Establishment of the operating principles of the deaerators used in industry and Eskom power stations**

This objective was achieved through a thorough literature search based on theoretical considerations and the operating manuals of some deaerator units that are installed within Eskom power stations.

It was established that both the tray and spray type deaerators consist of two deaerating stages, the first of which is similar between the two types and is called the preheater. In the preheater the water to be deaerated is mixed with the deaerating steam in a process which accounts for over 90% of the heating and deaeration. The steam heats the water to a degree or two within its saturation temperature thereby removing dissolved NCGs in accordance to the temperature-solubility relationship of gases in water and Henry's law. On a deeper level, the removal of NCGs can be treated as a convective mass transfer process where NCGs diffuse from the water body into the steam. The deaerating steam then condenses as it loses heat during deaeration, leaving the NCGs "floating" in the preheater from which they are expelled into the atmosphere or any other lower pressure vessel.

For the tray type deaerator, the second stage consists of slightly tilted perforated trays. The incoming water from the preheater trickles down these trays and is deaerated to completion. The NCGs are released into the steam and move up into the preheater where they are expelled as previously mentioned.

For the spray type deaerator, the second stage consists of a cavity into which water from the preheater is collected. High velocity steam is then bubbled through the water causing a violent mixing which facilitates the removal of the remaining NCGs. As with the tray type deaerator, the NCGs pass into the deaerating steam and move into the preheater where they are expelled from the vessel.

### 6.1.2 Development and validation of an analytical model of a deaerator in Mathcad

**Development of analytical model**

This objective was met through developing a mathematical algorithm representative of a thermal deaerator. The approach followed in developing the algorithm was derived from a combination of the efforts of [1], [40] , [41], [42] and [43] pertaining to deaerator modelling and heat and mass transfer in deaerators respectively.

As inputs, the model requires boundary process parameters (specifically two mass flow rates, three enthalpies, one pressure value, and inlet oxygen concentration), chemical properties of water and oxygen, deaerator design characteristics and other miscellaneous quantities. The model uses these to solve the unidirectional steady-state mass and energy conservation equations around the deaerator boundary together with the oxygen component continuity equation. The outputs, or results from the model are then the mass flow rates, thermodynamic properties and outlet oxygen concentrations of all streams crossing the physical boundary of the deaerator.

Due to the fact that some of the inputs to the model may be difficult to establish, particularly inputs relating to the detailed design of the equipment, the model includes a calibrations section. In this section the model uses the design case operating conditions to perform backward calculations and infer the unknown parameters. These parameters can then be used as inputs to the model for any other off-design case that the user may wish to simulate.

**Validation of the analytical model**

Due to the lack of information pertaining to the NCG removal characteristics of any existing deaerator unit, the validation of the analytical model was performed in two stages. The first stage involved the validation of the thermal hydraulic performance of the model by comparing its results to acceptance test data from Unit 2 of Eskom's Plant 1. The second validation exercise involved comparing selected trends, representative of the NCG gas extraction characteristics of the modelled deaerator, to those obtained by Sharma et al [43] after experimenting with a lab size deaerator experimental set up.

The results obtained from the first validation exercise showed satisfactory agreement between the model's thermal hydraulic predictions and the acceptance test values. The errors obtained ranged between 0% and 1.81% with an average of 0.128%. The average error was raised by the relatively high errors associated with the vent steam mass flow rates, which were seen to decrease with increasing loads and were attributable to certain assumptions made in the development of the model. In conclusion, the errors between the model predictions and acceptance data were very small and were not considered to significantly affect the accuracy of the entire model.

The results obtained from the second validation exercise generally showed satisfactory agreement between the trends produced by the model to those expected under similar conditions as shown by Sharma et al [43]. Two of the trends compared exhibited differences that could be explained by either certain simplifications made in the model, or possible experimental errors backed by fundamental theoretical considerations in mass transfer and statistics. These differences were analysed and deemed not to affect the functionality of the model significantly.

In conclusion, the overall performance of the analytical model was satisfactory and the model was deemed to be fit for its intended use as a verification reference for the development of the Flownex model.

### 6.1.3 Development, verification and validation of the Flownex model

**Development of Flownex model**

This objective was met through developing a Flownex network representative of a thermal deaerator. Since Flownex is not designed to perform any elaborate mass transfer computations, an external Excel component was added to the network. The component is responsible for solving the oxygen component continuity equation in order to determine the unknown oxygen concentrations in the deaerated water stream.

The inputs and outputs of the Flownex model are very similar to those of the analytical model. The major differences arise from the fact that Flownex also solves the unidirectional momentum conservation equation and so allows for less inputs and can provide more results, e.g. no mass flow rates need to be specified but the level changes inside the feedwater tank are provided as outputs. In addition, the process parameters recommended for the model are the pressure values of each stream at the deaerator boundary, together with the temperature or enthalpy values of the incoming streams. This recommendation steams from the fact that the model is primarily intended to be a building block in the full plant model and these parameters are most likely the ones it will be exposed to.

**Verification of Flownex model**

The Flownex model was verified by running it for the 100%, 80%, 60% and 46% load cases of Unit 2 of Plant 1, and comparing its results to those of the analytical model. The results obtained from these verification exercises showed good agreement between the predictions of the two models. The errors obtained ranged from 0.02% to 0.67% for the thermal hydraulic performance of the model and between 2.57% and 29.17% for the NCG extraction behaviour of the model. The high errors associated with the NCG extraction behaviour are somewhat exaggerated compared to the true magnitude of the errors since the concentrations in question are of very small magnitudes. A further look into these errors showed that the actual differences between the values predicted by the two models was very small, with a maximum value of -0.43 ppb at the 60% load case. In conclusion, it was decided that the Flownex model was a true representation of a deaerator system as it predicted results similar to those predicted by the validated analytical model. With this notion, further exercises were performed on the model.

**Validation of the Flownex model**

The Flownex model was validated through three separate case studies. In the first two case studies only the thermal hydraulic performance of the model was analysed since no different NCG

information was available. The trends observed for the NCG extraction characteristics of the analytical model also apply to the Flownex model since there are virtually no changes to the algorithm. The only possible differences are quantitative and therefore could not be validated because of the lack of data.

The first case study involved comparing the model results for the 100%, 80%, 60% and 46% load cases of Unit 2 of Plant 1 to the acceptance test data obtained during plant commissioning in 1978. The agreement between the model predictions and the acceptance test data was satisfactory. The errors obtained ranged from 0% to 2.32%. These errors were attributed to certain assumptions made in the development of the model and deemed to be insignificant with respect to the overall performance of the model.

The second case study involved comparing the model results for the 100%, 80%, 60% and 40% load cases of Unit 3 of Plant 2 with the power station's heat balance data. The agreement between the model predictions and the heat balance data was satisfactory. The errors obtained ranged between 0% and 5.97%. These errors were attributed to the same sources sighted for the Plant 1 case study and were deemed to be insignificant with respect to the overall performance of the model.

The third case study involved analysing the transient response of the deaerator model during a turbine trip simulation. Although there was no control system in place and the model trends could not be compared against real life trends, it was concluded that the integrity of the model when simulating transient scenarios was satisfactory. This conclusion was reached after analysing the trends using theoretical considerations and concluding that the trends observed where in agreement with what was expected under the given conditions.

## 6.2 Contributions and limitations of the study

### 6.2.1 Contributions of the study

The primary contribution of this study is a deaerator model that can be used as a building block for the plant model that the EPPEI Centre for Energy Efficiency intends to build. In addition to the other standalone functions for which the model can be used, a few other benefits can be realised from this work. The two main ones are discussed below.

Firstly, the study aids in understanding the technology employed in new and existing deaerator units, particularly the role played by spray nozzles. It is apparent from this study, that spray nozzles play a very important role in the heating and deaeration process and the design of the nozzles is therefore of primary importance. This information might be particularly helpful to

Eskom engineers who battle with tray type deaerators as the trays are susceptible to corrosion and other factors that lead to increased maintenance and added down time. It might be in their interests to investigate the option of redesigning the spray systems and ensuring that even more of the heating and deaeration is achieved in the preheaters. This eliminates the system's heavy dependence on the functionality of the tray section and it may be discovered that the same deaerating effect can be obtained even without the trays. This is particularly applicable to those power stations without proven spray technologies e.g. those with simple pipe and/or Chinese head spray devices.

Secondly, the study provides a method to infer internal design details by using process parameters and high level design information. This may be particularly useful in fault diagnosis exercises were a knowledge of the processes happening inside the equipment may provide some useful insights. This could also be linked to online condition monitoring of the spray nozzles.

### 6.2.2 Limitations of the study

The first limitations to this study was the unavailability of detailed design data. Although this limitation was overcome by using reverse calculations to infer what the design parameters would be, a significant number of assumptions were still made. The main assumptions made were those pertaining to the cone spray angle (60 degrees) and the pressure loss characteristics of the nozzle. In addition, it became impossible to separately include the contribution of the second deaerating stage as the number of unknown parameters would far exceed the equations available, making it impossible to infer the design parameters of the second stage. These assumptions and simplifications may result in losses of accuracy in some cases, especially those that are outside the typical operating range of the equipment.

The second limitation was the unavailability of NCG extraction characteristics data for use in the development of the model, and for the validation of the model. Again this limitation was partially overcome by making an assumption, that all Eskom deaerators were designed to the standards prescribed by [13] and [20]. Although this assumption is derived from credible sources and acceptable reasoning, it does mean that for deaerators not designed to the prescribed specifications the model may give erroneous quantitative results if the calibration exercises prescribed in chapters 4 and 5 are adopted. With regards to validating the model, the lack of NCG extraction characteristics data limited the validation exercise to a qualitative one as there was no quantitative data to use. This in turn means that the integrity of the numerical output of the model with regards to NCG concentrations was not confirmed.

## 6.3 Recommendations

### 6.3.1 Further studies

The deaerator model developed in this study is only applicable for deaerator systems fitted with pressure swirl simplex atomizers, and can only predict the concentrations of one NCG, oxygen. In light of the fact that many other nozzle types exist, and that there are other NCGs removed in the deaerator, it is recommended that further studies be pursued in these matters. The nozzle issue could be dealt with by devoting a study to the types of nozzles used in thermal deaerators and establishing the relations required to perform the same calculations performed in this work. As for the treatment of other NCGs, it may suffice to establish the correlations that govern the mass transfer parameters required to perform computations similar to those performed for oxygen in this study.

It is also recommended that a study of the mass transfer characteristics of the second deaerating stages be performed. This has the advantage of doing away with the assumption that all heating and deaeration are completed in the preheater and may increase the numerical accuracy of the model.

### 6.3.2 Benefit of spray nozzles in deaerators

In light of the issue raised in section 6.2.1 concerning the contribution of this study to understanding the technologies employed in deaerator design, it is recommended that Eskom consider a review of the spray systems in all of their tray type units. It may be beneficial to retrofit these units with better atomizing spray technologies thereby increasing the de-aeration efficiency. One could potentially remove some of the high-maintenance trays in that cose. However, spray nozzles introduce an additional pressure drop, which will need to be factored into the process implications of the entire system. It may be the case that this will require a higher main condensate pressure, requiring all the low pressure FWHs to operate at a higher pressures, perhaps exceeding their safe design pressure and/or shortening their operational life spans.

## 6.4 Closing remarks

The primary objective of this study was successfully met. The steps taken to meet this objective and results obtained are summarized in this chapter. In addition to the Flownex model, this study has revealed some key facts about deaerator operation that can be used by Eskom engineers to better understand and improve the performance of new and existing deaerator units. The model

developed in this study can still be improved and made applicable to an even wider range of activities. Some of the steps that can be taken towards this are documented in the recommendations section.

# 7. References


[1] I. Opris, “A de-aerator model,” Bucharest, 2013.

[2] Gallant, Mark; Hida, Gary;, “Power Plant Modeling: Restart with Confidence and Lower Risk During Emissions Control Revamp,” Aspen Technology, Inc., Burlington, 2011.

[3] E. J. Roldan-Villasana and A. K. Vazquesz, “Model of the Feed Water System Including a Generic Mdel of the Deaerator for a Full Scope Combined Cycle Power Plant Simulator,” in *UKSim Fourth European Symposium on Computer Modelling and Simulation*, Pisa, 2010.

[4] E. Ferro, E. Ghiazza, B. Bosio and P. Costa, “Modelling of flash and stripping phenomena in deaerators for seawater desalination,” *Desalination,* pp. 171-180, 2002.

[5] P. J. Potter, Power Plant Theory and Design, 2nd Edition, Auburn: The Ronald Press Company, 1959.

[6] P. O'Kelly, Computer Simulation of Thermal Plant Processes, 1st ed., New York : Springer, 2013.

[7] F. T. Morse, POWER PLANT ENGINEERING, the theory and practice of stationary electric generating plants, Toronto: D. Van Nostrand Company, Inc, 1953.

[8] M. A. B. Yunus A. Cengel, Thermodynamics: An engineering approach, 5th Edition, Boston: McGraw-Hill College, 2006.

[9] Alstom, “Feedwater heaters for nuclear power plants,” 2002. [Online]. Available: http://www.alstom.com/products-services/product-catalogue/power-generation/nuclear/heat-exchangers-for-nuclear/feedwater-heaters/. [Accessed 16 January 2015].

[10] The McGraw-Hill Companies, McGraw-Hill Dictionary of Scientific & Technical Terms, New York: The McGraw-Hill Companies, Inc, 2003.

[11] Lalonde Systhermique, “Deaeration of steam systems,” 2015. [Online]. Available: http://www.systhermique.com/steam-condensate/deaeration-noncondensables/. [Accessed 2014 November 2014].

[12] F. J. Mathews, Boiler Feedwater Treatment, London: Hutchinson's Scientific & Technical Publications, 1935.

[13] ASME, “ASME Performance Test Code on Deaerators,” New York, 1997.

[14] R. K. Mobley, Plant Engineers Handbook, Woburn: Butterworth-Heinemann, 2002.

[15] E. B. Woodruff, H. B. Lammers and T. F. Lammers, Steam Plant Operation, New York: The McGraw-Hill Companies, Inc., 2012.

[16] S. Y. Stevens, L. M. Sutherland and J. S. Krajcik, The Big Ideas of Nanoscale Science and Engineering, Arlington: National Science Teachers Association, 2009.

[17] “The deaerating principle,” Sterling Deaerator Company, 2014. [Online]. Available: http://www.sterlingdeaerator.com/principle.htm. [Accessed 15 September 2015].

[18] K. E. Heselton, Boiler Operators Handbook, Lilburn: Fairmount Press, 2005.

[19] K. Coleman and D. Gandy, “Repair of Dearators, 1008069, Technical Update,” EPRI, California, 2004.

[20] HEI, “Standards and Typical Specifications for Deaerators,” Cleveland, 1992.

[21] Ecodyne Limited, “Deaerating Products - Spray-Scrubber Deaerators,” 2014. [Online]. Available: http://www.ecodynedeaerators.com/deaerator-products-spray-scrubber.html. [Accessed 10 January 2015].

[22] Jack B. Pratt, “Does Your Deaerator Really Work,” Warminster, 2005.

[23] Stork, “Stork,” 1 January 2015. [Online]. Available: http://www.stork.com/en/products-services/power-services-products/thermeq-services/deaerators/operating-principle/. [Accessed 15 January 2015].

[24] Emmerson Process Management, “Deaerator Level Control (DALC) Application Discussion,” 2013. [Online]. Available: http://www.documentation.emersonprocess.com/groups/publicreadonly/documents/webpage/ad103_ots.hcsp. [Accessed 26 June 2015].

[25] G. Wamsley, “evaluating deaerator-operation,” HPAC Engineering, 1 January 2010. [Online]. Available: http://hpac.com/heating/evaluating-deaerator-operation. [Accessed 21 September 2015].

[26] J. P. Holman, Heat Transfer, Singapore: McGraw-Hill Book Company, 1986.

[27] Welty, Wicks, Wilson and Rorrer, Fundamentals of Momentum, Heat, and Mass Transfer, Oregon: John Wiley & Sons. Inc, 2008.

[28] L. Theodore and F. Ricci, Mass Transfer Operations For The Practicing Engineer, Hoboken: John Wiley & Sons, Inc., 2010.

[29] R. S. Subramanian, “Convective Mass Transfer - Clarkson University,” 2015. [Online]. Available: http://web2.clarkson.edu/projects/subramanian/ch330/notes/Convective%20Mass%20Transfer.pdf. [Accessed 10 June 2015].

[30] C. Skowland, M. Hlavinka, M. Lopez and C. Fits , “COMPARISON OF IDEAL STAGE AND MASS TRANSFER MODELS FOR SEPARATION PROCESSES WITH AND WITHOUT CHEMICAL REACTIONS”.

[31] D. W. Green and R. H. Perry, Perry's Chemical Engineer's Handbook, New York: McGraw-Hill Companies, Inc, 2008.

[32] R. W. Rousseau, Handbook of Seperation Process Technology, 1st ed., Canada: John Wiley & Sons, Inc, 1987.

[33] R. H. Weiland and W. A. Hatcher, “What are the benefits from mass transfer rater based simulation: models are highly detailed and predictive,” Gulf Publishing Company, Houston, 2011.

[34] A. H. Lefebvre, Atomization and Sprays, 1st ed., Boca Raton: CRC Press, 1989.

[35] L. Bayvel and Z. Orzechowski, Liquid Atomization, 1st ed., Washington DC: Taylor & Francis, 1993.

[36] Y. I. Khavkin, The Theory and Practice of Swirl Atomizers, New York: Taylor & Francis Group, 2003.

[37] W. A. Sirignano, Fluid Dynamics and Transport of Droplet and Sprays, New York: Cambridge University Press, 2010.

[38] ESKOM, *Water Distributor for Deaerator A & B Sectional Assembly (Drawing number*

*0.45/1048),* 1973.

[39] Balcke-Durr Akti Engesellscaft, *Kendal Power Station Feedwater Heater System and Deaerator System with Storage Tank,* Moers, 1978.

[40] P. Stephan , S. Kabelac, M. Kind, H. Martin, M. Dieter and K. Schaber, VDI Heat Atlas, 2 nd ed., Dusseldorf: Springer, 2010.

[41] K. V. Sharma, K. V. Suryanarayana, P. K. Sarma, V. Dharma Rao and P. S. V. Kurma Rao, "Effect of droplet diameter on oxygen stripping in deaerators," in *ICLASS-2006*, Kyoto, 2006.

[42] K. V. Sharma, K. V. Suryanarayana, P. K. Sarma, M. M. Rahman, M. M. Noor and K. Kadirgama, "Experimental investigations of oxygen stripping from boiler feedwater in a spray and tray type deaerator," *International Journal of Automotive and Mechanical Engineering (IJAME),* pp. 46-65, 2010.

[43] K. V. Sharma, K. V. Suryanarayana, P. K. Sarma, V. Dharma Rao and Subramanyam, "Oxygen stripping in deaerator feedwater: Condensation on spray droplets," *Heat Mass Transfer,* pp. 665-673, 2010.

[44] R. Sander, "Henry's Law Constants," 1 September 2015. [Online]. Available: http://www.henrys-law.org/. [Accessed 29 October 2015].

[45] Brown Boveri, *Kriel Heat Balance Diagram,* 1972.

[46] M-Tech, Flownex library theory manual, Johannesburg, 2014.

[47] M-Tec, *Flownex Library Manual,* 2015.

# Appendix A. Verification and Validation data

Analytical model validation inputs, intermediate results and final results

Plant 1 80% Load case

**Core model inputs**

| ***Parameter*** | ***Value*** | ***Unit*** |
|---|---|---|
| | | |
| *Bled steam enthalpy ($h_{bs}$)* | *3147.544* | *kJ/kg* |
| *Bled steam pressure ($P_{bs}$)* | *0.706* | *MPa* |
| *Main condensate mass flow rate ($m_{mc}$)* | *141.616* | *kg/s* |
| *Main condensate temperature ($T_{mc}$)* | *136.963* | *°C* |
| *Main condensate pressure ($P_{mc}$)* | *1.132* | *MPa* |
| *Return condensate mass flow rate ($m_{rc}$)* | *18.235* | *kg/s* |
| *Return condensate enthalpy ($h_{rc}$)* | *828.100* | *kJ/kg* |
| *Return condensate pressure ($P_{rc}$)* | *0.752* | *MPa* |
| *Vent pipe pressure loss coefficient ($C_{k.vp}$)* | *$1.745 \times 10^{7}$* | *$m^{-4}$* |

**Some intermediate results**

| ***Parameter*** | ***Value*** | ***Unit*** |
|---|---|---|
| | | |
| *Deaerator pressure ($P_{dea}$)* | *7.06* | *bar* |
| *Main condensate enthalpy ($h_{mc}$)* | *576.7* | *kJ/kg* |
| *Deaerated water enthalpy ($h_{dw}$)* | *698.647* | *kJ/kg* |
| *Vent steam enthalpy ($h_{vs}$)* | *2763.109* | *kJ/kg* |
| *Vent steam mass flow rate ($m_{vs}$)* | *0.271* | *kg/s* |

**Results**

| ***Parameter*** | ***Value*** | ***Unit*** |
|---|---|---|
| | | |
| *Bled steam mass flow rate ($m_{bs}$)* | *6.316* | *kJ/kg* |
| *Vent steam temperature ($T_{vs}$)* | *165.297* | *°C* |
| *Vent steam pressure ($P_{vs}$)* | *7.06* | *bar* |
| *Deaerated water mass flow rate ($m_{dw}$)* | *165.897* | *kJ/kg* |
| *Deaerated water temperature ($T_{dw}$)* | *165.297* | *°C* |
| *Deaerated water pressure ($P_{dw}$)* | *7.06* | *bar* |

Plant 1 60% Load case

**Core model inputs**

| ***Parameter*** | ***Value*** | ***Unit*** |
|---|---|---|
| | | |
| *Bled steam enthalpy ($h_{bs}$)* | *3162.327* | *kJ/kg* |
| *Bled steam pressure ($P_{bs}$)* | *0.536* | *MPa* |
| *Main condensate mass flow rate ($m_{mc}$)* | *105.824* | *kg/s* |
| *Main condensate temperature ($T_{mc}$)* | *128.168* | *°C* |
| *Main condensate pressure ($P_{mc}$)* | *0.934* | *MPa* |
| *Return condensate mass flow rate ($m_{rc}$)* | *12.778* | *kg/s* |
| *Return condensate enthalpy ($h_{rc}$)* | *770.600* | *kJ/kg* |
| *Return condensate pressure ($P_{rc}$)* | *0.562* | *MPa* |
| *Vent pipe pressure loss coefficient ($C_{k.vp}$)* | *$1.745 \times 10^{7}$* | *$m^{-4}$* |

**Some intermediate results**

| ***Parameter*** | ***Value*** | ***Unit*** |
|---|---|---|
| | | |
| *Deaerator pressure ($P_{dea}$)* | *5.36* | *bar* |
| *Main condensate enthalpy ($h_{mc}$)* | *539.03* | *kJ/kg* |
| *Deaerated water enthalpy ($h_{dw}$)* | *651.598* | *kJ/kg* |
| *Vent steam enthalpy ($h_{vs}$)* | *2751.193* | *kJ/kg* |
| *Vent steam mass flow rate ($m_{vs}$)* | *0.205* | *kg/s* |

**Results**

| ***Parameter*** | ***Value*** | ***Unit*** |
|---|---|---|
| | | |
| *Bled steam mass flow rate ($m_{bs}$)* | *4.311* | *kJ/kg* |
| *Vent steam temperature ($T_{vs}$)* | *154.474* | *°C* |
| *Vent steam pressure ($P_{vs}$)* | *5.36* | *bar* |
| *Deaerated water mass flow rate ($m_{dw}$)* | *122.707* | *kJ/kg* |
| *Deaerated water temperature ($T_{dw}$)* | *154.474* | *°C* |
| *Deaerated water pressure ($P_{dw}$)* | *5.36* | *bar* |

Plant 1 46% Load case

**Core model inputs**

| ***Parameter*** | ***Value*** | ***Unit*** |
|---|---|---|
| | | |
| *Bled steam enthalpy ($h_{bs}$)* | *3158.857* | *kJ/kg* |
| *Bled steam pressure ($P_{bs}$)* | *0.425* | *MPa* |
| *Main condensate mass flow rate ($m_{mc}$)* | *84.291* | *kg/s* |
| *Main condensate temperature ($T_{mc}$)* | *121.424* | *°C* |
| *Main condensate pressure ($P_{mc}$)* | *0.813* | *MPa* |
| *Return condensate mass flow rate ($m_{rc}$)* | *9.519* | *kg/s* |
| *Return condensate enthalpy ($h_{rc}$)* | *727.500* | *kJ/kg* |
| *Return condensate pressure ($P_{rc}$)* | *0.442* | *MPa* |
| *Vent pipe pressure loss coefficient ($C_{k.vp}$)* | *$1.745 \times 10^{7}$* | *$m^{-4}$* |

**Some intermediate results**

| ***Parameter*** | ***Value*** | ***Unit*** |
|---|---|---|
| | | |
| *Deaerator pressure ($P_{dea}$)* | *4.25* | *bar* |
| *Main condensate enthalpy ($h_{mc}$)* | *510.263* | *kJ/kg* |
| *Deaerated water enthalpy ($h_{dw}$)* | *614.187* | *kJ/kg* |
| *Vent steam enthalpy ($h_{vs}$)* | *2740.806* | *kJ/kg* |
| *Vent steam mass flow rate ($m_{vs}$)* | *0.162* | *kg/s* |

**Results**

| ***Parameter*** | ***Value*** | ***Unit*** |
|---|---|---|
| | | |
| *Bled steam mass flow rate ($m_{bs}$)* | *3.154* | *kJ/kg* |
| *Vent steam temperature ($T_{vs}$)* | *145.811* | *°C* |
| *Vent steam pressure ($P_{vs}$)* | *4.25* | *bar* |
| *Deaerated water mass flow rate ($m_{dw}$)* | *96.802* | *kJ/kg* |
| *Deaerated water temperature ($T_{dw}$)* | *145.811* | *°C* |
| *Deaerated water pressure ($P_{dw}$)* | *4.25* | *bar* |

## Flownex model verification inputs and results

### Plant 1 80% load case

**Inputs**

| ***Parameter*** | ***Value*** | ***Unit*** |
|---|---|---|
| | | |
| *Main condensate pressure ($P_{mc}$)* | *11.32* | *bar* |
| *Main condensate temperature ($T_{mc}$)* | *136.963* | *°C* |
| *Main condensate pressure loss coefficient ($C_{k.mc}$)* | *19736.2* | *$m^4$* |
| *Bled steam pressure ($P_{bs}$)* | *7.06* | *bar* |
| *Bled steam enthalpy ($h_{bs}$)* | *3147.54* | *kJ/kg* |
| *Return condensate pressure ($P_{rc}$)* | *7.52* | *bar* |
| *Return condensate enthalpy ($h_{rc}$)* | *828.1* | *kJ/kg* |
| *Return condensate pressure loss coefficient ($C_{k.rc}$)* | *8106.51* | *$m^4$* |
| *Vent steam pressure ($P_{vs}$)* | *1.013* | *bar* |
| *Vent steam pressure loss coefficient ($C_{k.vs}$)* | *$1.77 \times 10^7$* | *$m^4$* |
| *Deaerated water pressure ($P_{dw}$)* | *7.06* | *bar* |
| *Deaerated water outlet admittance ($Af_{.dw}$)* | *1.8294* | *-* |
| *Deaerator tank volume ($V_{dt}$)* | *218* | *$m^3$* |
| *Deaerator tank diameter ($D_{dt}$)* | *4.5* | *m* |
| *Deaerator tank initial pressure ($P_{dea.in}$)* | *7.06* | *bar* |
| *Deaerator tank quality (x)* | *0.001049543* | *-* |
| *Oxygen inlet concentration ($\omega_{o2.in}$)* | *22650.286* | *ppb* |

**Results**

| ***Parameter*** | ***Value*** | ***Unit*** |
|---|---|---|
| | | |
| *Main condensate mass flow rate ($m_{mc}$)* | *141.718* | *kg/s* |
| *Bled steam mass flow rate ($m_{bs}$)* | *6.29015* | *kg/s* |
| *Return condensate mass flow rate ($m_{rc}$)* | *18.4775930220632* | *kg/s* |
| *Vent steam mass flow rate ($m_{vs}$)* | *0.268876711425735* | *kg/s* |
| *Deaerated water mass flow rate ($m_{dw}$)* | *166.216572047586* | *kg/s* |
| *Deaerator pressure ($P_{dea}$)* | *7.05370985374519* | *bar* |
| *Deaerated water temperature ($T_{dw}$)* | *165.262033592759* | *°C* |
| *Main condensate mass flow rate ($m_{mc}$)* | *4.514* | *ppb* |

Plant 1 60% load case

**Inputs**

| ***Parameter*** | ***Value*** | ***Unit*** |
|---|---|---|
| | | |
| *Main condensate pressure ($P_{mc}$)* | *9.34* | *bar* |
| *Main condensate temperature ($T_{mc}$)* | *128.168* | *°C* |
| *Main condensate pressure loss coefficient ($C_{k.mc}$)* | *33287.5* | *$m^4$* |
| *Bled steam pressure ($P_{bs}$)* | *5.36* | *bar* |
| *Bled steam enthalpy ($h_{bs}$)* | *3162.33* | *kJ/kg* |
| *Return condensate pressure ($P_{rc}$)* | *5.62* | *bar* |
| *Return condensate enthalpy ($h_{rc}$)* | *770.6* | *kJ/kg* |
| *Return condensate pressure loss coefficient ($C_{k.rc}$)* | *8106.51* | *$m^4$* |
| *Vent steam pressure ($P_{vs}$)* | *1.013* | *bar* |
| *Vent steam pressure loss coefficient ($C_{k.vs}$)* | *$1.77 \times 10^7$* | *$m^4$* |
| *Deaerated water pressure ($P_{dw}$)* | *5.36* | *bar* |
| *Deaerated water outlet admittance ($Af_{.dw}$)* | *0.511644* | *-* |
| *Deaerator tank volume ($V_{dt}$)* | *218* | *$m^3$* |
| *Deaerator tank diameter ($D_{dt}$)* | *4.5* | *m* |
| *Deaerator tank initial pressure ($P_{dea.in}$)* | *5.36* | *bar* |
| *Deaerator tank quality (x)* | *0.0007998078* | *-* |
| *Oxygen inlet concentration ($\omega_{o2.in}$)* | *22650.286* | *ppb* |

**Results**

| ***Parameter*** | ***Value*** | ***Unit*** |
|---|---|---|
| | | |
| *Main condensate mass flow rate ($m_{mc}$)* | *105.879289121916* | *kg/s* |
| *Bled steam mass flow rate ($m_{bs}$)* | *4.3005312178703* | *kg/s* |
| *Return condensate mass flow rate ($m_{rc}$)* | *12.8003290119169* | *kg/s* |
| *Vent steam mass flow rate ($m_{vs}$)* | *0.204096258289493* | *kg/s* |
| *Deaerated water mass flow rate ($m_{dw}$)* | *122.776053093414* | *kg/s* |
| *Deaerator pressure ($P_{dea}$)* | *5.35569946878213* | *bar* |
| *Deaerated water temperature ($T_{dw}$)* | *154.445193671233* | *°C* |
| *Main condensate mass flow rate ($m_{mc}$)* | *2.546* | *ppb* |

Plant 1 46 % load case

**Inputs**

| ***Parameter*** | ***Value*** | ***Unit*** |
|---|---|---|
| | | |
| *Main condensate pressure ($P_{mc}$)* | *8.13* | *bar* |
| *Main condensate temperature ($T_{mc}$)* | *121.424* | *°C* |
| *Main condensate pressure loss coefficient ($C_{k.mc}$)* | *51451* | *$m^4$* |
| *Bled steam pressure ($P_{bs}$)* | *4.25* | *bar* |
| *Bled steam enthalpy ($h_{bs}$)* | *3158.86* | *kJ/kg* |
| *Return condensate pressure ($P_{rc}$)* | *4.42* | *bar* |
| *Return condensate enthalpy ($h_{rc}$)* | *727.5* | *kJ/kg* |
| *Return condensate pressure loss coefficient ($C_{k.rc}$)* | *8106.51* | *$m^4$* |
| *Vent steam pressure ($P_{vs}$)* | *1.013* | *bar* |
| *Vent steam pressure loss coefficient ($C_{k.vs}$)* | *$1.77 \times 10^7$* | *$m^4$* |
| *Deaerated water pressure ($P_{dw}$)* | *4.25* | *bar* |
| *Deaerated water outlet admittance ($Af_{.dw}$)* | *0.314515* | *-* |
| *Deaerator tank volume ($V_{dt}$)* | *218* | *$m^3$* |
| *Deaerator tank diameter ($D_{dt}$)* | *4.5* | *m* |
| *Deaerator tank initial pressure ($P_{dea.in}$)* | *8.73* | *bar* |
| *Deaerator tank quality (x)* | *0.0006372481* | *-* |
| *Oxygen inlet concentration ($\omega_{o2.in}$)* | *22650.286* | *ppb* |

**Results**

| ***Parameter*** | ***Value*** | ***Unit*** |
|---|---|---|
| | | |
| *Main condensate mass flow rate ($m_{mc}$)* | *84.3237195366475* | *kg/s* |
| *Bled steam mass flow rate ($m_{bs}$)* | *3.14514430898533* | *kg/s* |
| *Return condensate mass flow rate ($m_{rc}$)* | *9.57398755977454* | *kg/s* |
| *Vent steam mass flow rate ($m_{vs}$)* | *0.161151452967853* | *kg/s* |
| *Deaerated water mass flow rate ($m_{dw}$)* | *96.8816999524396* | *kg/s* |
| *Deaerator pressure ($P_{dea}$)* | *4.24685485569101* | *bar* |
| *Deaerated water temperature ($T_{dw}$)* | *145.787143560855* | *°C* |
| *Main condensate mass flow rate ($m_{mc}$)* | *1.290* | *ppb* |

Plant 2 80% load case

**Inputs**

| ***Parameter*** | ***Value*** | ***Unit*** |
|---|---|---|
| | | |
| *Main condensate pressure ($P_{mc}$)* | *8.98* | *bar* |
| *Main condensate temperature ($T_{mc}$)* | *138.343* | *°C* |
| *Main condensate pressure loss coefficient ($C_{k.mc}$)* | *1253.1* | *$m^4$* |
| *Bled steam pressure ($P_{bs}$)* | *7.02* | *bar* |
| *Bled steam enthalpy ($h_{bs}$)* | *3151.36* | *kJ/kg* |
| *Return condensate pressure ($P_{rc}$)* | *7.11* | *bar* |
| *Return condensate enthalpy ($h_{rc}$)* | *739.7* | *kJ/kg* |
| *Return condensate pressure loss coefficient ($C_{k.rc}$)* | *400.281* | *$m^4$* |
| *Vent steam pressure ($P_{vs}$)* | *0.136* | *bar* |
| *Vent steam pressure loss coefficient ($C_{k.vs}$)* | *$2.13 \times 10^6$* | *$m^4$* |
| *Deaerated water pressure ($P_{dw}$)* | *7.02* | *bar* |
| *Deaerated water outlet admittance ($Af_{.dw}$)* | *0.00748657* | *-* |
| *Deaerator tank volume ($V_{dt}$)* | *447* | *$m^3$* |
| *Deaerator tank diameter ($D_{dt}$)* | *4.5* | *m* |
| *Deaerator tank initial pressure ($P_{dea.in}$)* | *7.02* | *bar* |
| *Deaerator tank quality (x)* | *0.001912489* | *-* |

**Results**

| ***Parameter*** | ***Value*** | ***Unit*** |
|---|---|---|
| | | |
| *Main condensate mass flow rate ($m_{mc}$)* | *380.9534376* | *kg/s* |
| *Bled steam mass flow rate ($m_{bs}$)* | *17.51342423* | *kg/s* |
| *Return condensate mass flow rate ($m_{rc}$)* | *58.9758318* | *kg/s* |
| *Vent steam mass flow rate ($m_{vs}$)* | *0.779550452* | *kg/s* |
| *Deaerated water mass flow rate ($m_{dw}$)* | *456.6631432* | *kg/s* |
| *Deaerator pressure ($P_{dea}$)* | *7.019982487* | *bar* |
| *Deaerated water temperature ($T_{dw}$)* | *165.0630905* | *°C* |

Plant 2 60% load case

**Inputs**

| ***Parameter*** | ***Value*** | ***Unit*** |
|---|---|---|
| | | |
| *Main condensate pressure ($P_{mc}$)* | *7.27* | *bar* |
| *Main condensate temperature ($T_{mc}$)* | *129.584* | *°C* |
| *Main condensate pressure loss coefficient ($C_{k.mc}$)* | *2223.003* | *$m^4$* |
| *Bled steam pressure ($P_{bs}$)* | *5.30* | *bar* |
| *Bled steam enthalpy ($h_{bs}$)* | *3132.24* | *kJ/kg* |
| *Return condensate pressure ($P_{rc}$)* | *5.3437* | *bar* |
| *Return condensate enthalpy ($h_{rc}$)* | *683.9* | *kJ/kg* |
| *Return condensate pressure loss coefficient ($C_{k.rc}$)* | *400.281* | *$m^4$* |
| *Vent steam pressure ($P_{vs}$)* | *0.136* | *bar* |
| *Vent steam pressure loss coefficient ($C_{k.vs}$)* | *$2.13 \times 10^6$* | *$m^4$* |
| *Deaerated water pressure ($P_{dw}$)* | *5.30* | *bar* |
| *Deaerated water outlet admittance ($Af_{.dw}$)* | *0.00748657499235646* | *-* |
| *Deaerator tank volume ($V_{dt}$)* | *447* | *$m^3$* |
| *Deaerator tank diameter ($D_{dt}$)* | *4.5* | *m* |
| *Deaerator tank initial pressure ($P_{dea.in}$)* | *5.3* | *bar* |
| *Deaerator tank quality (x)* | *0.001449837* | *-* |

**Results**

| ***Parameter*** | ***Value*** | ***Unit*** |
|---|---|---|
| | | |
| *Main condensate mass flow rate ($m_{mc}$)* | *287.9077136* | *kg/s* |
| *Bled steam mass flow rate ($m_{bs}$)* | *12.09267213* | *kg/s* |
| *Return condensate mass flow rate ($m_{rc}$)* | *40.28436236* | *kg/s* |
| *Vent steam mass flow rate ($m_{vs}$)* | *0.5930922* | *kg/s* |
| *Deaerated water mass flow rate ($m_{dw}$)* | *339.6916559* | *kg/s* |
| *Deaerator pressure ($P_{dea}$)* | *5.299987907* | *bar* |
| *Deaerated water temperature ($T_{dw}$)* | *154.0413282* | *°C* |

Plant 2 40% load case

**Inputs**

| ***Parameter*** | ***Value*** | ***Unit*** |
|---|---|---|
| | | |
| *Main condensate pressure ($P_{mc}$)* | *5.45* | *bar* |
| *Main condensate temperature ($T_{mc}$)* | *117.05* | *°C* |
| *Main condensate pressure loss coefficient ($C_{k.mc}$)* | *5004.89* | *$m^4$* |
| *Bled steam pressure ($P_{bs}$)* | *3.48* | *bar* |
| *Bled steam enthalpy ($h_{bs}$)* | *3086.97* | *kJ/kg* |
| *Return condensate pressure ($P_{rc}$)* | *3.4981* | *bar* |
| *Return condensate enthalpy ($h_{rc}$)* | *609.7* | *kJ/kg* |
| *Return condensate pressure loss coefficient ($C_{k.rc}$)* | *400.281* | *$m^4$* |
| *Vent steam pressure ($P_{vs}$)* | *0.136* | *bar* |
| *Vent steam pressure loss coefficient ($C_{k.vs}$)* | *$2.13 \times 10^6$* | *$m^4$* |
| *Deaerated water pressure ($P_{dw}$)* | *3.48* | *bar* |
| *Deaerated water outlet admittance ($Af_{.dw}$)* | *0.00748657499235646* | *-* |
| *Deaerator tank volume ($V_{dt}$)* | *447* | *$m^3$* |
| *Deaerator tank diameter ($D_{dt}$)* | *4.5* | *m* |
| *Deaerator tank initial pressure ($P_{dea.in}$)* | *3.48* | *bar* |
| *Deaerator tank quality (x)* | *0.0009615752* | *-* |

**Results**

| ***Parameter*** | ***Value*** | ***Unit*** |
|---|---|---|
| | | |
| *Main condensate mass flow rate ($m_{mc}$)* | *192.9237595* | *kg/s* |
| *Bled steam mass flow rate ($m_{bs}$)* | *7.159159645* | *kg/s* |
| *Return condensate mass flow rate ($m_{rc}$)* | *24.71271249* | *kg/s* |
| *Vent steam mass flow rate ($m_{vs}$)* | *0.394162353* | *kg/s* |
| *Deaerated water mass flow rate ($m_{dw}$)* | *224.4014693* | *kg/s* |
| *Deaerator pressure ($P_{dea}$)* | *3.479992841* | *bar* |
| *Deaerated water temperature ($T_{dw}$)* | *138.6587875* | *°C* |

# Appendix B. Program code

## *DEAERATOR MODEL*

Reference:C:\Users\Richard\Documents\Water-Steam+IAPWS-IF97+rev+A.3.xmcd

### PRECALCULATION

#### *INPUTS*

**Process inputs**

Main condensate mass flow rate $m_{mc.d} := 180.360 \frac{kg}{s}$

Main condesnate pressure $P_{mc.d} := 13.34\,bar$

Main condesnate temperature $T_{mc.d} := 143.829\,°C$

Bled steam mass flow rate $m_{bs.d} := 8.707 \frac{kg}{s}$

Bled steam pressure $P_{bs.d} := 8.73 bar$

Bled steam enthalpy $h_{bs.d} := 3149.813 \frac{kJ}{kg}$

Return condensate mass flow rate $m_{rc.d} := 23.27 \frac{kg}{s}$

Return condensate pressure $P_{rc.d} := 9.39 bar$

Return condensate enthalpy $h_{rc.d} := 877.3 \frac{kJ}{kg}$

**Deaerator design features**

Number of nozzles $N_{noz} := 1$

Distance from nozzle discharge to first tray $L_{spray} := 0.5m$

Nozzle half spray angle $\theta := 60deg$

**Miscellaneous inputs**

Ambient temperature $T_\theta := 298.15K$

Ambient pressure $P_\theta := 101.3kPa$

**Chemical properties of water and Oxygen**

Ideal gas constant $R_{ideal} := 8.3144621 \cdot \frac{J}{mol \cdot K}$

Henry's Law constant at ambient conditions $k_{H\theta} := 1.3 \cdot 10^{-3} \frac{1000mol}{m^3 atm}$

Henry's law expression $k_H(T) := k_{H\theta} \cdot exp\left[1700K \cdot \left(\frac{1}{T} - \frac{1}{T_\theta}\right)\right]$

"association" parameter for solvent (water) $\Phi_{water} := 2.26$

Molecular weight of solvent (water) $M_{water} := 18$

Molal of solute (oxygen) volume at normal boiling point $V_{oxygen} := 31.2 \frac{cm^3}{mol}$

Molar mass of oxygen $M_{o2} := 32 \frac{gm}{mol}$

Oxygen mole fraction in air $mf_{o2.air} := 0.21$

Unit conversion factor $ppb := \frac{mg \cdot 10^{-3}}{L \cdot M_{o2}} = 3.125 \times 10^{-5} \frac{mol}{m^3}$

Target Oxygen outlet concentration $c_{o2.out.d} := 7ppb = 2.188 \times 10^{-4} \frac{mol}{m^3}$

## *EXECUTION*

Deaerator operating pressure

$$P_{dea.d} := P_{bs.d} = 8.73 \cdot bar$$

Main condensate enthalpy at deaerator inlet

$$h_{mc.d} := h_{steam}\left(P_{mc.d}, T_{mc.d}, "", "", ""\right) = 606.248 \cdot \frac{kJ}{kg}$$

Deaerated water enthalpy at deaerator outlet

$$h_{dw.d} := h_{steam}\left(P_{dea.d}, "", "", 0, ""\right) = 737.051 \cdot \frac{kJ}{kg}$$

Vent steam enthalpy at deaerator outlet

$$h_{vs.d} := h_{steam}\left(P_{dea.d}, "", "", 1, ""\right) = 2.772 \times 10^{3} \cdot \frac{kJ}{kg}$$

Main condensate pressure drop across deaerator nozzle

$$\Delta P_{noz.d} := P_{mc.d} - P_{dea.d} = 4.61 \cdot bar$$

Vent steam pressure drop across vent pipe

$$\Delta P_{vp.d} := P_{dea.d} - P_{\theta} = 7.717 \cdot bar$$

Main condensate temperature at nozzle inlet

$$T_{noz.in.d} := T_{mc.d} = 143.829 \cdot °C$$

Main condensate temperature at nozzle outlet

$$T_{noz.out.d} := T_{steam}\left(P_{dea.d}, "", h_{mc.d}, ""\right) = 143.918 \cdot °C$$

Main condensate temperature at deaerator inlet

$$T_{dea.in.d} := T_{steam}\left(P_{dea.d}, "", h_{mc.d}, ""\right) = 417.068 \cdot K$$

Main condensate temperature at deaerator outlet

$$T_{dea.out.d} := T_{steam}\left(P_{dea.d}, "", "", ""\right) = 447.217 \cdot K$$

Main condensate density at nozzle inlet

$$\rho_{noz.in.d} := \rho_{steam}\left(P_{mc.d}, T_{mc.d}, "", "", ""\right) = 923.202 \frac{kg}{m^3}$$

Main condensate density at nozzle outlet

$$\rho_{noz.out.d} := \rho_{steam}\left(P_{dea.d}, "", "", h_{mc.d}, ""\right) = 922.867 \frac{kg}{m^3}$$

Main condensate density at deaerator inlet

$$\rho_{dea.in.d} := \rho_{steam}\left(P_{dea.d}, "", "", h_{mc.d}, ""\right) = 922.867 \frac{kg}{m^3}$$

Main condensate density at deaerator outlet

$$\rho_{dea.out.d} := \rho_{steam}\left(P_{dea.d}, "", 0, "", ""\right) = 893.26 \frac{kg}{m^3}$$

Bled steam density at deaerator inlet

$$\rho_{s.dea.in.d} := \rho_{steam}\left(P_{bs.d}, "", "", h_{bs.d}, ""\right) = 3.111 \frac{kg}{m^3}$$

Bled steam density at deaerator outlet

$$\rho_{s.dea.out.d} := \rho_{steam}\left(P_{dea.d}, "", 1, "", ""\right) = 4.521\,\frac{kg}{m^3}$$

Vent steam density at vent pipe inlet

$$\rho_{vp.in.d} := \rho_{steam}\left(P_{dea.d}, "", 1, "", ""\right) = 4.521\,\frac{kg}{m^3}$$

Vent steam density at vent pipe outlet

$$\rho_{vp.out.d} := \rho_{steam}\left(P_{\theta}, "", "", h_{vs.d}, ""\right) = 0.526\,\frac{kg}{m^3}$$

Main condensate viscosity at nozzle inlet

$$\mu_{noz.in.d} := \mu_{steam}\left(P_{mc.d}, T_{mc.d}, "", "", "", ""\right) = 1.913 \times 10^{-4}\cdot Pa\cdot s$$

Main condensate viscosity at nozzle outlet

$$\mu_{noz.out.d} := \mu_{steam}\left(P_{dea.d}, "", "", "", h_{mc.d}, ""\right) = 1.91 \times 10^{-4}\cdot Pa\cdot s$$

Main condensate viscosity at deaerator outlet

$$\mu_{dea.out.d} := \mu_{steam}\left(P_{dea.d}, "", "", 0, "", ""\right) = 1.558 \times 10^{-4}\cdot Pa\cdot s$$

Bled steam viscosity at deaerator inlet

$$\mu_{s.dea.in.d} := \mu_{steam}\left(P_{bs.d}, "", "", "", h_{bs.d}, ""\right) = 2.212 \times 10^{-5}\cdot Pa\cdot s$$

Bled steam viscosity at deaerator outlet

$$\mu_{s.dea.out.d} := \mu_{steam}\left(P_{dea.d}, "", "", 1, "", ""\right) = 1.478 \times 10^{-5}\cdot Pa\cdot s$$

Main condensate surface tension at nozzle inlet

$$\sigma_{noz.in.d} := \sigma_{steam}\left("", T_{noz.in.d}\right) = 0.05\cdot\frac{N}{m}$$

Main condensate surface tension at nozzle outlet

$$\sigma_{noz.out.d} := \sigma_{steam}\left("", T_{noz.out.d}\right) = 0.05\cdot\frac{N}{m}$$

Main condensate conductivity at deaerator inlet

$$k_{dea.in.d} := \lambda_{steam}\left(P_{dea.d}, "", "", "", h_{mc.d}, ""\right) = 0.685\,\frac{kg\cdot m}{K\cdot s^3}$$

Main condensate conductivity at deaerator outlet

$$k_{dea.out.d} := \lambda_{steam}\left(P_{dea.d}, "", "", 0, "", ""\right) = 0.677\,\frac{kg\cdot m}{K\cdot s^3}$$

Main condensate specific heat at constant pressure at deaerator inlet

$$c_{P.dea.in.d} := Cp_{steam}\left(P_{dea.d}, "", "", "", h_{mc.d}, ""\right) = 4.294\cdot\frac{kJ}{kg\cdot K}$$

Main condensate specific heat at constant pressure at deaerator outlet

$$c_{P.dea.out.d} := Cp_{steam}\left(P_{dea.d}, "", "", 0, "", ""\right) = 4.384\cdot\frac{kJ}{kg\cdot K}$$

Average main condensate density across nozzle

$$\rho_{noz.d} := \frac{\rho_{noz.in.d} + \rho_{noz.out.d}}{2} = 923.035 \frac{kg}{m^3}$$

Average main condensate density in deaerator

$$\rho_{dea.d} := \frac{\rho_{dea.in.d} + \rho_{dea.out.d}}{2} = 908.064 \frac{kg}{m^3}$$

Average steam density in deaerator

$$\rho_{s.dea.d} := \frac{\rho_{s.dea.in.d} + \rho_{s.dea.out.d}}{2} = 3.816 \frac{kg}{m^3}$$

Average steam density across vent pipe

$$\rho_{vp.d} := \frac{\rho_{vp.in.d} + \rho_{vp.out.d}}{2} = 2.524 \frac{kg}{m^3}$$

Avergage main condensate viscosity across nozzle

$$\mu_{noz.d} := \frac{\mu_{noz.in.d} + \mu_{noz.out.d}}{2} = 1.911 \times 10^{-4} \cdot Pa \cdot s$$

Average steam viscosity in deaerator

$$\mu_{s.dea.d} := \frac{\mu_{s.dea.in.d} + \mu_{s.dea.out.d}}{2} = 1.845 \times 10^{-5} \frac{kg}{s \cdot m}$$

Average main condensate surface tension across nozzle

$$\sigma_{noz.d} := \frac{\sigma_{noz.in.d} + \sigma_{noz.out.d}}{2} = 0.05 \cdot \frac{N}{m}$$

Average main condensate conductivity in deaerator

$$k_{dea.d} := \frac{k_{dea.in.d} + k_{dea.out.d}}{2} = 0.681 \frac{kg \cdot m}{K \cdot s^3}$$

Average main condensate specific heat in deaerator

$$c_{p.dea.d} := \frac{c_{P.dea.in.d} + c_{P.dea.out.d}}{2} = 4.339 \cdot \frac{kJ}{kg \cdot K}$$

Temperature tolerance

$$\Delta k := 0.05$$

Target temperature (Temp at which deaeration takes place)

$$T_{target.d} := T_{dea.out.d} - \Delta k \ K$$

Distance travelled by droplet

$$L_d := \frac{L_{spray}}{cos(\theta)} = 1 m$$

Oxygen inlet partial pressure - main condensate

$$p_{o2.in.d} := mf_{o2.air} \cdot P_{mc.d} = 2.8014 \cdot bar$$

Oxygen Inlet concentration - main condensate

$$c_{o2.in.d} := p_{o2.in.d} \cdot k_H\left(T_{mc.d}\right) = 22650.2855030843 \cdot ppb$$

Guess value for Nozzle "X" factor

$$Xg := 0.1$$

Guess value for outlet orifice diameter

$$d_{og} := 0.01$$

Guess value for sheet thickness

$$tg := 0.005$$

*Given*

Spray angle - nozzle geometry relationship

$$\cos(\theta)^2 = \frac{1 - Xg}{1 + Xg}$$

$$X := Find(Xg) = 0.6$$

Nozzle "X" factor

$$X = 0.6$$

Spray Sauter Mean Diameter (SMD)

$$d_{32.d} := 2.25\sigma_{noz.d}^{\frac{1}{4}} \cdot \mu_{noz.d}^{\frac{1}{4}} \cdot \left(\frac{m_{mc.d}}{N_{noz}}\right)^{\frac{1}{4}} \cdot \Delta P_{noz.d}^{\frac{-1}{2}} \cdot \rho_{s.dea.d}^{\frac{-1}{4}} = 0.483 \cdot mm$$

Mean dimensionless temperature

$$\theta_{m.d} := \frac{T_{target.d} - T_{dea.in.d}}{T_{dea.out.d} - T_{dea.in.d}} = 0.998$$

Fourier number

$$Fo_d := -\frac{ln\left(1 - \theta_{m.d}^2\right)}{\pi^2} = 0.579$$

Time taken to heat water to saturation

$$t_{heat.d} := \frac{Fo_d \cdot c_{p.dea.d} \cdot d_{32.d}^{2} \cdot \rho_{dea.d}}{4 \cdot k_{dea.d}} = 0.195\,s$$

Oxygen diffusivity in water

$$D_{o2.water.d} := \left[ \frac{117.3 \cdot 10^{-18} \cdot \left(\Phi_{water} \cdot M_{water}\right)^{\frac{1}{2}} \cdot \frac{T_{dea.out.d}}{K}}{\left( \frac{V_{oxygen}}{1000 \cdot \frac{cm^3}{mol}} \right)^{0.6} \cdot \frac{\mu_{dea.out.d}}{\frac{kg}{m \cdot s}}} \right] \cdot \frac{m^2}{s} = 1.72 \times 10^{-8} \frac{m^2}{s}$$

$$tol_1 := 1 \cdot 10^{-6} \frac{m}{s}$$

Iterative solver initialisation

$$v_{new} := 1 \frac{m}{s}$$

$$v_{old} := 10 \frac{m}{s}$$

Schmidt number

$$Sc_d := \frac{\mu_{dea.out.d}}{\rho_{dea.out.d} \cdot D_{o2.water.d}} = 10.144$$

Grashof number

$$Gr_d := \frac{d_{32.d}^{3} \cdot \rho_{dea.out.d} \cdot g \cdot \left(\rho_{dea.out.d} - \rho_{s.dea.d}\right)}{\mu_{dea.out.d}^{2}} = 3.621 \times 10^{4}$$

Droplet velocity

$$U_{drop} := \left| \begin{array}{l} i \leftarrow 0 \\ \text{while} \quad \left| v_{new} - v_{old} \right| \geq tol_1 \\ \quad \left| \begin{array}{l} Re_{dea} \leftarrow \dfrac{\rho_{s.dea.d} \cdot v_{new} \cdot d_{32.d}}{\mu_{s.dea.d}} \\ Sh_0 \leftarrow \left| \begin{array}{ll} 2 + 0.569 \left( Gr_d \cdot Sc_d \right)^{0.25} & \text{if} \quad Gr_d \cdot Sc_d \leq 1 \cdot 10^8 \\ 2 + 0.0254 \left( Gr_d \cdot Sc_d \right)^{\frac{1}{3}} \cdot Sc_d^{\,0.244} & \text{otherwise} \end{array} \right. \\ Sh \leftarrow Sh_0 + 0.347 \cdot \left( Re_{dea} \cdot Sc_d^{\,\frac{1}{2}} \right)^{0.62} \\ t_{res} \leftarrow -\dfrac{d_{32.d}^{\,2} \cdot \ln\left( \dfrac{c_{o2.out.d}}{c_{o2.in.d}} \right)}{6 \cdot D_{o2.water.d} \cdot Sh} \\ v_{old} \leftarrow v_{new} \\ v_{new} \leftarrow \dfrac{L_d}{t_{res} + t_{heat.d}} \\ v_{n_i} \leftarrow v_{new} \\ i \leftarrow i + 1 \end{array} \right. \\ v_n \end{array} \right.$$

$$n := last\left( U_{drop} \right) = 9$$

Droplet/Spray velocity

$$U_{droplet.d} := U_{drop_n} = 1.248 \frac{m}{s}$$

Time taken for heat and mass transfer to be completed

$$t_{residence} := \frac{L_d}{U_{droplet.d}} = 0.801\,s$$

Vent steam mass flow rate

$$m_{vs.d} := -\frac{h_{mc.d} \cdot m_{mc.d} - h_{dw.d} \cdot \left( m_{mc.d} + m_{bs.d} + m_{rc.d} \right) + h_{bs.d} \cdot m_{bs.d} + h_{rc.d} \cdot m_{rc.d}}{h_{dw.d} - h_{vs.d}} = 0.334 \frac{kg}{s}$$

Deaerated water mass flow rate

$$m_{dw.d} := m_{mc.d} + m_{bs.d} + m_{rc.d} - m_{vs.d} = 212.003\,\frac{kg}{s}$$

Vent pipe loss coefficient

$$C_{k.vp} := \frac{\Delta P_{vp.d} \cdot \rho_{vp.d}}{m_{vs.d}^{2}} = 1.745 \times 10^{7}\,\frac{1}{m^{4}}$$

Nozzle flow area

$$A_0 := \frac{\frac{m_{mc.d}}{N_{noz}}}{\rho_{noz.d} \cdot U_{droplet.d} \cdot (1 - X)} = 391406.411 \cdot mm^{2}$$

Nozzle discharge diameter

$$d_0 := \sqrt{\frac{4 \cdot A_0}{\pi}} = 0.70594201 \cdot m$$

Nozzle "X" factor as a function of discharge port deameter and sheet thickness

$$X = \frac{\left(d_0 - 2t_{sheet}\right)^{2}}{d_0^{2}}$$

Conical sheet thickness

$$t_{sheet.d} := \begin{pmatrix} \frac{d_0}{2} + \frac{\sqrt{X} \cdot d_0}{2} \\ \frac{d_0}{2} - \frac{\sqrt{X} \cdot d_0}{2} \end{pmatrix} = \begin{pmatrix} 626.381 \\ 79.561 \end{pmatrix} \cdot mm$$

## *OUTPUTS*

Vent pipe loss coefficient

$$C_{k.vp} = 1.745 \times 10^{7}\,\frac{1}{m^{4}}$$

Nozzle discharge diameter

$$d_0 = 0.70594201\,m$$

# CORE MODEL

## *INPUTS*

Main condensate mass flow $m_{mc} := 180.360 \frac{kg}{s}$

Main condesnate pressure $P_{mc} := 13.34\,bar$

Main condesnate temperature $T_{mc} := 143.829\ °C$

Bled steam pressure $P_{bs} := 8.73 bar$

Bled steam enthalpy $h_{bs} := 3149.813 \frac{kJ}{kg}$

Return condensate mass flow rate $m_{rc} := 23.27 \frac{kg}{s}$

Return condensate DA inlet pressure $P_{rc} := 9.39 bar$

Return condensate DA inlet enthalpy $h_{rc} := 877.300 \frac{kJ}{kg}$

## *EXECUTION*

Deaerator operating pressure $P_{dea} := P_{bs} = 8.73 \cdot bar$

Main condensate enthalpy at deaerator inlet $h_{mc} := h_{steam}\left(P_{mc}, T_{mc}, "", "", ""\right) = 606.248 \cdot \frac{kJ}{kg}$

Deaerated water enthalpy at deaerator outlet $h_{dw} := h_{steam}\left(P_{dea}, "", "", 0, ""\right) = 737.051 \cdot \frac{kJ}{kg}$

Vent steam enthalpy at deaerator outlet

$$h_{vs} := h_{steam}(P_{dea}, "", "", 1, "") = 2.772 \times 10^3 \cdot \frac{kJ}{kg}$$

Main condensate pressure drop across deaerator nozzle

$$\Delta P_{noz} := P_{mc} - P_{dea} = 4.61 \cdot bar$$

Vent steam pressure drop across vent pipe

$$\Delta P_{vp} := P_{dea} - P_{\theta} = 7.717 \cdot bar$$

Main condensate temperature at nozzle inlet

$$T_{noz.in} := T_{mc} = 143.829 \cdot °C$$

Main condensate temperature at nozzle outlet

$$T_{noz.out} := T_{steam}(P_{dea}, "", h_{mc}, "") = 143.918 \cdot °C$$

Main condensate temperature at deaerator inlet

$$T_{dea.in} := T_{steam}(P_{dea}, "", h_{mc}, "") = 143.918 \cdot °C$$

Main condensate temperature at deaerator outlet

$$T_{dea.out} := T_{steam}(P_{dea}, "", "", "") = 174.067 \cdot °C$$

Main condensate density at nozzle inlet

$$\rho_{noz.in} := \rho_{steam}(P_{mc}, T_{mc}, "", "", "") = 923.202 \frac{kg}{m^3}$$

Main condensate density at nozzle outlet

$$\rho_{noz.out} := \rho_{steam}(P_{dea}, "", "", h_{mc}, "") = 922.867 \frac{kg}{m^3}$$

Main condensate density at deaerator inlet

$$\rho_{dea.in} := \rho_{steam}(P_{dea}, "", "", h_{mc}, "") = 922.867 \frac{kg}{m^3}$$

Main condensate density at deaerator outlet

$$\rho_{dea.out} := \rho_{steam}(P_{dea}, "", 0, "", "") = 893.26 \frac{kg}{m^3}$$

Bled steam density at deaerator inlet

$$\rho_{s.dea.in} := \rho_{steam}(P_{bs}, "", "", h_{bs}, "") = 3.111 \frac{kg}{m^3}$$

Bled steam density at deaerator outlet

$$\rho_{s.dea.out} := \rho_{steam}(P_{dea}, "", 1, "", "") = 4.521 \frac{kg}{m^3}$$

Vent steam density at vent pipe inlet

$$\rho_{vp.in} := \rho_{steam}(P_{dea}, "", 1, "", "") = 4.521 \frac{kg}{m^3}$$

Vent steam density at vent pipe outlet

$$\rho_{vp.out} := \rho_{steam}(P_{\theta}, "", "", h_{vs}, "") = 0.526 \frac{kg}{m^3}$$

Main condensate viscosity at nozzle inlet

$$\mu_{noz.in} := \mu_{steam}(P_{mc}, T_{mc}, "", "", "", "") = 1.913 \times 10^{-4} \cdot Pa \cdot s$$

Main condensate viscosity at nozzle outlet

$$\mu_{noz.out} := \mu_{steam}(P_{dea}, "", "", "", h_{mc}, "") = 1.91 \times 10^{-4} \cdot Pa \cdot s$$

Main condensate viscosity at deaerator outlet

$$\mu_{dea.out} := \mu_{steam}(P_{dea}, "", "", 0, "", "") = 1.558 \times 10^{-4} \cdot Pa \cdot s$$

Bled steam viscosity at deaerator inlet

$$\mu_{s.dea.in} := \mu_{steam}(P_{bs}, "", "", "", h_{bs}, "") = 2.212 \times 10^{-5} \cdot Pa \cdot s$$

Bled steam viscosity at deaerator outlet

$$\mu_{s.dea.out} := \mu_{steam}(P_{dea}, "", "", 1, "", "") = 1.478 \times 10^{-5} \cdot Pa \cdot s$$

Main condensate surface tension at nozzle inlet

$$\sigma_{noz.in} := \sigma_{steam}("", T_{noz.in}) = 0.05 \cdot \frac{N}{m}$$

Main condensate surface tension at nozzle outlet

$$\sigma_{noz.out} := \sigma_{steam}("", T_{noz.out}) = 0.05 \cdot \frac{N}{m}$$

Main condensate conductivity at deaerator inlet

$$k_{dea.in} := \lambda_{steam}(P_{dea}, T_{dea.in}, "", "", "", "") = 0.685 \frac{kg \cdot m}{K \cdot s^3}$$

Main condensate conductivity at deaerator outlet

$$k_{dea.out} := \lambda_{steam}(P_{dea}, "", "", 0, "", "") = 0.677 \frac{kg \cdot m}{K \cdot s^3}$$

Main condensate specific heat at constant pressure at deaerator inlet

$$c_{P.dea.in} := Cp_{steam}(P_{dea}, "", "", "", h_{mc}, "") = 4.294 \cdot \frac{kJ}{kg \cdot K}$$

Main condensate specific heat at constant pressure at deaerator outlet

$$c_{P.dea.out} := Cp_{steam}(P_{dea}, "", "", 0, "", "") = 4.384 \cdot \frac{kJ}{kg \cdot K}$$

Average main condensate density across nozzle

$$\rho_{noz} := \frac{\rho_{noz.in} + \rho_{noz.out}}{2} = 923.035 \frac{kg}{m^3}$$

Average main condensate density in deaerator

$$\rho_{dea} := \frac{\rho_{dea.in} + \rho_{dea.out}}{2} = 908.064 \frac{kg}{m^3}$$

Average steam density in deaerator

$$\rho_{s.dea} := \frac{\rho_{s.dea.in} + \rho_{s.dea.out}}{2} = 3.816 \frac{kg}{m^3}$$

Average steam density across vent pipe

$$\rho_{vp} := \frac{\rho_{vp.in} + \rho_{vp.out}}{2} = 2.524\,\frac{kg}{m^3}$$

Avergage main condensate viscosity across nozzle

$$\mu_{noz} := \frac{\mu_{noz.in} + \mu_{noz.out}}{2} = 1.911 \times 10^{-4}\cdot Pa\cdot s$$

Average steam viscosity in deaerator

$$\mu_{s.dea} := \frac{\mu_{s.dea.in} + \mu_{s.dea.out}}{2} = 1.845 \times 10^{-5}\cdot Pa\cdot s$$

Average main condensate surface tension across nozzle

$$\sigma_{noz} := \frac{\sigma_{noz.in} + \sigma_{noz.out}}{2} = 0.05\cdot\frac{N}{m}$$

Average main condensate conductivity in deaerator

$$k_{dea} := \frac{k_{dea.in} + k_{dea.out}}{2} = 0.681\,\frac{kg\cdot m}{K\cdot s^3}$$

Average main condensate specific heat in deaerator

$$c_{p.dea} := \frac{c_{P.dea.in} + c_{P.dea.out}}{2} = 4.339\cdot\frac{kJ}{kg\cdot K}$$

Target temperature (Temp at which deaeration takes place)

$$T_{target} := T_{dea.out} - \Delta k\ K$$

Deaerated water pressure at dearator outlet

$$P_{dw} := P_{dea} = 8.73\cdot bar$$

Deaerated water temperature at deaerator outlet

$$T_{dw} := T_{steam}\left(P_{dea}, "", "", ""\right) = 174.067\cdot °C$$

Oxygen inlet partial pressure - main condensate

$$p_{o2.in} := mf_{o2.air}\cdot P_{mc} = 2.8014\cdot bar$$

Oxygen Inlet concentration - main condensate

$$c_{o2.in} := p_{o2.in}\cdot k_H\left(T_{mc}\right) = 0.708\,\frac{mol}{m^3}$$

Spray Sauter mean diameter

$$d_{32} := 2.25\sigma_{noz}^{\frac{1}{4}}\cdot\mu_{noz}^{\frac{1}{4}}\cdot\left(\frac{m_{mc}}{N_{noz}}\right)^{\frac{1}{4}}\cdot\Delta P_{noz}^{\frac{-1}{2}}\cdot\rho_{s.dea}^{\frac{-1}{4}} = 0.483\cdot mm$$

Droplet velocity

$$U_{droplet} := \frac{\frac{m_{mc}}{N_{noz}}}{\rho_{noz} \cdot A_0 \cdot (1 - X)} = 1.248 \frac{m}{s}$$

Mean dimensionless temperature

$$\theta_m := \frac{T_{target} - T_{dea.in}}{T_{dea.out} - T_{dea.in}} = 0.998$$

Fourier number

$$Fo := -\frac{ln\left(1 - \theta_m^{\,2}\right)}{\pi^2} = 0.579$$

Time taken to heat water to target temperature

$$t_{ht} := \frac{Fo \cdot c_{p.dea} \cdot d_{32}^{\,2} \cdot \rho_{dea}}{4 \cdot k_{dea}} = 0.195\,s$$

Oxygen diffusivity in water

$$D_{o2.water} := \left[ \frac{117.3 \cdot 10^{-18} \cdot \left(\Phi_{water} \cdot M_{water}\right)^{\frac{1}{2}} \cdot \frac{T_{dea.out}}{K}}{\left( \frac{V_{oxygen}}{1000 \cdot \frac{cm^3}{mol}} \right)^{0.6} \cdot \frac{\mu_{dea.out}}{\frac{kg}{m \cdot s}}} \right] \cdot \frac{m^2}{s} = 1.72 \times 10^{-8} \frac{m^2}{s}$$

Droplet resisdence time

$$t_r := \frac{L_d}{U_{droplet}} = 0.801\,s$$

Time available for mass transfer

$$t_{mt} := t_r - t_{ht} = 0.606\,s$$

Reynolds number

$$Re_{dea} := \frac{\rho_{s.dea} \cdot U_{droplet} \cdot d_{32}}{\mu_{s.dea}} = 124.719$$

Schmidt number

$$Sc := \frac{\mu_{dea.out}}{\rho_{dea.out} \cdot D_{o2.water}} = 10.144$$

Grashof number

$$Gr := \frac{{d_{32}}^3 \cdot \rho_{dea.out} \cdot g \cdot \left(\rho_{dea.out} - \rho_{s.dea}\right)}{{\mu_{dea.out}}^2} = 3.621 \times 10^4$$

Initial Sherwoods number

$$Sh_0 := \begin{cases} 2 + 0.569\,(Gr \cdot Sc)^{0.25} & \text{if } Gr \cdot Sc \le 1 \cdot 10^8 \\ 2 + 0.0254\,(Gr \cdot Sc)^{\frac{1}{3}} \cdot Sc^{0.244} & \text{otherwise} \end{cases}$$

$$Sh_0 = 16.008$$

Sherwoods number

$$Sh := Sh_0 + 0.347 \cdot \left(Re_{dea} \cdot Sc^{\frac{1}{2}}\right)^{0.62} = 30.19$$

Liquid side mass-transfer coefficient

$$K_L := \frac{Sh \cdot D_{o2.water}}{d_{32}} = 0.0011 \frac{m}{s}$$

Vent steam mass flow rate

$$m_{vs} := \sqrt{\frac{\Delta P_{vp} \cdot \rho_{vp}}{C_{k.vp}}} = 0.334 \frac{kg}{s}$$

bled steam mass flow rate

$$m_{bs} := \frac{h_{dw} \cdot \left(m_{mc} + m_{rc} - m_{vs}\right) - h_{mc} \cdot m_{mc} - h_{rc} \cdot m_{rc} + h_{vs} \cdot m_{vs}}{h_{bs} - h_{dw}} = 8.707 \frac{kg}{s}$$

Deaerated water mass flow rate

$$m_{dw} := m_{mc} + m_{rc} + m_{bs} - m_{vs} = 212.003 \frac{kg}{s}$$

Outlet concentration

$$c_{o2.out} := c_{o2.in} \cdot e^{-6 \cdot \left(\frac{Sh \cdot D_{o2.water}}{{d_{32}}^2}\right) \cdot t_{mt}} = 7 \cdot ppb$$

## *OUTPUTS*

deaerator pressure $P_{dea} = 8.73 \cdot bar$

main condensate mass flow rate $m_{mc} = 180.36 \frac{kg}{s}$

rewturn condensate mass flow rate $m_{rc} = 23.27 \frac{kg}{s}$

bled steam mass flow rate $m_{bs} = 8.707 \frac{kg}{s}$

vent steam mass flow rate $m_{vs} = 0.3341105298 \frac{kg}{s}$

deaerated water mass flow rate $m_{dw} = 212.003 \frac{kg}{s}$

deaerated water temperature $T_{dw} = 174.067 \cdot °C$

deaerated water pressure $P_{dw} = 8.73 \cdot bar$

Deaerated water outlet concentration $c_{o2.out} = 7 \cdot ppb$

Liquid side mass-transfer coefficient $K_L := \frac{Sh \cdot D_{o2.water}}{d_{32}} = 1.0743 \times 10^{-3} \frac{m}{s}$